

**Detection of the Calreticulin type 1 and type 2 mutations in a group of
myeloproliferative neoplasm patients using molecular methods**

by

LOUISE DE VILLIERS DU TOIT

Submitted in accordance with the requirements for the degree

Magister Scientiae

(MSc Haematology)

Department of Haematology

Faculty of Health Sciences

University of Pretoria

Pretoria

South Africa

November 2016

Declaration

I declare that this dissertation hereby submitted by me for the Master's degree in Haematology (MSc. Haematology) at the University of Pretoria is my own independent work and has not previously been submitted by me at another university. I furthermore cede copyright of the dissertation in favour of the University of Pretoria. There is no conflict of interest with regard to the proposed study and principle investigator Ms LDV du Toit. Furthermore, there is no contractual obligation limiting the publication of the results from this study.



LDV du Toit

Dedication

I would like to dedicate this dissertation to the friends and family that have supported me in my pursuit of the unknown and my incessant need to keep learning. Without you, the support system for pursuing my goals would not exist and I would not have found happiness in science.

Thank you.

Acknowledgements

I would like to acknowledge the following people for their part in making this dissertation possible:

- My supervisor, Dr Walda van Zyl.
- My co-supervisor, Mrs Andrea Prinsloo.
- The NHLS core laboratory in Steve Biko Academic Hospital for assisting with the collection of samples.
- The National Health Laboratory Service (NHLS) Research Trust Development Grant (Grant004_94524) and the School of Medicine Research Committee (SOM RESCOM) for the funding received for this project.
- Prof Piet Becker, for providing input with the statistical aspects of the study.
- The Department of Haematology at the University of Pretoria, for providing the backdrop for my study and helping me to grow as a scientist.
- The Virtual Molecular Laboratory at the Department of Human Genetics for nucleotide sequence analysis.
- Dr Johan Potgieter, for introducing me to Calreticulin and the potential it holds for study, and also for providing me with extra guidance.
- The head of our department, Prof Roger Pool.
- Dr Chantal van Niekerk, for the use of the Rotor-Gene® Q and for providing assistance when needed.
- My family and friends for their continued support.

Table of Contents

Declaration.....	i
Dedication.....	ii
Acknowledgements	iii
List of Tables	viii
List of Figures.....	xi
List of Abbreviations	xv
Summary.....	xxi
Chapter 1	1
Literature Review	1
1.1. Introduction to haematological malignancies.....	1
1.2. The Myeloproliferative Neoplasms	4
1.2.1. Introduction to the Myeloproliferative Neoplasms	4
1.2.2. Polycythaemia vera	8
1.2.3. Essential thrombocythaemia	10
1.2.4. Primary myelofibrosis/Myelofibrosis	11
1.3. Calreticulin	14
1.3.1. Introduction to Calreticulin	14
1.3.2. Structure of Calreticulin	15
1.3.3. Function of Calreticulin	16
1.3.4. Pathogenesis of Calreticulin.....	17
1.4. Treatment of the myeloproliferative neoplasms.....	20
1.5. Current <i>CALR</i> mutation detection methods.....	21
1.5.1. Assays involving conventional polymerase chain reaction.....	21
1.5.2. Assays involving sequencing	22

1.5.3. Assays involving real-time PCR	23
1.5.4. Assays involving other methods	24
1.6. Conclusion	25
References	27
Chapter 2	36
DNA Preparation and Conventional PCR for the Detection of Calreticulin Type 1 and 2 Mutations	36
2.1. Introduction to techniques	36
2.1.1. DNA extraction	36
2.1.2. Conventional PCR.....	37
2.1.3. Restriction enzyme analyses	38
2.1.4. Agarose gel electrophoresis	38
2.2. Materials and Methods	39
2.2.1. Study population and data analysis performed	40
2.2.2. DNA extraction	41
2.2.3. DNA analysis	42
2.2.4. Design and synthesis of primers.....	43
2.2.5. Design and synthesis of control fragments	44
2.2.6. Conventional in-house PCR.....	44
2.2.7. Purification of PCR products	46
2.2.8. Restriction enzyme analysis	47
2.2.9. Agarose gel electrophoresis	47
2.2.10. Conventional PCR using a commercial kit	48
2.3. Results and Discussion	53
2.4. Conclusion	64
References	65
Chapter 3	68

Sequencing	68
3.1. Introduction to techniques	68
3.1.1. Sanger sequencing.....	68
3.1.2. Next generation sequencing	69
3.2. Materials and Methods	70
3.2.1. Sanger sequencing.....	70
3.3. Results and Discussion	72
3.4. Conclusion.....	74
References	75
Chapter 4	76
Real-time PCR.....	76
4.1. Introduction to techniques	76
4.1.1. Real-time PCR.....	76
4.2. Materials and Methods	79
4.2.1. Real-time PCR using SYBR Green.....	79
4.2.1.1. QuantiNova™ SYBR® Green PCR.....	79
4.2.1.2. SensiFAST™ SYBR® Green PCR.....	82
4.2.1.3. SensiFAST™ High Resolution Melt PCR	83
4.2.2. Probe design for real-time PCR	84
4.2.3. Real-time PCR using probes	85
4.3. Results and Discussion	88
4.3.1. Real-time PCR using SYBR Green	88
4.3.2. Real-time PCR using probes	97
4.4. Conclusion.....	109
References	110
Chapter 5	112
Study Outcome	112

References	115
Appendices	117
A1. MSc Committee approval form	118
A2. Ethics Committee approval form.....	119
A3. Ethics Committee amendment approval form	120
A4. Informed consent form for the collection of blood samples from non-government institutions	121
A5. DNA concentration of samples used	127
A6. Manufactured control sequences with primer binding sites and the <i>MfeI</i> restriction enzyme digestion site	129

List of Tables

Table 1.1	Established and suspected risk factors for malignant disease (Zeeb and Blettner, 1998)	3
Table 1.2	Guidelines for using the revised WHO classification of myeloid neoplasms (Van Der Walt, 2015)	8
Table 2.1	Primer sequences and characteristics	43
Table 2.2	Conventional PCR reaction setup	45
Table 2.3	Conventional PCR cycling protocol on the BioRad DNA Engine® Peltier Thermal Cycler (Bio-Rad)	46
Table 2.4	Restriction enzyme digestion reaction setup	47
Table 2.5	Conventional PCR using a commercial kit reaction setup (AB Analytica)	49
Table 2.6	Conventional PCR using a commercial kit's cycling profile on the BioRad DNA Engine® Peltier Thermal Cycler (Bio-Rad) (AB Analytica, 2015)	49
Table 2.7	Pre-treatment of PCR product cycling conditions (AB Analytica, 2015)	50
Table 2.8	Method for preparing samples on parafilm before electrophoresis (AB Analytica, 2015)	51
Table 2.9	Indication of expected results (AB Analytica, 2015)	51
Table 2.10	Evaluation of the commercial PCR session (AB Analytica, 2015)	51
Table 2.11	Guide to interpreting results of the commercial PCR (AB Analytica, 2015)	52
Table 2.12	Cost analysis of the in-house conventional PCR assay	62

Table 2.13	Cost analysis of the commercially available PCR kit	62
Table 3.1	Preparation of reaction mixtures for Sanger sequencing	70
Table 3.2	Cycle sequencing program on the BioRad DNA Engine® Peltier Thermal Cycler (Bio-Rad)	71
Table 3.3	Samples found to contain type 1 or type 2 mutations	74
Table 4.1	Preparation of real-time PCR with QuantiNova (Qiagen) SYBR Green reaction setup on the SmartCycler® (Cepheid)	80
Table 4.2	Real-time PCR with QuantiNova (Qiagen) SYBR Green cycler conditions on the SmartCycler® (Cepheid)	80
Table 4.3	Real-time PCR with QuantiNova (Qiagen) SYBR Green reaction setup on the Rotor-Gene® Q (Qiagen)	81
Table 4.4	Real-time PCR with QuantiNova (Qiagen) SYBR Green cycler conditions on the Rotor-Gene® Q (Qiagen)	81
Table 4.5	Real-time PCR with SensiFAST™ SYBR® No-ROX (Bioline) SYBR Green reaction setup on the Rotor-Gene® Q (Qiagen)	82
Table 4.6	Real-time PCR with SensiFAST™ SYBR® No-ROX (Bioline) SYBR Green cycler conditions on the Rotor-Gene® Q (Qiagen)	83
Table 4.7	Real-time PCR with SensiFAST™ HRM (Bioline) reaction setup on the Rotor-Gene® Q (Qiagen)	83
Table 4.8	Real-time PCR with SensiFAST™ HRM (Bioline) SYBR Green cycler conditions on the Rotor-Gene® Q (Qiagen)	84
Table 4.9	Probe sequences and characteristics	85

Table 4.10	Real-time PCR with QuantiNova (Qiagen) Probe PCR kit reaction setup on the SmartCycler® (Cepheid)	86
Table 4.11	Real-time PCR with QuantiNova (Qiagen) Probe PCR kit cyclers conditions on the SmartCycler® (Cepheid)	86
Table 4.12	Real-time PCR with QuantiNova (Qiagen) Probe PCR kit reaction setup on the Rotor-Gene® Q (Qiagen)	87
Table 4.13	Real-time PCR with QuantiNova (Qiagen) Probe PCR kit cyclers conditions on the Rotor-Gene® Q (Qiagen)	87
Table A1	DNA concentrations of samples	127

List of Figures

Figure 1.1	Diagrammatic representation of the bone marrow pluripotent stem cell and the cell lines that arise from it (Hoffbrand and Moss, 2012c)	2
Figure 1.2	Laboratory features of polycythaemia vera, essential thrombocythaemia, and idiopathic myelofibrosis	13
Figure 1.3	The protein structure and putative functions of calreticulin domain (Lu <i>et al.</i> , 2015)	15
Figure 1.4	Immunostaining of bone marrow biopsies with the anti-mutated CALR antibody	25
Figure 2.1	Representative example of a gel and the interpretation of its results	52
Figure 2.2	Agarose gel electrophoresis of <i>CALR</i> exon 9 amplicons from selected patients, namely 23-30	54
Figure 2.3	Agarose gel electrophoresis of <i>CALR</i> exon 9 amplicons from selected patients, namely J36-J45	55
Figure 2.4	Agarose gel electrophoresis of <i>CALR</i> exon 9 amplicons from selected patients, namely 6.2, J22, DEL and INS	56
Figure 2.5	Agarose gel electrophoresis of <i>CALR</i> exon 9 amplicons, after RE digest, from selected patients, namely J22 and INS	58
Figure 2.6	Agarose gel electrophoresis of <i>CALR</i> exon 9 amplicons, after RE digest, from selected patients, namely DEL and INS	58

Figure 2.7	Agarose gel electrophoresis of <i>CALR</i> exon 9 amplicons detected using a commercially available conventional PCR kit, from selected patients namely 5, 10, 16, 21, 23, DEL and INS	60
Figure 2.8	Agarose gel electrophoresis of <i>CALR</i> exon 9 amplicons detected using a commercially available conventional PCR kit, from selected patients namely J43, 31, J9, J22, 18 and J6	61
Figure 3.1	Sanger sequencing electropherograms of sequences exhibiting no type 1 (A) or type 2 (B) mutations. The asterisks (*) indicate where mutations would have occurred in both cases. Both sequences are from patient 19	72
Figure 3.2	Sanger sequencing electropherograms of the two samples representative of the type 1 (A) and type 2 (B) mutations. A: sample DEL, B: sample INS. The top row of nucleotides refers to the sequence of the wild type strand and the bottom row refers to the sequence of the mutated strand. The box below each figure indicates the change to the strand and the sequence of the specific change	73
Figure 4.1	Hydrolysis probes (e.g., <i>TaqMan</i> assay)	78
Figure 4.2	SYBR Green analysis using the SmartCycler® (Cepheid) system. A) Amplification curve, B) melting curve (middle) and C) a zoomed in view of the yellow square on the melting curve of a SYBR Green analysis using the QuantiNova (Qiagen) kit	89
Figure 4.3:	Agarose gel electrophoresis of <i>CALR</i> exon 9 amplicons produced by a real-time PCR using SYBR Green QuantiNova (Qiagen) kit on the SmartCycler® (Cepheid) system	90

Figure 4.4	Agarose gel electrophoresis of <i>CALR</i> exon 9 amplicons produced by a real-time PCR using SYBR Green, comparing the QuantiNova (Qiagen) and SensiFAST™ (Bioline) kits on the Rotor-Gene® Q (Qiagen)	91
Figure 4.5	Figure 4.5: Analysis of the HRM run on the Rotor-Gene® Q (Qiagen). A) Melt curve analysis and B) Amplification plot	92
Figure 4.6	Agarose gel electrophoresis of <i>CALR</i> exon 9 amplicons produced by a real-time PCR using HRM analysis on the Rotor-Gene® Q (Qiagen)	93
Figure 4.7	Amplification curve analysis of the real-time PCR using SYBR Green on the LightCycler® 2.0 (Roche)	94
Figure 4.8	Melting curve analysis of the real-time PCR using SYBR Green on the LightCycler® 2.0 (Roche)	94
Figure 4.9	Melting peaks of the real-time PCR using SYBR Green on the LightCycler® 2.0 (Roche)	95
Figure 4.10	Agarose gel electrophoresis of <i>CALR</i> exon 9 amplicons produced by a real-time PCR using SYBR Green on the LightCycler® 2.0 (Roche)	95
Figure 4.11	A) Melt curve and B) amplification curve analysis of a SYBR Green run using a more optimized protocol on the SmartCycler® (Cepheid)	96
Figure 4.12	Amplification curves of the first attempt at real-time PCR using probes run on the SmartCycler® (Cepheid)	98
Figure 4.13	Agarose gel electrophoresis of the first real-time PCR amplicons using probes on the SmartCycler® (Cepheid)	98
Figure 4.14	Amplification curves of a real-time PCR using probes run using one probe per tube on the SmartCycler® (Cepheid)	99

Figure 4.15	Amplification curves of a real-time PCR using probes run with annealing temperature changed on the SmartCycler® (Cepheid)	100
Figure 4.16	Amplification curves of a real-time PCR using new probes run with one probe per tube on the SmartCycler® (Cepheid)	101
Figure 4.17	Amplification curves of a real-time PCR using new probes run with one probe per tube and different amounts of DNA on the SmartCycler® (Cepheid)	102
Figure 4.18	Amplification curves of a real-time PCR, using new probes, run with one probe per tube (type 1 probes) and different DNA concentrations on the Rotor-Gene® Q (Qiagen)	103
Figure 4.19	Amplification curves of a real-time PCR using new probes run with two probes per tube for the type 1 mutation on the Rotor-Gene® Q (Qiagen)	104
Figure 4.20	Amplification curves of a real-time PCR using new probes run with two probes per tube for the type 1 and type 2 mutations on the Rotor-Gene® Q (Qiagen)	106
Figure 4.21	Amplification curves of a real-time PCR using a probe from IDT on the Rotor-Gene® Q (Qiagen)	107

List of Abbreviations

6-FAM	6-carboxyfluorescein
A	adenine
<i>ABL1</i>	Abelson murine leukaemia viral oncogene homolog 1
AML	Acute myeloid/myelogenous leukaemia
ASCT	Allogeneic stem cell transplant
<i>ASXLI</i>	Additional sex combs like 1
Baso	basophil
BB	Bromophenol Blue
<i>BCR</i>	breakpoint cluster region
BFU	burst-forming unit
BM	bone marrow
bp	base pairs
C	cytosine
Ca ²⁺	Calcium
<i>CALR</i>	calreticulin
Cat.	Catalogue
CCD	charge-coupled device
CD	cluster of differentiation
cDNA	complementary DNA
<i>CEBPA</i>	CCAAT/enhancer binding protein (C/EBP), Alpha

CEL	chronic eosinophilic leukaemia
CFU	colony-forming unit
cm	centimetres
CML	chronic myeloid/myelogenous leukaemia
CMPD	chronic myeloproliferative disease
CNL	chronic neutrophilic leukaemia
COOH	carboxyl group
D; Asp	aspartic acid
DAMPs	danger associated molecular pattern molecules
ddH ₂ O	double distilled H ₂ O
DEAE	diethylaminoethyl
dL	decilitre
DNA	deoxyribonucleic acid
<i>DNMT3A</i>	DNA methyltransferase 3A
DNase	deoxyribonuclease
E	erythroid
E; Glu	glutamic acid
EDTA	ethylenediaminetetraacetic acid
e.g.	for example
Eo	eosinophil
ER	endoplasmic reticulum
EtOH	ethanol

ET	essential thrombocythaemia
<i>et al.</i>	and others
etc.	<i>et cetera</i> ; and so on
FBC	full blood count
FISH	fluorescence <i>in situ</i> hybridisation
<i>FLT3</i>	fms-related tyrosine kinase 3
FRET	fluorescent resonance energy transfer
g	grams
G	Guanine
GEMM	granulocyte, erythroid, monocyte and megakaryocyte
GM	granulocyte, monocyte
H ₂ O	water
HACBP	high affinity calcium-binding protein
HEX	6-carboxyfluorescein hexachloride
HCl	hydrogen chloride
HRM	high resolution melt
HSC	haematopoietic stem cell
HTLV	human T-cell leukaemia/lymphoma virus
i.e.	that is
<i>IDH1/2</i>	isocitrate dehydrogenase 1 and 2
IDT	Integrated DNA Technologies
IFN- α	interferon alpha
IHC	immunohistochemistry

indels	insertions/deletions
<i>JAK2</i>	Janus-kinase 2
JAK-STAT	Janus-kinase/signal transducer and activator of transcription
K; Lys	lysine
kb	kilobases
kDa	kiloDalton
<i>KIT</i>	v-kit Hardy-Zuckerman 4 feline sarcoma viral oncogene homolog
l	Litre
L; Leu	Leucine
LNA	Locked nucleic acid
<i>LNK</i>	SH2B adaptor protein 3
LoD	limit of detection
M	Molar
MDS	myelodysplastic syndrome
Meg	megakaryocyte
MF	myelofibrosis
MGB	minor groove binding
MHC	major histocompatibility
mM	microMolar
mm	millimetre
ml	millilitre
<i>MPL</i>	myeloproliferative leukaemia virus oncogene



MPN	myeloproliferative neoplasm
MPO	myeloperoxidase
MRD	minimal residual disease
mU	milliunits
NaAc	sodium acetate
ng	nanogram
NGS	next generation sequencing
NH ₂	amine group
NK	natural killer
<i>NPM1</i>	nucleophosmin
<i>NRAS</i>	neuroblastoma RAS viral (v-ras) oncogene homolog
NTC	no template control
PB	peripheral blood
PCR	polymerase chain reaction
Ph	Philadelphia
PMF	primary myelofibrosis
pmol	picomol
<i>PTPN11</i>	protein tyrosine phosphatase, non-receptor type 11
PV	polycythaemia vera
qPCR	real-time PCR
RBC	red blood cell
RE	restriction enzyme

RNA	ribonucleic acid
RNase	ribonuclease
RT-PCR	reverse transcription PCR
STAT	signal transducer and activator of transcription
T	thymine
TAE	Tris/acetic acid/EDTA
TBE	Tris/Borate/EDTA
<i>TET2</i>	ten-eleven-translocation-2
T _m	melting temperature
USA	United States of America
UV	ultraviolet
V	volt
VAT	value added tax
vs.	versus
WBC	white blood cell
WHO	World Health Organization
°C	degrees Celsius
μl	microlitre
%	per cent
X	times (multiplication)
x g	times gravity

**Detection of the Calreticulin type 1 and type 2 mutations in a group of
myeloproliferative neoplasm patients using molecular methods**

by

Louise de Villiers du Toit

Supervisor **Dr WB van Zyl (University of Pretoria)**
Co-supervisor **Mrs A Prinsloo (University of Pretoria/NHLS)**
Department **Haematology, Faculty of Health Sciences, University of
Pretoria**
Degree **MSc (Haematology)**

Summary

The myeloproliferative neoplasms (MPN), formerly referred to as chronic myeloproliferative disorders, are a group of haematopoietic stem cell disorders that are characterized by clonal proliferation of one or more mature myeloid lineages. The group of disorders, now classified as the classic MPNs, include chronic myeloid leukaemia (CML), as well as the Philadelphia (Ph) chromosome-negative MPNs: polycythaemia vera (PV), essential thrombocythaemia (ET) and primary myelofibrosis (PMF) or myelofibrosis (MF).

In 2013, somatic mutations at exon 9 of *CALR*, the gene that encodes for calreticulin, were discovered through whole-exome sequencing and targeted re-sequencing in patients with MPNs. Among these mutations, more than 80% of *CALR* mutated patients possessed one of only two mutation types: type 1 (a 52-bp deletion) and type 2 (a 5-bp insertion).

In MPNs, patients positive for a mutation in their calreticulin gene have shown milder symptoms and an overall better survival rate than patients who had one of the other common phenotypic driver mutations i.e. JAK2 or MPL. Determining which driver mutation is responsible for the manifestation of the MPN is therefore important in monitoring the treatment and prognosis of the patient. In the South African sector, a simple, efficient, cost effective and sensitive detection method for testing for *CALR* type 1 and type 2 mutations is necessary to fill the current diagnostic gap regarding the diagnosis of MPNs.

This study aimed to evaluate the use of conventional PCR followed by restriction enzyme digestion, confirmation of the PCR results by nucleotide sequencing, as well as real-time PCR (qPCR) to detect these mutations. A conventional PCR commercial kit was also compared to that of the developed conventional PCR. For this study 24 blood samples were collected from the tertiary hospital haematology clinic, 24 archived DNA samples from a colleague's previous *JAK2* mutation study were used and two DNA samples were obtained from a private pathology laboratory. A total of 50 samples were thus analysed.

The newly developed in-house conventional PCR was successful in detecting the *CALR* type 1 and type 2 mutations in patients and the results were confirmed by Sanger sequencing. The results obtained using the commercial conventional PCR kit corresponded 100% with the results obtained by the in-house conventional PCR assay, followed by restriction enzyme digestion and finally confirmation of results by nucleotide sequencing analysis. The kit was, however, much more expensive than the in-house PCR assay. The qPCR using SYBR Green as well as the qPCR using probes were unable to detect the type 1 and type 2 mutations and further troubleshooting was not possible due to budgetary constraints. Overall, 3/50 patients contained the type 1 mutation and 2/50 contained the type 2 mutation, indicating the possibility of a low prevalence for the *CALR* type 1 and type 2 mutations in the South African population.

Chapter 1

Literature Review

1.1. Introduction to haematological malignancies

In our modern day and age, cancer has become an increasingly significant cause of morbidity and mortality, with haematological malignancies consisting of roughly 7% of all malignant disease (Hoffbrand and Moss, 2012c). These haematopoietic malignancies represent clonal diseases that derive from a single progenitor cell or haematopoietic stem cell (HSC) that has undergone genetic alterations or lesions, which usually occurs in the bone marrow (BM) or in the peripheral lymphoid tissue (Hoffbrand and Moss, 2012c; Chi and Costeas, 2015).

The HSC was discovered in the BM in 1961 (Till and McCulloch, 1961; Li *et al.*, 2015). A HSC is a multipotent cell that can produce progenitor cells which are capable of differentiating into the myeloid and lymphoid components that make up the various cells of the peripheral blood (PB) (Szilvassy, 2003; Li *et al.*, 2015). Haematopoietic stem cells are also crucial in the maintenance and regeneration of all cells that make up the BM, the thymus and the spleen and have been known to differentiate into cells of tissues that are non-haematopoietic, e.g. liver, kidney, heart, pancreas and brain, when the need arose (Szilvassy, 2003). Stem cells have an important property that distinguishes them from other cells: self-renewal (generation of daughter cells that have the same biological characteristics of the parental stem cell) (Jordan *et al.*, 2006; Li *et al.*, 2015). Stem cells also exhibit the ability to differentiate (the potential to develop into numerous cell lineages) (illustrated in Figure 1.1), and proliferate (Jordan *et al.*, 2006; Li *et al.*, 2015).

In general, the factors that are associated with the development of malignant disease can be classified into, 1) environmental, 2) genetic and familial, and 3) medical and therapy related factors (Table 1.1) (Zeeb and Blettner, 1998). Development of a malignant disorder, is in most cases, however, a combination of environmental influence and genetic background (Hoffbrand and Moss, 2012c).

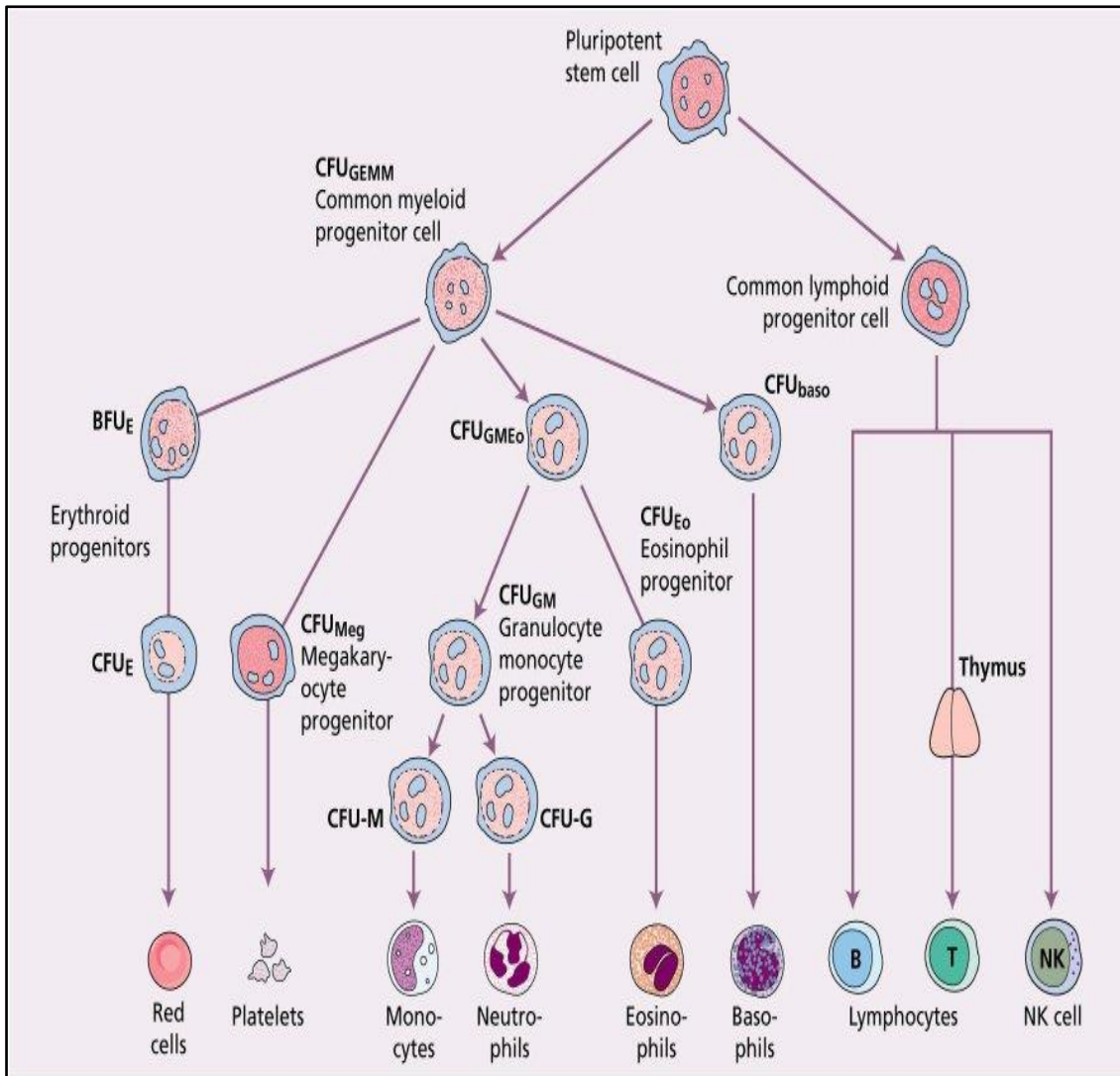


Figure 1.1: Diagrammatic representation of the bone marrow pluripotent stem cell and the cell lines that arise from it. Various progenitor cells can be identified by culture in semi-solid medium by the type of colony they form. It is possible that an erythroid/megakaryocytic progenitor may be formed before the common lymphoid progenitor diverges from the mixed granulocytic/monocyte/eosinophil myeloid progenitor. Baso, basophil; BFU, burst-forming unit; CFU, colony-forming unit; E, erythroid; Eo, eosinophil; GEMM, granulocyte, erythroid, monocyte and megakaryocyte; GM, granulocyte, monocyte; Meg, megakaryocyte; NK, natural killer (Hoffbrand and Moss, 2012b)

Haematopoietic malignancies are usually diagnosed and studied using various techniques (Bain *et al.*, 2012). These techniques include examination of white cell morphology, performing a white cell differential count, karyotype analysis, fluorescence *in situ* hybridisation (FISH), polymerase chain reaction (PCR) and flow cytometry (Bain *et al.*, 2012; Hoffbrand and Moss, 2012c; Béné *et al.*, 2015).

Table 1.1: Established and suspected risk factors for malignant disease (Zeeb and Blettner, 1998)

Environmental factors	<ul style="list-style-type: none"> • Occupational exposures, e.g. leather, printing industry • Ionizing radiation • Non-ionizing radiation • Chemicals, e.g. benzene • Pesticides • Smoking • Others, e.g. diet
Familial and genetic factors	<ul style="list-style-type: none"> • Inherited diseases, e.g. Down Syndrome • Other chromosomal abnormalities, e.g. Philadelphia chromosome
Medical and therapy related factors	<ul style="list-style-type: none"> • Radiotherapy • Diagnostic radiology • Chemotherapy • Medication, e.g. chloramphenicol • Viruses, e.g. human T-cell leukaemia/lymphoma virus (HTLV), herpes viruses

1.2. The Myeloproliferative Neoplasms

1.2.1. Introduction to the Myeloproliferative Neoplasms

The myeloproliferative neoplasms (MPN), formerly referred to as chronic myeloproliferative disorders, are a group of HSC disorders that are characterized by clonal proliferation of one or more mature myeloid lineages i.e. erythroid, megakaryocytic, or granulocytic cells in the bone marrow and, in some cases, the liver and spleen (Klco *et al.*, 2010; Hoffbrand and Moss, 2012d; Turgeon, 2012; Skoda *et al.*, 2015). While these disorders had been recognized as separate clinical entities more than 50 years ago, their interrelatedness was only described in 1951 by William Dameshek, who suggested that they be classified as a group of phenotypically related myeloproliferative disorders or neoplasms (Campbell and Green, 2006; Levine and Gilliland, 2008).

The group of disorders, now classified as the classic MPNs, include chronic myeloid leukaemia (CML), as well as the Philadelphia (Ph) chromosome-negative MPNs: polycythaemia vera (PV), essential thrombocythaemia (ET) and primary myelofibrosis (PMF) or myelofibrosis (MF) (Santos and Verstovsek, 2012; Klampfl *et al.*, 2013). In 2001, the World Health Organization (WHO) committee for the organisation of myeloid neoplasms assigned the classic MPNs under the broader category of chronic myeloproliferative diseases (CMPDs) (Vardiman *et al.*, 2002; Tefferi and Vardiman, 2008; Arber *et al.*, 2016). This group of disorders also include chronic eosinophilic leukaemia (CEL), chronic neutrophilic leukaemia (CNL) and ‘CMPD unclassifiable’ (Tefferi and Vardiman, 2008). In 2016, the WHO classification of the myeloproliferative neoplasms was revised which was the first revision made to the classification system since 2008 (Arber *et al.*, 2016). The categories of MPNs have not changed much since the 2008 edition; however, discoveries of novel mutations and a better understanding of the morphological characteristics of the MPNs, have made an impact on the diagnostic criteria for the diseases (Arber *et al.*, 2016). This is especially true involving genetic abnormalities and the significance they hold for the diagnosis and prognosis of the disease (Arber *et al.*, 2016).

The Ph-chromosome was discovered in 1960 in the leukocytes from patients with CML (P Nowell and Hungerford, 1960a; P C Nowell and Hungerford, 1960b). Chronic myeloid leukaemia is termed Ph-chromosome positive when this characteristic shortened derivative chromosome 22, that is created by a reciprocal translocation between chromosomes 9 and 22, is present (Holyoake *et al.*, 2002; Hoffbrand and Moss, 2012a). When this translocation occurs, part of the oncogene, Abelson murine leukaemia viral oncogene homolog 1 (*ABL1*), on chromosome 9, is moved to the breakpoint cluster (*BCR*) gene on chromosome 22 which results in a chimeric fusion gene *BCR-ABL1* (Holyoake *et al.*, 2002; Hoffbrand and Moss, 2012a). The resultant chimeric gene codes for a fusion protein that is 210-kDa in size vs. the normal *ABL1* product of 145-kDa (Hoffbrand and Moss, 2012a). This abnormal chromosome 22 is the Ph-chromosome which is associated with an increased tyrosine kinase activity compared to the normal *ABL1* product (Holyoake *et al.*, 2002; Hoffbrand and Moss, 2012a).

Mutations that are responsible for the manifestation of the MPNs can fall into two main categories: 1) phenotypic driver mutations that are directly linked to the hyperproliferation of haematopoietic cells and 2) mutations that can enhance and modify the effects of the phenotypic driver mutations for example, ten-eleven-translocation-2 (*TET2*), DNA methyltransferase 3A (*DNMT3A*) and additional sex combs like 1 (*ASXL1*) (Skoda *et al.*, 2015). The three most frequently occurring phenotypic driver mutations include those of Janus kinase 2 (*JAK2*) gene, the thrombopoietin receptor gene (myeloproliferative leukaemia virus oncogene (*MPL*)), and mutations of the calreticulin (*CALR*) gene (Skoda *et al.*, 2015).

The most frequently occurring mutation associated with patients with *BCR-ABL* negative MPN, is the *JAK2* V617F mutation (Skoda *et al.*, 2015). In PV, almost all patients (about 95%) exhibit a mutation in the *JAK2* gene, whereas only 50% to 60% of ET and PMF patients have the *JAK2*V617F mutation (Kilpivaara and Levine, 2008; Thiele and Kvasnicka, 2009; Rotunno *et al.*, 2014). The *JAK2* gene is found on the short arm of chromosome nine at position 9p24 and consists of 25 exons (Tefferi, 2010). The 1132 amino acid protein *JAK2* is one of four non-receptor protein tyrosine kinases in the Janus family (Tefferi, 2010).

A guanine-to-thymidine base-pair change in exon 14 results in a substitution of valine for phenylalanine at amino acid position 617 of the *JAK2* gene which causes the *JAK2V617F* mutation (Levine *et al.*, 2007; Thiele and Kvasnicka, 2009; Nangalia *et al.*, 2013). This gain-of-function, missense mutation is responsible for constitutive Janus kinase/signal transducer and activator of transcription (JAK-STAT) signalling, abolished apoptosis and wide-ranging cellular hyperplasia (Malherbe *et al.*, 2015). A number of mutations have also been observed in exon 12 of the *JAK2* gene and usually account for the PV patients without a *JAK2V617F* mutation (Scott, 2011).

The thrombopoietin receptor gene, *MPL*, exhibits a mutation in 3% to 5% of patients with ET and PMF, with non-mutated *JAK2* (Klampfl *et al.*, 2013; Rotunno *et al.*, 2014). The *MPL* gene is located on the short arm of chromosome one at position 1p34, encodes for a 635-680 amino acid protein, which includes 12 exons and is a crucial component for the survival and growth of megakaryocytes and, therefore, platelets (Tefferi, 2010; Langabeer *et al.*, 2015).

The most frequently occurring mutations of the *MPL* gene are gain of function mutations which group together in exon ten around amino acid number 51 (Choi *et al.*, 2015; Langabeer *et al.*, 2015). These include the W515L and W515K mutations, which result in the substitution of tryptophan with leucine and lysine, respectively, and induce continuous signalling of the downstream JAK/STAT pathway (Ipek *et al.*, 2015; Langabeer *et al.*, 2015). The *MPL* W515L mutation has been shown to induce myeloproliferation marked by leucocytosis, splenomegaly, characteristic thrombocytosis without PV features, extramedullary haematopoiesis by the spleen and, myelofibrosis (Ipek *et al.*, 2015).

Somatic mutations in the *CALR* gene were discovered in 2013 (Klampfl *et al.*, 2013; Nangalia *et al.*, 2013). This was achieved through whole-exome sequencing and targeted re-sequencing in 50% to 70% and 33% to 58% of European and Asian patients, respectively, with ET and PMF who had neither mutated *JAK2* nor *MPL* (Klampfl *et al.*, 2013; Nangalia *et al.*, 2013). More than 50 different mutations have been found in exon 9 of the *CALR* gene (Pietra *et al.*, 2015).

A small minority of patients, exhibit additional mutations that fall into two main classes: 1) signalling mutations that activate the thrombopoietin receptor (*MPL*) or inactivate negative regulators (*LNK*) and 2) mutations in epigenetic regulators of deoxyribonucleic acid (DNA) methylation or chromatin structure (*TET2*, *DNMT3A*, *IDH1/2*) (Nangalia *et al.*, 2013). The most common trait of these mutations is that they alone do not cause a MPN phenotype; rather these mutations are acquired in cells that already carry a mutation in one of the phenotypic driver genes i.e. *JAK2V617F* and they are suspected to be involved in the progression of disease (Skoda *et al.*, 2015). These mutations are also commonly found in other haematological malignancies such as myelodysplastic syndrome (MDS) and acute leukaemias (Skoda *et al.*, 2015).

A small subset of MPN patients lack mutations in all three phenotypic driver genes i.e. *JAK2*, *MPL* or *CALR*, and have become designated as a subgroup termed “triple negative” (Klampfl *et al.*, 2013; Harrison *et al.*, 2015). The lack of mutations in these genes have been shown by several studies to have the worst prognosis compared to the subgroups with mutations in these phenotypic driver genes (Harrison *et al.*, 2015).

In Europe, the MPNs occur at a frequency of approximately 3.1/100 000 per year and primarily affect adults aged 55 years and older but can occur in younger subjects (Visser *et al.*, 2012). The incidence data for myeloproliferative neoplasms in South Africa is, however lacking. The National Cancer Registry does not make provision for the reporting of different types of blood malignancies. However, in 2008, the National Cancer Registry did register 392 males and 311 females that were diagnosed with leukaemia (Herbst, 2015). In the South African public sector, the molecular diagnosis of MPN is mostly done using only *JAK2* mutation analysis. The method of diagnosis regarding the myeloproliferative neoplasms must take into account factors of a clinical, haematological, morphological and especially a genetic nature (Table 1.2) (Van der Walt, 2015).

Signs and symptoms of the MPNs include haemorrhages, thrombosis (arterial and venous), microcirculatory problems and visual and neurological disturbances (Klco *et al.*, 2010; Schmaier and Lazarus, 2012; Mehta *et al.*, 2014). The most important features of the Ph-negative MPN's are: increased red blood cell (RBC) production in PV, a persistent high platelet count in ET, and fibrosis of the BM in PMF/MF (Choi *et al.*, 2015).

Table 1.2: Guidelines for using the revised WHO classification of myeloid neoplasms (Van der Walt, 2015)

Specimen requirements	<ul style="list-style-type: none"> • PB and BM specimens collected prior to any definitive therapy. • PB and cellular BM aspirate smears and/or touch preparations stained with Wright/Giemsa or similar stain. • BM biopsy specimen, at least 1.5 cm in length and at right angles to the cortical bone, is recommended for all cases if feasible. • BM specimens for complete cytogenetic analysis and, when indicated for flow cytometry, with an additional specimen cryopreserved for molecular genetic studies. The latter studies should be performed based on initial karyotypic, clinical, morphologic, and immunophenotypic studies.
Assessment of blasts	<ul style="list-style-type: none"> • Blast percentage in PB and BM is determined by visual inspection. • Myeloblasts, monoblasts, promonocytes, megakaryoblasts (but not dysplastic megakaryocytes) are counted as blasts when summing blast percentage for diagnosis of AML or blast transformation; count abnormal promyelocytes as “blast equivalents” in APL. • Proerythroblasts are not counted as blasts except in rare instances of “pure” acute erythroleukaemia. • Flow cytometric assessment of CD34+ cells is not recommended as a substitute for visual inspection; not all blasts express CD34, and artifacts introduced by specimen processing may result in erroneous estimates. • If the aspirate is poor and/or marrow fibrosis is present, immunohistochemistry (IHC) on biopsy sections for CD34 may be informative if blasts are CD34+.
Assessment of blast lineage	<ul style="list-style-type: none"> • Multiparameter flow cytometry (at least three colours) is recommended; the panel should be sufficient to determine lineage as well as aberrant antigen profile of a neoplastic population. • Cytochemistry, such as myeloperoxidase or nonspecific esterase, may be helpful, particularly in AML, NOS, but it is not essential in all cases. • IHC on biopsy sections may be helpful; many antibodies are now available for recognition of myeloid and lymphoid antigens.
Assessment of genetic features	<ul style="list-style-type: none"> • Complete cytogenetic analysis from BM at initial diagnosis when possible. • Additional studies, such as FISH, RT-PCR, and mutational status should be guided by clinical, laboratory, and morphologic information. • Mutational studies for mutated <i>NPM1</i>, <i>CEBPA</i>, and <i>FLT3</i> are recommended in all cytogenetically normal AML; mutated <i>JAK2</i> should be sought in <i>BCR-ABL1</i> negative MPN, and mutational analysis for <i>MPL</i>, <i>CALR</i>, <i>KIT</i>, <i>NRAS</i>, <i>PTNP11</i>, etc., should be performed as clinically indicated.
Correlation/reporting of data	<ul style="list-style-type: none"> • All data should be assimilated into one report that states the WHO diagnosis.

1.2.2. Polycythaemia vera

Polycythaemia can be described as an increase in the haemoglobin concentration above the upper limit of which is normal for the age and the sex of the patient (Hoffbrand and Moss, 2012d). Polycythaemia vera is a clonal stem cell disorder, distinguished by an increase in the production of RBCs independent of the mechanisms that control erythropoiesis (Tefferi *et al.*, 2000; Choi *et al.*, 2015).

The disease is characterized by an increased haemoglobin count, decreased serum erythropoietin, hypercellular bone marrow with panmyelosis (Figure 1.2), the presence of the *JAK2* mutation in the BM and PB granulocytes in more than 95% of patients (Hoffbrand and Moss, 2012d; Choi *et al.*, 2015). Clinical features of PV are mainly due to hyperviscosity, hypermetabolism or hypervolaemia (Hoffbrand and Moss, 2012d). These include headaches, blurred vision, dyspnoea, night sweats, a plethoric appearance, splenomegaly in about 75% of patients, haemorrhage or thrombosis, hypertension and gout (Hoffbrand and Moss, 2012d).

The major diagnostic criteria are: 1) a haemoglobin count of >16.5 g/dL in men and >16.0 g/dL in women or a haematocrit of >49% in men and >48% in women or other signs of an increased red cell mass, 2) a BM biopsy showing hypercellularity for age with tri-lineage growth and 3) the presence of the *JAK2V617F* mutation or another functionally similar mutation (Arber *et al.*, 2016). The minor diagnostic criteria includes 1) a BM biopsy showing hypercellularity for age with panmyelosis with marked erythroid, megakaryocytic and granulocyte proliferation, 2) a serum erythropoietin level below that which is normal (normal range: 4.1-19.5 mU/mL), and 3) the formation of an endogenous erythroid colony *in vitro* (Arber *et al.*, 2016). The diagnosis of PV requires meeting all three major criteria, or the first two major criteria and the minor criterion (Arber *et al.*, 2016).

The prevalence of patients with PV differs greatly in various parts of the world with annual incidence rates ranging from 0.02 to 2.6 cases per 100 000 people (Kutti and Ridell, 2001). Polycythaemia vera has a similar incidence among males and females and occurs primarily in adults (Kutti and Ridell, 2001). The median survival of patients with PV is approximately 10 to 16 years (Barbui *et al.*, 2011; Hoffbrand and Moss, 2012d).

1.2.3. Essential thrombocythaemia

Essential thrombocythaemia was first described in 1934 and was known by the name haemorrhagic thrombocythaemia at the time (Epstein and Goedel, 1934; Ahmadzadeh *et al.*, 2015). Essential thrombocythaemia is a MPN that occurs due to an acquired genetic defect of haematopoietic stem cells that lead to clonal proliferation of the myelogenous blood cell lineage (Tefferi *et al.*, 2000; Gauthaman and Al-Sayes, 2015). Thrombocytosis is a characteristic feature of ET (Figure 1.2), which predisposes the patient to frequent haemorrhagic and thrombotic incidents, although approximately half of patients with ET are asymptomatic (Tefferi, 2001; Carobbio *et al.*, 2008; Gauthaman and Al-Sayes, 2015).

Most cases of ET are asymptomatic and are only suspected once a full blood count (FBC) is performed (Ahmadzadeh *et al.*, 2015). The increase in platelet number can be attributed to uncontrolled megakaryocyte proliferation and overproduction of platelets and causes occlusion of the micro vessels (arteries/veins) (Hoffbrand and Moss, 2012d; Gauthaman and Al-Sayes, 2015). The occlusion of the micro vessels can, in turn, lead to vascular disturbances such as headache, stroke, light-headedness, transient ischaemic attacks and visual disturbances (Hoffbrand and Moss, 2012d; Gauthaman and Al-Sayes, 2015).

The major diagnostic criteria are: 1) a persistent platelet count of $>450 \times 10^9/L$, 2) a BM biopsy indicating proliferation of the megakaryocyte lineage with increased numbers of enlarged, mature megakaryocytes containing hyperlobulated nuclei, 3) not meeting the WHO diagnostic criteria for PMF, PV, CML or any other myeloid neoplasm or myelodysplastic syndrome and, 4) presence of *JAK2*, *CALR*, or *MPL* mutation (Arber *et al.*, 2016). The minor diagnostic criterion involves the presence of a clonal marker or an absence of evidence for a reactive thrombocytosis (Arber *et al.*, 2016). The diagnosis of ET requires meeting all four major diagnostic criteria or the first three major criteria and the minor criterion (Arber *et al.*, 2016).

Essential thrombocythaemia has previously shown a tendency to spontaneously transform into PV, MF, myelodysplastic syndrome (MDS), and finally, acute leukaemia (Schafer, 2006; Carobbio *et al.*, 2008). In the United States of America (USA) general population, ET occurs in about 30/100 000 individuals and can occur at any age, but the median age of onset has been found to be between 60-70 years (Tefferi *et al.*, 2000; Gauthaman and Al-Sayes, 2015). Essential thrombocythaemia has a slight increase in incidence in females between the ages of 25 and 50 years, with a ratio of 2:1 (Tefferi *et al.*, 2000; Gauthaman and Al-Sayes, 2015). The complications associated with ET are often not fatal and the incidence of both transformation to acute leukaemia and thrombotic death is less than 5%, which is why patients with ET usually have a good prognosis (Tefferi, 2001).

1.2.4. Primary myelofibrosis/Myelofibrosis

Myelofibrosis is a clonal HSC disorder that is distinguished by marrow fibrosis, aberrant cytokine expression that causes serious systemic symptoms, anaemia, a leukoerythroblastic blood picture (Figure 1.2), extramedullary haematopoiesis and enlargement of the spleen (Thiele and Kvasnicka, 2009; Hobbs and Rampal, 2015).

In some patients, osteosclerosis occurs (Hoffbrand and Moss, 2012d). The bone marrow fibrosis is due to the hyperplasia of abnormal megakaryocytes and it is thought that fibroblasts are stimulated by platelet-derived growth factor and other cytokines that are produced by platelets and megakaryocytes (Hoffbrand and Moss, 2012d).

The disease can originate *de novo*, known as, primary myelofibrosis, or it can occur as end stage manifestation of PV (post-PV MF) and ET (post-ET MF), which is referred to as myelofibrosis or secondary myelofibrosis (Tefferi *et al.*, 2012; Hobbs and Rampal, 2015). Progression to acute leukaemia is observed in approximately 20% of patients (Cervantes *et al.*, 2012).

The major criteria are: 1) proliferation of megakaryocytes and atypical megakaryocytic cells accompanied by reticulin and/or collagen fibrosis, 2) not meeting the WHO criteria for MDS, PV, CML or another myelogenous neoplasm, 3) presence of *JAK2*, *CALR*, or *MPL* mutation or in the absence of these mutations, the presence of another clonal marker or no evidence of reactive marrow fibrosis (Tefferi, 2013). The minor criteria are: 1) anaemia not attributed to a comorbid condition 2) leucocytosis $\geq 11 \times 10^9/L$, 3) palpable splenomegaly, 4) increased serum LDH levels, and 5) leukoerythroblastosis (Arber *et al.*, 2016). The diagnosis of PMF is currently based on the 2016 WHO diagnostic criteria for MPNs and requires the fulfilment of all three of the major criteria and at least one of the minor criteria (Arber *et al.*, 2016).

Among the classic MPNs, PMF is the most aggressive and is associated with a significantly shorter life expectancy than PV or ET (Hobbs and Rampal, 2015). It is, however, the least common of the three classic MPNs (Hobbs and Rampal, 2015). According to data obtained in the USA, primary myelofibrosis occurs at a frequency of approximately 1.5/100 000 people and has an equal incidence among male and female patients (Singh, 2015).

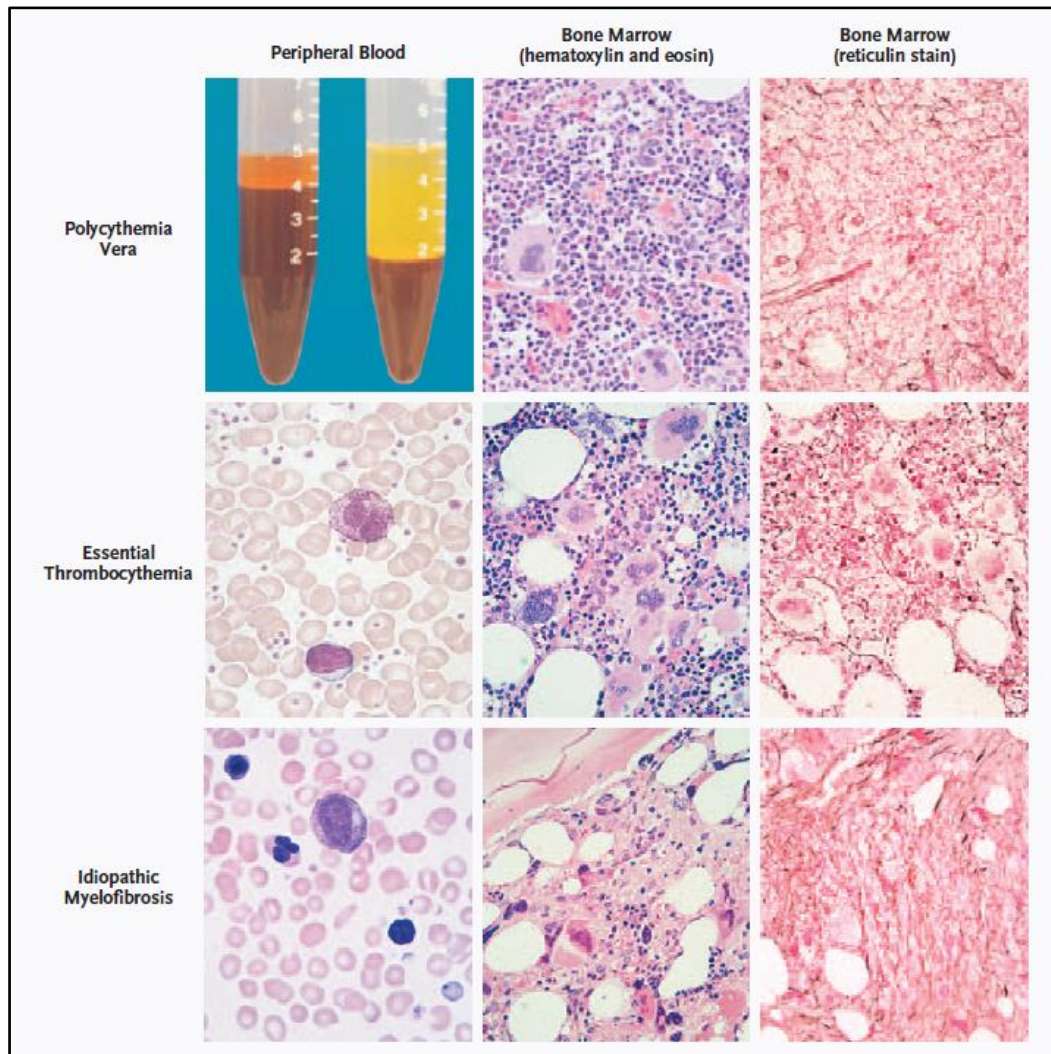


Figure 1.2: Laboratory features of polycythaemia vera, essential thrombocythaemia, and idiopathic myelofibrosis. Polycythaemia vera is characterized by an increased haematocrit in the peripheral blood (test tube on left); a hypercellular marrow with increased numbers of erythroid, megakaryocytic, and granulocytic precursor cells; and a variable increase in the number of reticulin fibres. Essential thrombocythaemia is characterized by an increase in the number of platelets in the peripheral blood and an increased number of megakaryocytes in the marrow, which tend to cluster together and have hyperbolated nuclei. Idiopathic myelofibrosis is characterized by the presence of immature red and white cells (a leukoerythroblastic blood film) and “teardrop” red cells, disordered cellular architecture, dysplastic megakaryocytes, new bone formation in the marrow, and the formation of collagen fibres (Campbell and Green, 2006)

1.3. Calreticulin

1.3.1. Introduction to Calreticulin

In 1974, researchers Ostwald and MacLennan were the first to isolate a protein, which showed a high affinity for binding calcium (Ca^{2+}), from the sarcoplasmic reticulum of rabbit muscle (Ostwald and MacLennan, 1974; Johnson *et al.*, 2001). The sarcoplasmic reticulum was prepared from the muscles of rabbits and was suspended at a protein concentration of 25 mg/ml buffer (Ostwald and MacLennan, 1974). The supernatant was removed and passed through a column of diethylaminoethyl-cellulose (DEAE-cellulose) which was then eluted using a buffer made up of 5 mM TRIS-HCl (Ostwald and MacLennan, 1974). The second eluted peak contained a high affinity calcium-binding protein (Ostwald and MacLennan, 1974). The protein was then concentrated and processed to obtain a purified high affinity calcium binding protein at a yield of 1 mg from 800 g of wet muscle tissue (Ostwald and MacLennan, 1974).

The protein was initially named high affinity calcium-binding protein (HACBP) but was later dubbed calreticulin (Ostwald and MacLennan, 1974; Smith and Koch, 1989). ‘Calreticulin’ was considered a more appropriate name for the protein as it more accurately reflected the established properties of the protein i.e. the ability to bind calcium and the location of the protein in the endoplasmic reticulum (ER) (Fliegel *et al.*, 1989; Smith and Koch, 1989).

In 1989, the calreticulin gene was cloned and the complementary DNA (cDNA) isolated simultaneously by the groups of Koch and Michalak (Fliegel *et al.*, 1989; Smith and Koch, 1989; Johnson *et al.*, 2001). In both Koch’s and Michalak’s studies, the complete amino acid sequence of calreticulin was gathered from the murine cDNA nucleotide sequence and was used to better understand the various components and functions of the protein (Fliegel *et al.*, 1989; Smith and Koch, 1989). Calreticulin was found to be the most abundant calcium-binding protein in all nucleated cells present in the lumen of the ER (Tarr *et al.*, 2010).

Among many different organisms, calreticulin amino acid identity is highly conserved, with over 90% similarity existing between human, rabbit, mouse and rat forms of the protein (Coppolino and Dedhar, 1998). The calreticulin gene has also been found in many other vertebrate and invertebrate species as well as in some higher plant species (Coppolino and Dedhar, 1998; Michalak *et al.*, 1999).

1.3.2. Structure of Calreticulin

In humans, the calreticulin gene is found on the short arm of chromosome 19, is approximately 3.6 kb long and it consists of nine exons (Ha and Kim, 2015; Luo and Yu, 2015). The 46-kDa calreticulin protein contains 400 amino acids, is encoded by a single gene and contains a cleavable signal-sequence at the start of the protein which has a $-NH_2$ group (N-terminal) and an ER retrieval signal consisting of the amino acids lysine (K; Lys), aspartic acid (D; Asp), glutamic acid (E; Glu) and leucine (L; Leucine) (KDEL) at the end of the protein which has a $-COOH$ group (C-terminal) (Lu *et al.*, 2015). Calreticulin consists of three structural domains: an N-domain, P-domain and a C-domain (Figure 1.3) (Lu *et al.*, 2015).

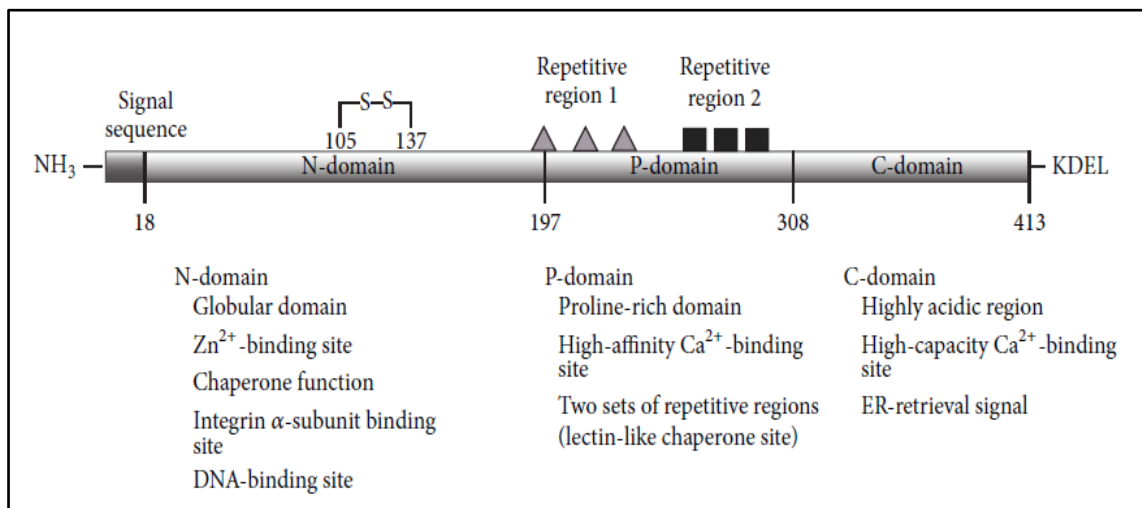


Figure 1.3: The protein structure and putative functions of calreticulin domains. The figure represents a schema of calreticulin. (Lu *et al.*, 2015)

The first third of calreticulin, the N-domain, which is so named for containing the N-terminal, has a globular structure with eight anti-parallel β -sheets (Coppolino and Dedhar, 1998; Lu *et al.*, 2015). The function of this domain is to interact with α -integrins and steroid receptors as well as interacting with the proline-rich P-domain to create the chaperone functions of calreticulin (Lu *et al.*, 2015).

The middle third is the P-domain which contains two sets of three repetitive regions (Lu *et al.*, 2015). These regions form the chaperone structures that are responsible for the protein-folding capability of calreticulin (Lu *et al.*, 2015).

The last third of the protein, the C-domain, so named for containing the C-terminal end of the protein, is highly negatively charged which makes it acidic in nature and is very important for Ca^{2+} -buffering reactions (Coppolino and Dedhar, 1998; Lu *et al.*, 2015). This region is able to bind Ca^{2+} in a low-affinity/high capacity Ca^{2+} binding site (Coppolino and Dedhar, 1998; Lu *et al.*, 2015).

1.3.3. Function of Calreticulin

Calreticulin is a Ca^{2+} binding chaperone that plays an important role in the regulation of calcium homeostasis and protein chaperoning inside the ER (Rotunno *et al.*, 2014; Ha and Kim, 2015). The ER is an important organelle for the synthesis, folding and transportation of various secretory proteins (Lu *et al.*, 2015). These duties are the responsibility of molecular chaperones which ensure that these functions are carried out correctly (Lu *et al.*, 2015). Calreticulin is one of these well-characterized protein chaperones in the ER and it is there that calreticulin operates with calnexin (an integral ER membrane protein) and a few other proteins as part of a quality control system that oversees the production of *N*-linked glycoproteins (Lu *et al.*, 2015; Nauseef, 2016).

Calreticulin acts as a chaperone in the ER for endogenous glycoproteins such as myeloperoxidase (MPO) which, in the normal state interacts transiently with calreticulin and calnexin (Nauseef, 2016). Inherited MPO deficiency is caused by mutant forms of MPO which exhibit aberrant interactions with ER chaperones such as calreticulin (Nauseef, 2016).

Calcium is mainly stored in the ER lumen and is a signalling molecule that influences developmental and cellular processes (Lu *et al.*, 2015). Since calreticulin contains two protein binding sites (one in the P-domain and one in the C-domain which contains the KDEL sequence), it is considered an intracellular regulator of Ca^{2+} homeostasis (Lu *et al.*, 2015). More than half of the Ca^{2+} stored inside the ER lumen associates with calreticulin and therefore increased levels of calreticulin may lead to raised intracellular Ca^{2+} storage (Lu *et al.*, 2015).

Endoplasmic reticulum-resident calreticulin is also involved in the regulation of loading of antigenic peptides into the major histocompatibility (MHC) class I and thus has a crucial role in the development and execution of immunity (Rotunno *et al.*, 2014; De Bruyn *et al.*, 2015; Ha and Kim, 2015). Outside the ER it is responsible for the regulation of integrin-mediated cell adhesion, programmed cell removal and immunological cell death (Rotunno *et al.*, 2014; Ha and Kim, 2015).

In the extracellular space, calreticulin has been found to have immunomodulatory effects (De Bruyn *et al.*, 2015). Chaperone molecules such as calreticulin, function as danger associated molecular pattern molecules (DAMPs) once they are outside the cell (De Bruyn *et al.*, 2015). This is evident, for instance, when calreticulin is found on the surface of dendritic cells where it acts as a receptor for autocrine-produced complement factor 1q which is upregulated for effective dendritic cell maturation (De Bruyn *et al.*, 2015). Calreticulin also acts to promote the differentiation of B-cells into antibody-secreting cells (De Bruyn *et al.*, 2015).

1.3.4. Pathogenesis of Calreticulin

In 2013, somatic mutations at exon 9 of *CALR*, the gene that encodes for calreticulin, were discovered through whole-exome sequencing and targeted re-sequencing in 50% to 70% and 33% to 58% of European and Asian patients, respectively, with ET and PMF who had neither mutated *JAK2* nor *MPL* (Klampfl *et al.*, 2013; Nangalia *et al.*, 2013; Ha and Kim, 2015). Mutations in the *CALR* gene have also been found in familial cases of ET (11%) and PMF (30%) (Assaf *et al.*, 2015).

Initially it was found that *JAK2*, *MPL* and *CALR* mutations occurred in a mutually exclusive manner (Tefferi *et al.*, 2014; Luo and Yu, 2015). However, there have been reports, for example, of both a PV and an ET patient that were double positive for *CALR* and *JAK2* mutations but researchers have argued that the *CALR* mutations in question did not cause a disease state as they did not cause a +1 shift in the reading frame of the protein (He *et al.*, 2015; Xu *et al.*, 2015). However, a recent study performed in the Free State (province of South Africa) disproved this theory, as a patient with a PV phenotype was discovered harbouring both a *JAK2* mutation and a homozygous *CALR* type 1 mutation which did in fact cause a +1 frameshift (De Kock, 2016). A mutation in *CALR* has also been demonstrated in a Ph-chromosome positive patient where it has been found to have preceded the *BCR-ABL1* mutation (Cabagnols *et al.*, 2015).

More than 50 different indels (insertions and deletions) have been found in exon 9 of the *CALR* gene (Pietra *et al.*, 2015). Among these mutations, more than 80% of *CALR* mutated patients possess one of only two mutation types: type 1 which is a 52-bp deletion (c.1092_1143del) and type 2 which is a 5-bp insertion (c.1154_1155insTTGTC) (Klampfl *et al.*, 2013; Tefferi *et al.*, 2014). The other indels can be grouped, based on their molecular characteristics, into the categories type 1-like or type 2-like (Guglielmelli *et al.*, 2015b). The majority of the calreticulin mutations are heterozygous in nature, with homozygous mutations occurring mostly as 5-bp insertions (Luo and Yu, 2015).

All mutant *CALR* proteins, that result from most of the mutations, share a novel amino acid sequence at the C-terminal (Klampfl *et al.*, 2013). This is due to the fact that these mutations cause a frameshift to alternative reading frame 1 and therefore a defective KDEL signal arises (Klampfl *et al.*, 2013). The mutant peptide contains many positively charged amino acids whereas the wild type is largely negatively charged and contains the endoplasmic reticulum-retention motif at the C-terminal end, which is lost in all mutant variants (Klampfl *et al.*, 2013). The mutant KDEL results in abnormal functioning of calreticulin as a chaperone, for example, even with normal MPO expression, the dysfunctional calreticulin does not productively process or package MPO (Nauseef, 2016; Theocharides *et al.*, 2016).

Variable presentations of disease occur depending on which *CALR* mutation is present (Klampfl *et al.*, 2013). This is due to the fact that the mutant protein may possess varying amounts of negatively charged amino acids (Klampfl *et al.*, 2013). Therefore, type 1/type 1-like and type 2/type 2-like mutations are phenotypically very different (Klampfl *et al.*, 2013; Guglielmelli *et al.*, 2015b; Pietra *et al.*, 2015).

Type 1/type 1-like mutations are associated with a significant thrombocytosis and an accelerated development to myelofibrosis-like disease with consequential splenomegaly, anaemia, and thrombocytopenia (Guglielmelli *et al.*, 2015b). Type 2/type 2-like mutations present with a much milder phenotype as less thrombocytosis is observed as well as a reduced disposition to evolve (Guglielmelli *et al.*, 2015b).

In patients with ET, those with type 2/type 2-like *CALR* mutations were younger, had a higher platelet count and lower risk for thrombosis at the time of diagnosis as compared to those with a type 1/type 1-like or *JAK2* mutation (Pietra *et al.*, 2015). It has been noted that the type 1 mutation occurs much more frequently in PMF than in ET (Klampfl *et al.*, 2013). Within the PMF patients, no compelling differences were found between those with type 1-like *CALR* mutations and those with type 2-like *CALR* mutations (Pietra *et al.*, 2015).

Within the MPNs, disease presentation also differs between the *JAK2*, *MPL* and *CALR* mutations. In patients with ET, those with a *CALR* mutation have a lower WBC count, a lower haemoglobin level and a higher platelet count at diagnosis as well as a lower risk of thrombosis than those patients who have mutated *JAK2* (Klampfl *et al.*, 2013; Ahmadzadeh *et al.*, 2015). These patients also have a better thrombosis free survival rate than those with a *JAK2* mutation (Ahmadzadeh *et al.*, 2015).

Patients with PMF who have mutated *CALR* are found to have a lower white-cell count and higher platelet count than patients with mutated *JAK2* (Klampfl *et al.*, 2013). Overall there is a marked difference in the survival rates among the three subgroups of patients with PMF i.e. patients with a somatic mutation of *CALR* have a longer overall survival than those with mutated *JAK2* or *MPL* (Klampfl *et al.*, 2013).

1.4. Treatment of the myeloproliferative neoplasms

It has been shown that overexpression of *CALR* mutations result in cytokine-independent proliferation of Ba/F3 cells and activation of STAT5 and that these effects can be suppressed *in vitro* by Fedratinib (Selleck Chemicals LLC, Houston, TX), a JAK2 inhibitor (Klampfl *et al.*, 2013). Palpable spleen length, as well as symptoms in two patients with myelofibrosis, has been reduced using Fedratinib (Passamonti *et al.*, 2014). These results have indicated that the inhibition of abnormal JAK/STAT signalling can be used as a therapeutic option for *CALR* mutated patients (Guglielmelli *et al.*, 2015a).

Before the commencement of therapy, information that is used in the risk stratification of MPN patients must be collected (Barbui *et al.*, 2011). This includes information such as thrombotic history and age for patients with PV; thrombotic history, age, and platelet count for patients with ET; and age, blast count, white blood cell (WBC) count, haemoglobin and constitutional symptoms for PMF (Barbui *et al.*, 2011). Current therapy in PV and ET is aimed at lowering the risk of thrombosis and alleviating symptoms (Barbui *et al.*, 2011; Tefferi and Pardanani, 2015).

Polycythaemia vera patients should be managed with phlebotomy to ensure that the haematocrit is maintained at less than 45% (Barbui *et al.*, 2011; Tefferi, 2015). Low dose aspirin (81 mg/day) should be included in the antithrombotic treatment of PV as well as ET (Barbui *et al.*, 2011; Tefferi and Pardanani, 2015).

Treatment with aspirin has also been shown to be effective in reducing microvascular symptoms such as headaches and erythromelalgia (Tefferi and Pardanani, 2015). In high risk PV or ET patients, cytoreductive therapy is indicated (Barbui *et al.*, 2011; Tefferi and Pardanani, 2015). This includes patients with a low tolerance of phlebotomy or a continual phlebotomy requirement, severe disease related symptoms, platelet counts greater than $1,500 \times 10^9/L$, progressive or symptomatic enlargement of the spleen, and continuous leucocytosis (Barbui *et al.*, 2011).

The first line cytoreductive therapy at any age is either interferon alpha (IFN- α) (Intron®A, Merck, Darmstadt, Germany) or hydroxyuria (Hydrea, Bristol-Myers Squibb Company, USA) although hydroxyuria should be used with caution in younger patients (age < 40 years) (Barbui *et al.*, 2011; Harrison *et al.*, 2015). In PMF/MF patients, current drug therapy is not curative and is very unlikely to prolong survival (Tefferi, 2015).

Allogeneic stem cell transplant (ASCT) seems to be the only treatment that is able to cure patients or prolong their lives and is only recommended in very high risk patients as transplant related death or severe morbidity occurs in more than 50% of transplant recipients (Tefferi, 2015; Tefferi and Pardanani, 2015). In intermediate risk patients ASCT or investigational drug therapy and observation are acceptable treatment approaches (Tefferi, 2015; Tefferi and Pardanani, 2015).

1.5. Current *CALR* mutation detection methods

1.5.1. Assays involving conventional polymerase chain reaction

Conventional PCR is used in many cases, to amplify the DNA region of interest before the detection technique itself is performed. Polymerase chain reaction is therefore not the final step when looking for mutations but rather a means to an end. A PCR step is required when performing techniques such as fragment analysis, gel electrophoresis and Sanger sequencing.

A study published in 2015, evaluated the use of fragment analysis PCR to detect *CALR* mutations in exon 9 (Jones *et al.*, 2015). Fragment analysis PCR requires that a size difference in labelled PCR products be visualised using capillary gel electrophoresis (Jones *et al.*, 2015). This method uses forward primers that are labelled by fluorescent dyes such as 6-carboxyfluorescein (6-FAM) or 6-carboxyfluorescein hexachloride (HEX) (Jones *et al.*, 2015). According to a number of studies, fragment analysis has the lowest monetary and time costs, is the easiest detection method to establish in laboratories and it provides reasonable sensitivity for *CALR* mutation detection (Jones *et al.*, 2015; Maier *et al.*, 2015; Park *et al.*, 2015).

Fragment analysis has been validated as a method for diagnostic purposes in the United States of America (Maier *et al.*, 2015). A study performed in 2015 compared fragment analysis PCR, high resolution melt (HRM) analysis and Sanger sequencing and found that the sensitivity and specificity of fragment analysis PCR is 98.2% and 100%, respectively (Park *et al.*, 2015). It cannot, however, distinguish between the wild type sequence of calreticulin and any point mutation (Lim *et al.*, 2015).

A recently published article described the use of a conventional PCR followed by agarose gel electrophoresis that was developed to screen for *CALR* type 1 and type 2 mutations before using Sanger sequencing to confirm the results (Jeong *et al.*, 2016). The researchers used a method whereby two forward primers and one reverse primer was added to a reaction mix and a PCR was performed (Jeong *et al.*, 2016). Depending on the presence of the wild type, type 1 or type 2 mutations the length of the fragments would be 357-bp, 302-bp or 272-bp respectively (Jeong *et al.*, 2016).

1.5.2. Assays involving sequencing

The initial discovery of the calreticulin exon 9 mutations occurred in 2013 when the groups of Klampf *et al.*, (2013) and Nangalia *et al.*, (2013) simultaneously performed whole exome sequencing, a next generation sequencing technique, in patients with myeloproliferative neoplasms. Targeted resequencing was then performed on genomic regions of interest that had been amplified by PCR and these sequencing products were used to screen for insertions and deletions within *CALR* exon 9 (Klampfl *et al.*, 2013; Nangalia *et al.*, 2013).

In the majority of published studies about mutation analysis of calreticulin, the tests are done using PCR followed by Sanger sequencing (Bilbao-Sieyro *et al.*, 2014). Sequencing is considered to be the reference method when it comes to the detection and screening of *CALR* mutations and is often used as a control assay when other techniques are evaluated for the detection of mutations.

As previously mentioned, a study performed in 2015 compared fragment analysis PCR, HRM and Sanger sequencing and found that the sensitivity and specificity of Sanger sequencing to be 89.3% and 100%, respectively (Park *et al.*, 2015). The study previously mentioned and conducted by Jones *et al.* (2015) found next generation sequencing (NGS) to be the most robust technique and have the lowest limit of detection (Lod).

However, it is more expensive and time consuming when compared to other techniques such as fragment analysis PCR and HRM (Park *et al.*, 2015). Due to the expensive and time consuming nature of Sanger sequencing, it has been proposed to serve as a confirmation of *CALR* mutation presence and type, after initial screening tests have been performed (Park *et al.*, 2015).

1.5.3. Assays involving real-time PCR

A study performed in 2014 evaluated the use of a real-time PCR (qPCR) assay using TaqMan[®] probes to detect and differentiate between type 1 and type 2 *CALR* mutations (Chi *et al.*, 2015). The assay used a common reverse primer and a pair of different forward primers; one specific for the 52-bp deletion of the type 1 mutation and the other specific for the 5-bp insertion of the type 2 mutation (Chi *et al.*, 2015). The samples were all tested multiple times and it was found that the assay showed complete differentiation between type 1, type 2 and wild type samples (Chi *et al.*, 2015). It was also determined that this assay could be used for minimal residual disease (MRD) monitoring (Chi *et al.*, 2015).

Another recent study compared the following methods of detecting the *CALR* mutations in MPN patients: Sanger sequencing, fragment analysis PCR, high resolution melt (HRM) analysis, and targeted next generation sequencing (Jones *et al.*, 2015). The study found that the ability to quantitate *CALR* mutations using qPCR techniques would, in the future, allow the monitoring of molecular responses to treatment similar to what is being done currently with the treatment of *JAK2V617F* (Jones *et al.*, 2015). The researchers also found that each assay was able to detect the range of *CALR* mutations that were originally detected by Sanger sequencing (Jones *et al.*, 2015).

High resolution melt analysis is a closed tube technique that detects genetic polymorphisms and mutations by measuring the change in a DNA duplex while melting (Lim *et al.*, 2015). High resolution melt analysis is a well-established method for detecting mutations and has, for example, shown high sensitivity and specificity for the detection of *JAK2* mutations in MPN patients (Lim *et al.*, 2015). Another study that evaluated the use of a HRM analysis showed that there were distinct HRM patterns to be observed between the type 1 and type 2 mutations and that the HRM used displayed no false positives and mutants could be detected in up to a 3.13% dilution (Bilbao-Sieyro *et al.*, 2014).

As previously mentioned, a comparison of three techniques was tested and it was found that the sensitivity and specificity of HRM was 96.4% and 96.3% respectively (Park *et al.*, 2015). This technique has proven to be a fast, reliable, economical and high-throughput screening method for the detection of *CALR* mutation status. Sanger sequencing is; however, necessary to correctly categorize the mutants seeing as, for example, type 2 mutations are not the only 5-bp insertions that can occur (Bilbao-Sieyro *et al.*, 2014).

1.5.4. Assays involving other methods

In 2014, an article published by Vannucchi *et al.*, (2014) evaluated the use of calreticulin specific immunostaining as a diagnostic tool for the detection of all *CALR* mutations (Figure 1.4). As previously discussed, all pathogenic *CALR* mutations cause a +1 frameshift in exon 9 of the *CALR* gene creating a unique alternative reading frame that results in a novel C-terminus of approximately 36 amino acids (Klampfl *et al.*, 2013; Vannucchi *et al.*, 2014). The researchers showed that an antibody that was specifically raised against a peptide located in the novel C-terminus of mutated *CALR*, can be used to stain mutated cells in BM biopsies of ET and PMF patients that carry all mutations that cause a +1 frameshift in the *CALR* gene (Vannucchi *et al.*, 2014).

Myeloproliferative neoplasm patients with the *JAK2V617F* or *MPLW515* mutations as well as those patients, who were triple negative for all three common MPN mutations, showed no staining with the developed antibody (Vannucchi *et al.*, 2014). The three types of *CALR* mutations all showed positive staining with the developed antibody, indicating the presence of a *CALR* mutation (Vannucchi *et al.*, 2014).

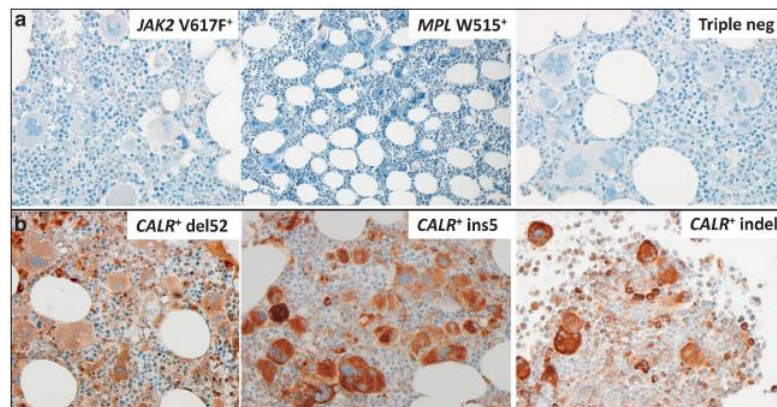


Figure 1.4: Immunostaining of bone marrow biopsies with the anti-mutated *CALR* antibody. Representative sections from *CALR*-unmutated ET/PMF patients (*JAK2V617F* mutated, *MPLW515L* mutated and triple-negative mutation) and from *CALR*-mutated patients (*CALRdel52*, *CALR ins* and *CALR indel*) are shown in panel a and panel b, respectively. Pictures were taken with a LEICA DM LS2 microscope using a N-Plan x 40/0.65 objective. The number of immunostained megakaryocytes over total number of morphologically recognizable megakaryocytes was calculated by counting at least 100 megakaryocytes/slide from 10 patients with ET and 10 patients with PMF (n=2 for the *CALR indel*), and expressed as per cent of total megakaryocytes (c); as there was no significant difference between the two groups, all individual data were pooled (Vannucchi *et al.*, 2014)

1.6. Conclusion

From the literature it is clear that simple, efficient, cost effective and sensitive mutation testing for *CALR* is a necessity in all diagnostic laboratories aiming to fill the current diagnostic gap regarding the diagnosis of MPNs. This study aimed to evaluate the use of PCR and qPCR due to the popularity and widespread use of these techniques as well as the lack of a qPCR technique in the South African sector.

A PCR and qPCR for the detection of the type 1 and 2 mutations in *CALR* was deemed most beneficial as these techniques are most readily available in the context of the study setting as well as in most diagnostic laboratories in South Africa. The objectives of this study were:

- To design primers for the detection of the *CALR* type 1 and type 2 mutations using a conventional PCR.
- To compare the results of the in-house conventional PCR with a commercially available conventional PCR to compare the accuracy and pricing between the two methods.
- To determine the nucleotide sequence of the calreticulin genes of MPN patients, in parallel to PCR, to determine whether a mutation in the *CALR* gene is present and whether it is type 1 or type 2.
- To optimize and evaluate the use of a qPCR assay using SYBR Green to detect the *CALR* type 1 and type 2 mutations.
- To design fluorescently labelled hydrolysis probes, to optimize and to evaluate the use of qPCR using these hydrolysis probes to detect the *CALR* type 1 and type 2 mutations.

References

Ahmadzadeh, A, Shirzad, R, Golchin, A, S, S, Shahjahani, M, Seghatoleslami, M and Saki, N 2015. Calreticulin and JAK2^{V617F} Mutations in Essential Thrombocythemia and Their Potential Role in Diagnostics and Prognosis. *Cellular and Molecular Medicine*, 1, 1-11.

Arber, D, Orazi, A, Hasserjian, R, Thiele, J, Borowitz, M, Le Beau, M, Bloomfield, C, Cazzola, M and Vardiman, J 2016. The 2016 revision to the World Health Organization (WHO) classification of myeloid neoplasms and acute leukemia. *Blood*, 127, 2391-2405.

Assaf, CA, Van-Obbergh, F, Billiet, J, Lierman, E, Devos, T, Graux, C, Hervent, AS, Emmerechts, J, Tousseyn, T, De-Paepe, P, Papadopoulos, P, Michaux, L and Vandenberghe, P 2015. Analysis of Phenotype and Outcome in Essential Thrombocythemia with CALR or JAK2 mutations. *Haematologica*, 100.

Bain, BJ, Bates, I, Laffan, MA and Lewis, SM 2012. Molecular and cytogenetic analysis. In: Houston, M. (ed.) *Dacie and Lewis Practical Haematology*. Churchill Livingstone Elsevier, 139-174.

Barbui, T, Barosi, G, Birgegard, G, Cervantes, F, Finazzi, G, Griesshammer, M, Harrison, C, Hasselbalch, HC, Hehlmann, R, Hoffman, R and Kiladjian, J 2011. Philadelphia-Negative Classical Myeloproliferative Neoplasms: Critical Concepts and Management Recommendations From European LeukemiaNet. *Journal of Clinical Oncology*, 29, 761-770.

Béné, MC, Grimwade, D, Haferlach, C, Haferlach, T and Zini, G 2015. Leukemia diagnosis: today and tomorrow. *European Journal of Haematology*, 10, 1-9.

Bilbao-Sieyro, C, Santana, G, Moreno, M, Torres, L, Santana-Lopez, G, Rodriguez-Medina, C, Perera, M, Bellosillo, B, De la Iglesia, S, Molero, T and Gomez-Casares, M 2014. High Resolution Melting Analysis: A Rapid and Accurate Method to Detect CALR Mutations. *PLoS One*, 9, 1-5.

Cabagnols, X, Cayuela, JM and Vainchenker, W 2015. A CALR Mutation Preceding BCR-ABL1 in an Atypical Myeloproliferative Neoplasm. *New England Journal of Medicine*, 372, 688-690.

Campbell, PJ and Green, AR 2006. The Myeloproliferative Disorders. *New England Journal of Medicine*, 355, 2452-2466.

Carobbio, A, Antonioli, E, Guglielmelli, P, Vannucchi, AM, Delaini, F, Guerini, V, Finazzi, G, Rambaldi, A and Barbui, T 2008. Leukocytosis and Risk Stratification Assessment in Essential Thrombocythemia. *Journal of Clinical Oncology*, 26, 2732-2736.

Cervantes, F, Dupriez, B, Passamonti, F, Vannucchi, AM, Morra, E, Reilly, JT, Demory, J-L, Rumi, E, Guglielmelli, P, Roncoroni, E, Tefferi, A and Pereira, A 2012. Improving Survival Trends in Primary Myelofibrosis: An International Study. *Journal of Clinical Oncology*, 30, 2981-2987.

Chi, J and Costeas, P 2015. The Evolution of Genetics Techniques for Leukemia Diagnosis. *Advanced Techniques in Biology & Medicine*, 3, 1-2.

Chi, J, Manoloukos, M, Pierides, C, Nicolaidou, V, Nicolaou, K, Kleopa, M, Vassiliou, G and Costeas, P 2015. *Calreticulin* mutations in myeloproliferative neoplasms and new methodology for their detection and monitoring. *Annals of Hematology*, 94, 399-408.

Choi, CW, Bang, S-M, Jang, S, Jung, CW, Kim, H-J, Kim, HY, Kim, S-J, Kim, Y-K, Park, J and Won, J-H 2015. Guidelines for the management of myeloproliferative neoplasms. *Korean Journal of Internal Medicine*, 30, 771-788.

Coppolino, MG and Dedhar, S 1998. Molecules in focus Calreticulin. *International Journal of Biochemistry and Cell Biology*, 30, 553-558.

De Bruyn, M, Wiersma, VR, Helfrich, W, Eggleton, P and Bremer, E 2015. The ever-expanding immunomodulatory role of calreticulin in cancer immunity. *Frontiers in Oncology*, 5, 1-6.

De Kock, A. 2016. *RE: Screening for calreticulin mutations in a Free State cohort suspected of having a myeloproliferative neoplasm*. Type to Prinsloo, A.

Epstein, E and Goedel, A 1934. Hemorrhagic thrombocythemia with a cascular, sclerotic spleen. *Virchows Archiv für Pathologische Anatomie und Physiologie und für Klinische Medizin*, 293, 233-248.

Fliegel, L, Burns, K, MacLennan, DH, Reithmeier, RA and Michalak, M 1989. Molecular Cloning of the High Affinity Calcium-binding Protein (Calreticulin) of Skeletal Muscle Sarcoplasmic Reticulum. *Journal of Biological Chemistry*, 264, 21522-21528.

Gauthaman, K and Al-Sayes, FM 2015. Essential Thrombocythemia: Current Molecular and Therapeutic Insights. *Saudi Journal of Internal Medicine*, 5, 5-10.

Guglielmelli, P, Rotunno, G, Bogani, C, Mannarelli, C, Giunti, L, Provenzano, A, Giglio, S, Squires, M and Stalbovskay, V 2015a. Ruxolitinib is an effective treatment for CALR-positive patients with myelofibrosis. *British Journal of Haematology*, 1-3.

Guglielmelli, P, Rotunno, G, Fanelli, T, Pacilli, A, Brogi, G, Calabresi, L, Pancrazzi, A and Vannucchi, AM 2015b. Validation of the differential prognostic impact of type 1/type 1-like versus type 2/type 2-like *CALR* mutations in myelofibrosis. *Blood Cancer Journal*, 5, 1-3.

Ha, JS and Kim, YK 2015. Calreticulin Exon 9 Mutations in Myeloproliferative Neoplasms. *Annals of Laboratory Medicine*, 35, 22-27.

Harrison, CN, Loman, DPM, Francis, YA, Woodley, C, Provis, L and Radia, DH 2015. How We Treat Myeloproliferative Neoplasms. *Clinical Lymphoma, Myeloma & Leukemia*, 15, 19-26.

He, R, Hanson, CA, Oliveira, JL, Pardanani, A, Reichard, KK and Viswanatha, DS 2015. Not all *CALR* mutations are created equal. *Leukemia & Lymphoma*, 56, 2482-2483.

Herbst, MC 2015. Fact Sheet on Polycythaemia Vera. In: Africa, C. a. O. S. (ed.). South Africa: CANSA.

Hobbs, GS and Rampal, RK 2015. Clinical and molecular genetic characterization of myelofibrosis. *Current Opinion in Hematology*, 22, 177-183.

Hoffbrand, AV and Moss, PA 2012a. Chronic myeloid leukaemia. *Essential Haematology*. 6th ed. West Sussex, UK: Wiley-Blackwell Publishing Ltd, 191-199.

Hoffbrand, AV and Moss, PA 2012b. Haematopoiesis. *Essential Haematology*. 6th ed. West Sussex, UK: Wiley-Blackwell Publishing Ltd, 1-14.

Hoffbrand, AV and Moss, PA 2012c. Haematological malignancy: aetiology and genetics. *Essential Haematology*. 6th ed. West Sussex, UK: Wiley-Blackwell Publishing Ltd, 150-165.

Hoffbrand, AV and Moss, PA 2012d. The non-leukaemic myeloproliferative neoplasms. *Essential Haematology*. 6th ed. West Sussex, UK: Wiley-Blackwell Publishing Ltd, 200-213.

Holyoake, TL, Jiang, X, Drummond, MW, Eaves, AC and Eaves, CJ 2002. Elucidating critical mechanisms of deregulated stem cell turnover in the chronic phase of chronic myeloid leukemia. *Leukemia*, 16, 549-558.

Ipek, Y-H, Fehmi, H and Deniz, S 2015. Pathogenesis and Mutations of Myeloproliferative Neoplasms: An Overview. *British Journal of Medical and Medical Research*, 9, 1-24.

Jeong, JH, Lee, HT, Seo, JY, Seo, YH, Kim, KH, Kim, MJ, Lee, JH, Park, J, Hong, J, Park, PW and Ahn, JY 2016. Screening PCR Versus Sanger Sequencing: Detection of CALR Mutations in Patients With Thrombocytosis. *Annals of Laboratory Medicine*, 36, 291-299.

Johnson, S, Michalak, M, Opas, M and Eggleton, P 2001. The ins and outs of calreticulin: from the ER lumen to the extracellular space. *Trends in Cell Biology*, 11, 122-129.

Jones, AV, Ward, D, Lyon, M, Leung, W, Callaway, A, Chase, A, Dent, CL, White, HE, Drexler, HG, Nangalia, J, Mattocks, C and Cross, NCP 2015. Evaluation of methods to detect CALR mutations in myeloproliferative neoplasms. *Leukemia Research*, 39, 82-87.

Jordan, CT, Guzman, ML and Noble, M 2006. Cancer Stem Cells. *New England Journal of Medicine*, 355, 1253-1261.

Kilpivaara, O and Levine, RL 2008. JAK2 and MPL mutations in myeloproliferative neoplasms: discovery and science. *Leukemia*, 22, 1813-1817.

Klampfl, T, Gisslinger, H, Harutyunyan, AS, Nivarthi, H, Rumi, E, Milosevic, JD, Them, NCC, Berg, T and Gisslinger, B 2013. Somatic Mutations of Calreticulin in Myeloproliferative Neoplasms. *New England Journal of Medicine*, 369, 2379-2390.

Klco, JM, Vij, R, Kriesel, FH, Hassan, A and Frater, JL 2010. Molecular Pathology of Myeloproliferative Neoplasms. *American Journal of Clinical Pathology*, 133, 602-615.

Kutti, J and Ridell, B 2001. Epidemiology of the myeloproliferative disorders: essential thrombocythaemia, polycythaemia vera and idiopathic myelofibrosis. *Pathologie Biologie*, 49, 164-166.

Langabeer, SE, Andrikovics, H, Asp, J, Bellosillo, B, Carillo, S, Haslam, K, Kjaer, L, Lippert, E, Mansier, O, Leibundgut, EO, Percy, MJ, Porret, N, Palmqvist, L, Schwarz, J, McMullin, MF, Schnittger, S, Pallisgaard, N and Hermouet, S 2015. Molecular diagnostics of myeloproliferative neoplasms. *European Journal of Haematology*, 95, 270-279.

Levine, RL and Gilliland, DG 2008. Myeloproliferative disorders. *Blood*, 112, 2190-2198.

Levine, RL, Pardanani, A, Tefferi, A and Gilliland, DG 2007. Role of JAK2 in the pathogenesis and therapy of myeloproliferative disorders. *Nature Reviews Cancer*, 7, 673-683.

Li, X-L, Xue, Y, Yang, Y-J, Zhang, C-X, Wang, Y, Duan, Y-Y, Meng, Y-N and Fu, J 2015. Hematopoietic Stem Cells: Cancer Involvement and Myeloid Leukemia. *European Review for Medical and Pharmacological Sciences*, 19, 1829-1836.

Lim, K-H, Lin, H-C, Chen, CG-S, Wang, W-T, Chang, Y-C, Chiang, Y-H, Lin, C-S, Su, N-W, Su, Y-W, Lin, J, Chang, Y-F, Chang, M-C, Hsieh, R-K, Kuo, Y-Y and Chou, W-C 2015. Rapid and sensitive detection of *CALR* exon 9 mutations using high-resolution melting analysis. *Clinica Chimica Acta*, 440, 133-139.

Lu, Y-C, Weng, W-C and Lee, H 2015. Functional Roles of Calreticulin in Cancer Biology. *Biomed Research International*, 2015, 1-9.

Luo, W and Yu, Z 2015. Calreticulin (*CALR*) mutation in myeloproliferative neoplasms (MPNs). *Stem Cell Investigation*, 2, 1-10.

Maier, CL, Fisher, KE, Jones, HH, Hill, CE, Mann, KP and Zhang, L 2015. Development and Validation of *CALR* Mutation Testing for Clinical Diagnosis. *American Journal of Clinical Pathology*, 144, 738-745.

Malherbe, JA, Fuller, KA, Arshad, A, Nangalia, J, Romeo, G, Hall, SL, Meehan, KS, Guo, B, Howman, R and Erber, WN 2015. Megakaryocytic hyperplasia in myeloproliferative neoplasms is driven by disordered proliferative, apoptotic and epigenetic mechanisms. *Journal of Clinical Oncology*, 0, 1-9.

Mehta, J, Wnag, H, Iqbal, SU and Mesa, R 2014. Epidemiology of myeloproliferative neoplasms in the United States. *Leukemia & Lymphoma*, 55, 595-600.

Michalak, M, Corbett, EF, Mesaeli, N, Nakamura, K and Opas, M 1999. Calreticulin: one protein, one gene, many functions. *Biochemical Journal*, 344, 281-292.

Nangalia, J, Massie, CE, Baxter, EJ, Nice, FL, Gundem, G, Wedge, DC, Avezov, E, Li, J, Kollman, K, Kent, DG, Aziz, A, Godfrey, AL, Hinton, J, Martincorena, I, Van Loo, P, Jones, AV, Guglielmelli, P, Tarpey, P and Harding, HP 2013. Somatic *CALR* Mutations in Myeloproliferative Neoplasms with Nonmutated JAK 2. *New England Journal of Medicine*, 369, 2391-2405.

Nauseef, WM 2016. In the beginning and at the end: calreticulin. *Blood*, 127, 3113-3114.

Nowell, P and Hungerford, D 1960a. A minute chromosome in human chronic granulocytic leukemia. *Science*, 132, 1497.

Nowell, PC and Hungerford, DA 1960b. Chromosome studies on normal and leukemic human leukocytes. *Journal of the National Cancer Institute*, 25, 85-109.

Ostwald, TJ and MacLennan, DH 1974. Isolation of a high affinity calcium-binding protein from sarcoplasmic reticulum. *Journal of Biological Chemistry*, 249, 974-979.

Park, J-H, Sevin, M, Ramla, S, Truffot, A, Verrier, T, Bouchot, D, Courtois, M, Bas, M, Benali, S, Bailly, F, Favre, B, Guy, J, Martin, L, Maynadié, M, Carillo, S and Girodon, F 2015. Calreticulin Mutations in Myeloproliferative Neoplasms: Comparison of Three Diagnostic Methods. *PLoS One*, 10, 1-7.

Passamonti, F, Caramazza, D and Maffioli, M 2014. JAK Inhibitor in *CALR*-Mutant Myelofibrosis. *New England Journal of Medicine*, 370, 1168-1169.

Pietra, D, Rumi, E, Ferretti, VV, Di Buduo, CA, Milanesi, C, Cavalloni, C, Sant'Antonio, E, Abbonante, V, Moccia, F, Casetti, IC, Bellini, M, Renna, MC, Rancoroni, E, Fugazza, E, Astori, C, Boveri, E, Rosti, V, Barosi, G, Balduini, A and Cazzola, M 2015. Differential clinical effects of different mutation subtypes in *CALR*-mutant myeloproliferative neoplasms. *Leukemia*, 1-8.

Rotunno, G, Mannarelli, C, Guglielmelli, P, Pacilli, A, Pancrazzi, A, Pieri, L, Fanelli, T, Bosi, A and Vannucchi, AM 2014. Impact of calreticulin mutations on clinical and haematological phenotype and outcome in essential thrombocythemia. *Blood*, 123, 1552-1555.

Santos, FPS and Verstovsek, S 2012. Breakthroughs in myeloproliferative neoplasms. *Hematology*, 17, 55-58.

Schafer, AI 2006. Molecular basis of the diagnosis and treatment of polycythemia vera and essential thrombocythemia. *Blood*, 107, 4214-4222.

Schmaier, AH and Lazarus, HA 2012. Myeloproliferative Neoplasms and Myelodysplastic Syndromes. *Concise Guide to Hematology*. West Sussex, UK: Blackwell Publishing Ltd., 220-234.

Scott, LM 2011. The JAK2 exon 12 mutations: A comprehensive review. *American Journal of Hematology*, 86, 668-676.

Singh, NR 2015. Genomic diversity in myeloproliferative neoplasms: focus on myelofibrosis. *Translational Pediatrics*, 4, 107-115.

Skoda, RC, Duek, A and Grisouard, J 2015. Pathogenesis of myeloproliferative neoplasms. *Experimental Hematology*, 43, 599-608.

Smith, MJ and Koch, GLE 1989. Multiple zones in the sequence of calreticulin (CRP55, calregulin, HACBP), a major calcium binding ER/SR protein. *EMBO Journal*, 8, 3581-3586.

Szilvassy, SJ 2003. The Biology of Hematopoietic Stem Cells. *Archives of Medical Research* 34, 446-460.

Tarr, JM, Young, P, Morse, R, Shaw, DJ, Haigh, R, Petrov, PG, Johnson, SJ, Winyard, PG and Eggleton, P 2010. A Mechanism of Release of Calreticulin from Cells During Apoptosis. *Journal of Molecular Biology*, 401, 799-812.

Tefferi, A 2001. Recent progress in the pathogenesis and management of essential thrombocythemia. *Leukemia Research*, 25, 369-377.

Tefferi, A 2010. Novel mutations and their functional and clinical relevance in myeloproliferative neoplasms: *JAK2*, *MPL*, *TET2*, *ASXL1*, *CBL*, *IDH* and *IKZF1*. *Leukemia*, 24, 1128-1138.

Tefferi, A 2013. Primary myelofibrosis: 2013 update on diagnosis, risk-stratification, and management. *American Journal of Hematology*, 88, 142-150.

Tefferi, A 2015. Myeloproliferative Neoplasms: A Decade of Discoveries and Treatment Advances. *American Journal of Hematology*, n/a-n/a.

Tefferi, A, Lasho, TL, Jimma, T, Finke, CM, Gangat, N, Vaidya, R, Begna, KH, Al-Kali, A, Ketterling, RP, Hanson, CA and Pardanani, A 2012. One Thousand Patients With Primary Myelofibrosis: The Mayo Clinic Experience. *Mayo Clinic Proceedings*, 87, 25-33.

Tefferi, A and Pardanani, A 2015. Myeloproliferative Neoplasms: A Contemporary Review. *JAMA Onc*, 1, 97-105.

Tefferi, A, Solberg, LA and Silverstein, MN 2000. A Clinical Update in Polycythemia Vera and Essential Thrombocythemia. *American Journal of Medicine*, 109, 141-149.

Tefferi, A and Vardiman, JW 2008. Classification and diagnosis of myeloproliferative neoplasms: The 2008 World Health Organization criteria and point-of-care diagnostic algorithms. *Leukemia*, 22, 14-22.

Tefferi, A, Wassie, EA, Guglielmelli, P, Gangat, N, Belachew, AA, Lasho, TI, Finke, C, Ketterling, RP, Hanson, CA, Pardanani, A, Wolanskyj, AP, Maffioli, M, Casalone, R, Pacilli, A, Vannucchi, AM and Passamonti, F 2014. Type 1 versus Type 2 calreticulin mutations in essential thrombocythemia: A collaborative study of 1027 patients. *American Journal of Hematology*, 89, 121-124.

Theocharides, APA, Lundberg, P, Lakkaraju, AKK, Lysenko, V, Myburgh, R, Aguzzi, A, Skoda, RC and Manz, MG 2016. Homozygous *calreticulin* mutations in patients with myelofibrosis lead to acquired myeloperoxidase deficiency. *Blood*, 127, 3253-3259.

Thiele, J and Kvasnicka, HM 2009. The 2008 WHO Diagnostic Criteria for Polycythemia Vera, Essential Thrombocythemia, and Primary Myelofibrosis. *Current Hematologic Malignancy Reports*, 4, 33-40.

Till, JE and McCulloch, EA 1961. A Direct Measurement of the Radiation Sensitivity of Normal Mouse Bone Marrow Cells. *Radiation Research*, 14, 213-222.

Turgeon, ML 2012. Myeloproliferative Neoplasms. *Clinical Haematology: Theory and Procedures*. 5th ed. Philadelphia PA: Lippincott Williams and Wilkins, 361-385.

Van der Walt, JD 2015. An update on *BCR-ABL1*-negative myeloproliferative neoplasms. *Diagnostic Pathology*, 21, 190-197.

Vannucchi, AM, Rotunno, G, Bartalucci, N, Raugei, G, Carrai, V, Balliu, M, Mannarelli, C, Pacilli, A, Calabresi, L, Fjerza, R, Pieri, L, Bosi, A, Manfredini, R and Guglielmelli, P 2014. Calreticulin mutation-specific immunostaining in

myeloproliferative neoplasms: pathogenic insight and diagnostic value. *Leukemia*, 28, 1811-1818.

Vardiman, JW, Harris, NL and Brunning, RD 2002. The World Health Organization (WHO) classification of the myeloid neoplasms. *Blood*, 100.

Visser, O, Trama, A, Maynadié, M, Stiller, C, Marcos-Gragera, R, Angelis, RD, Mallone, S, Tereanu, C, Allemani, C, Ricardi, U and Schouten, HC 2012. Incidence, survival and prevalence of myeloid malignancies in Europe. *European Journal of Cancer*, 48, 3257-3266.

Xu, N, Ding, L, Yin, C, Zhou, X, Li, L, Li, Y, Lu, Q and Lu, X-L 2015. A report on the co-occurrence of JAK2V617F and CALR mutations in myeloproliferative neoplasm patients. *Annals of Hematology*, 94, 865-867.

Zeeb, H and Blettner, M 1998. Adult leukaemia: what is the role of currently known risk factors? *Radiation and Environmental Biophysics*, 36, 217-228.

Chapter 2

DNA Preparation and Conventional PCR for the Detection of Calreticulin Type 1 and 2 Mutations

2.1. Introduction to techniques

2.1.1. DNA extraction

Most molecular biology techniques require the use of isolated deoxyribonucleic acid (DNA) and therefore extraction of DNA is a vital step required to perform these molecular laboratory procedures (Chacon-Cortes and Griffiths, 2014). Methods that are used to extract DNA, all follow some common steps that are designed for the effective disruption of cells (thereby releasing DNA), denaturation of nucleoproteins, inactivation of enzymes, removal of all contaminants (whether chemical or biological), and finally the precipitation of DNA (Chacon-Cortes and Griffiths, 2014). Most extraction methods include the use of organic and non-organic reagents as well as centrifugation to achieve separation (Chacon-Cortes and Griffiths, 2014).

The GenElute™ Blood Genomic DNA Kit (Sigma-Aldrich, USA) uses the advantages of silica binding with a microspin format. Silica matrices are positively charged which gives them the ability to effectively bind negatively charged DNA (Chacon-Cortes and Griffiths, 2014). A lysis buffer ensures that cell membranes are disrupted in order to release the DNA, and the enzyme proteinase K actively cleaves nucleoproteins as well as any enzymes that degrade DNA or RNA (ribonucleic acid) such as deoxyribonucleases (DNases) or ribonucleases (RNases) (Chacon-Cortes and Griffiths, 2014).

A high pH and salt concentration, to ensure precipitation of DNA, are achieved by adding sodium cations which have a high affinity for the negatively charged oxygen molecules in the DNA backbone (Chacon-Cortes and Griffiths, 2014). Contaminants are removed with two washing steps and DNA is eluted using a buffer with a low ionic strength (Chacon-Cortes and Griffiths, 2014).

2.1.2. Conventional PCR

The polymerase chain reaction (PCR) is an *in vitro* enzymatic reaction that has made detection and generation of unlimited amounts of DNA sequences of interest possible (Mullis *et al.*, 1986; Malacinski, 2003; Lalam, 2006; Nussbaum *et al.*, 2007). A PCR assay can amplify a single piece or a few copies of DNA billions of times in just a few hours and therefore PCR has revolutionised molecular diagnostics and analysis of genetic disease (Nussbaum *et al.*, 2007; Solanki, 2012). The technique is now a common and crucial part of any medical or biological laboratory as it is simple, quick and relatively inexpensive (Solanki, 2012).

The PCR reaction is divided into three main steps: 1) denaturation, 2) primer annealing and 3) primer extension (Solanki, 2012). In the first step, DNA is denatured at very high temperatures (90-97°C) to form single strands to which the primers can bind (Solanki, 2012; Turgeon, 2012). During the second step, the PCR reaction uses two oligonucleotide primers of 16 to 20 base pairs (bp) long that bind at a lower temperature (50°C to 60°C) on either side of the fragment of interest (Nussbaum *et al.*, 2007). One primer is complementary to the 5'-3' strand of the DNA upstream from the sequence of interest and the other is complementary to the 3'-5' strand of the DNA molecule downstream from the sequence of interest (Nussbaum *et al.*, 2007). During the third step, extension of the primers occurs at approximately 72°C, during which synthesis of the new strands of DNA takes place (Dehar and Singh, 2006; Solanki, 2012). The extension step is dependent on the help of an enzyme called *Taq* polymerase (Malacinski, 2003; Nussbaum *et al.*, 2007; Solanki, 2012). It is a type of DNA polymerase, which is stable at very high temperatures (Malacinski, 2003; Nussbaum *et al.*, 2007; Solanki, 2012).

These three steps are generally repeated 25 to 30 times ensuring that an exponential increase in copy number of the original DNA sample will occur by the time that the PCR is completed (Solanki, 2012; Turgeon, 2012). After the last cycle, a final extension step, lasting 10 to 15 min is used to guarantee that all the remaining single stranded DNA is completely copied (Dehar and Singh, 2006). The PCR product is then detected using gel electrophoresis and staining with an intercalating dye indicating the presence of the sought after DNA sequence (Turgeon, 2012).

2.1.3. Restriction enzyme analyses

A restriction enzyme (RE) is a molecule that cleaves DNA sequences at short palindromic sequences (Bain *et al.*, 2012). Due to the fact that many REs are available, it frequently occurs that point mutations may create or destroy an RE recognition sequence (Bain *et al.*, 2012). This is the case with the 5-bp insertion of the type 2 *CALR* mutation which results in a recognition site for the RE *MfeI*. The RE *MfeI* recognises the target sequence 5'-caattg-3' and cuts between the cytosine (C) and the adenine (A) bases. Digestion of the PCR product with RE prior to agarose gel electrophoresis, enables visualisation of the PCR product based on size differences created when the DNA is completely digested (Bain *et al.*, 2012).

2.1.4. Agarose gel electrophoresis

The study and use of gel electrophoresis dates as far back as 1937 (Tiselius, 1937). Agarose gel electrophoresis is a technique with a high resolving power for the analysis of nucleic acid function and structure (Johnson, 1977). Using gel electrophoresis, mixtures of DNA, RNA or proteins can be separated according to their molecular size by travelling through a gel that contains many tiny pores (Scitable, 2014).

This is done by applying an electrical field to the molecules which causes them to migrate through the pores at a speed that is inversely related to the fragments' lengths, which means that smaller molecules migrate faster through the gel than larger ones (Scitable, 2014). The electrical field applied has a positive charge at one end and a negative charge at the other which causes the nucleic acid molecules to migrate in a direction opposite to their own electrical charge (Scitable, 2014). This means that negatively charged DNA and RNA will migrate towards the positively charged end of the gel (Scitable, 2014). When the nucleic acid molecules have been separated using electrophoresis, bands that represent the molecules of different sizes can be detected by staining of the gels with an intercalating dye and visualisation of the bands under ultraviolet (UV) light (Scitable, 2014).

Polymerase chain reaction assays have previously been used to detect other mutations responsible for the presentation of myeloproliferative neoplasms (MPN) including *JAK2V617F* and *MPL* (Baxter *et al.*, 2005; Steensma, 2006; Furtado *et al.*, 2013). The assays used allele-specific PCR to detect the *JAK2V617F* and *MPL* mutations as well as a restriction fragment length polymorphism assay to detect the *JAK2V617F* mutation (Baxter *et al.*, 2005; Steensma, 2006; Furtado *et al.*, 2013).

The first aim of this chapter was to develop a conventional PCR to detect the calreticulin type 1 and type 2 mutations in a group of patients with MPN. The second aim was to compare the in-house developed conventional PCR to a commercial conventional PCR both in cost and accuracy.

2.2. Materials and Methods

Approval to perform this study was given by the MSc Committee of the Faculty of Health Sciences at the University of Pretoria (Appendix A1), as well as the Research Ethics Committee of the Faculty of Health Sciences at the University of Pretoria (Appendix A2). The ethics reference number is 335/2015.

2.2.1. Study population and data analysis performed

From August 2015 – September 2016 24 blood specimens were collected from the tertiary academic hospital's haematology clinic. One DNA sample from a patient, identified as patient 6, produced a DNA sample that did not give a satisfactory result and was thus collected again and labelled 6.2. In addition, two DNA samples, a known deletion (DEL) and a known insertion (INS), were sourced from a private pathology laboratory as controls.

On most Wednesdays, existing patients visit the haematology clinic for routine follow-up or new patients are admitted. The samples taken from these patients fall under a blanket consent form (approved by the research ethics committee) that states that samples may be used anonymously for research purposes by the Department of Haematology once they are collected for diagnostic testing in the core laboratory. Research Ethics Committee approval was later sought to be able to source samples from private pathology laboratories (Appendix A3). An informed consent form was approved to be used to obtain blood samples from patients at non-government institutions (Appendix A4).

In addition, 24 DNA samples were obtained from a colleague's study that determined the Janus kinase 2 (*JAK2*) mutation status of patients [ethics reference number S32 (2012)]. Of these samples, 14 were negative for the *JAK1V167F* mutation and 10 were positive for the mutation. The researchers did not know the mutational status of the patients and thus a blinded component was included in this study. The final number of samples tested for this study was 50 patient samples.

Samples were included when a patient was older than 18 years and was diagnosed as having polycythaemia vera (PV), essential thrombocythaemia (ET) or primary myelofibrosis/myelofibrosis (PMF/MF) or when patients were listed as having a MPN. Both male and female patients were included, as well as people from any ethnicity. The exclusion criterion was that a patient could not be younger than 18 years of age.

Desirable for a new test is to achieve high sensitivity and specificity, i.e. a high level of agreement between the diagnosis of the new test and that of the reference method (sequencing). The analysis initially required 62 samples but unfortunately only 50 samples could be obtained due to lack of patient availability. The observed results were such that the reduced sample size did not compromise the statistical significance of the study. Additional measures were taken in an attempt to source more samples, which were unsuccessful. The data analysis was primarily based on the agreement of the newly developed PCR assay and sequencing and the diagnostic parameters for the new assay. The Cohen's Kappa-statistic was to be reported along with a 95% confidence interval and its interpretation as well as the diagnostic parameters and sensitivity and specificity using 2x2 tables.

2.2.2. DNA extraction

DNA was extracted using the GenElute™ Blood Genomic DNA kit (Sigma-Aldrich, St. Louis, MO, USA) protocol according to the manufacturer's instructions. Whole blood was collected in ethylenediaminetetraaceticacid (EDTA) anticoagulant tubes.

Twenty microlitres of the Proteinase K solution (Sigma-Aldrich) was placed into a 1.5 ml microcentrifuge tube. Two hundred microlitres of the whole blood sample was added to the tube. Two hundred microlitres of Lysis Solution C (Sigma-Aldrich) was added to the sample and vortexed using the RX3 vortex mixer (Velp Scientifica, Usmate Velate, Italy) thoroughly for fifteen seconds. The sample was incubated at 55°C in the AccuBlock™ Digital Dry Bath (Labnet International Inc., Edison, NJ, USA) for ten minutes. Five hundred microlitres of the Column Preparation Solution (Sigma-Aldrich) was added to each pre-assembled GenElute Miniprep Binding Column (Sigma-Aldrich) and centrifuged using the Mikro 200R (Hettich, Tuttlingen, Germany) centrifuge at 12,000 x g for one minute. The flow-through liquid was then discarded. Two hundred microlitres of ethanol (95% to 100%) was added to the lysate and mixed thoroughly by vortexing (Velp Scientifica) for ten seconds to ensure a homogeneous solution. The entire contents of the tube were transferred into the treated column followed by a centrifugation (Hettich) step, at 6,500 x g, for one minute.

The collection tube containing the flow-through liquid was discarded and the column was placed in a new two ml collection tube. Five hundred microlitres of the Prewash Solution (Sigma-Aldrich) was added to the column and centrifuged (Hettich) for one minute at 6,500 x g. The collection tube containing the flow-through liquid was discarded and the column was placed in a new two ml collection tube. Five hundred microlitres of Wash Solution (Sigma-Aldrich) was added to the column and centrifuged (Hettich) for three minutes at 14,000 x g to dry the column. The column had to be free of ethanol before eluting the DNA and therefore it was centrifuged (Hettich) for one additional minute at 14,000 x g speed. The collection tube containing the flow-through liquid was discarded and the column was placed into a new two ml collection tube. Two hundred microlitres of the Elution Solution (Sigma-Aldrich) was pipetted directly into the centre of the column, incubated at room temperature (20°C to 24°C) for five minutes and then centrifuged (Hettich) for one minute at 6,500 x g to elute the DNA.

Quality control measures included the use of different rooms for DNA extraction and analysis of PCR products to avoid possible contamination. Unidirectional flow from pre-amplification to post-amplification was maintained to minimise the risk of contamination. One extraction negative tube, containing nuclease free water, was included in each set of specimens that was extracted. This was done to account for any carry-over DNA contamination during the extraction process.

2.2.3. DNA analysis

In order to perform PCR reactions that are uniform, the concentration of each extracted sample had to be determined to ensure that all PCR reactions contained almost equal concentrations of DNA. The quality and concentration of the DNA samples was determined using the NanoDrop™ 2000c Spectrophotometer (Thermo Fisher Scientific, Waltham, MA, USA). The Elution Solution from the GenElute™ Blood Genomic DNA kit (Sigma-Aldrich) was used as the blank for the calibration of the NanoDrop™ (Thermo Fisher Scientific) in which the DNA was eluted.

One microlitre of the extracted DNA sample was pipetted onto the pedestal of the NanoDrop™ (Thermo Fisher Scientific), after which the arm was lowered and the concentration of the DNA sample was determined. The NanoDrop (Thermo Fisher Scientific) software recorded and saved all the readings onto an Excel spread sheet which was later used when the amount of DNA needed for each assay was determined. For conventional PCR a total DNA content of 100 ng was used.

2.2.4. Design and synthesis of primers

Primers were designed using the online primer design tool on the PrimerQuest Tool page of Integrated DNA Technologies' (IDT) (Integrated DNA Technologies, Coralville, IO, USA) website (Integrated DNA Technologies, 2015). Primers were designed using the following guidelines (Wang and Seed, 2006; Prediger, 2015): 1) primer specificity was ensured by comparing sequence similarity between primers and the template sequence in the design space to prevent mispriming, 2) the length of the primers had to fall between 16 to 28 nucleotides to prevent non-specific binding (when primers are too short) and to prevent the formation of secondary structures such as primer dimers (when primers are too long), 3) the GC content of the primers had to lie between 35% to 65% to prevent poor primer binding (when GC content is too low) and to prevent mispriming (when GC content is too high), and, 4) the forward and reverse primers had to have similar melting temperatures (T_m), with the optimal range being 60°C to 64°C to ensure optimum PCR enzyme function. The same primers were used for the detection of mutation type 1 and type 2 and are shown in Table 2.1.

Table 2.1: Primer sequences and characteristics

Primer	Sequence	Length	GC Content	T_m	Nucleotide number binding site
Forward primer	5'-TGG TCC TGG TCC TGA TGT CCG-3'	21-bp	61.9%	61.0°C	5039-5060
Reverse Primer	5'-CCC AAA TCC GAA CCA GCC TGG-3'	21-bp	61.9%	60.9°C	5417-5437

The product size for wild type PCR products were expected to be 399-bp in length whereas the product sizes of the type 1 mutation PCR products and the type 2 mutation PCR products were expected to be 347-bp and 404-bp respectively. Primers were subsequently manufactured by IDT.

2.2.5. Design and synthesis of control fragments

Gene fragments that were used as synthesized control samples were designed and then manufactured by Inqaba Biotec (Inqaba Biotechnical Industries, Pretoria, South Africa). Three fragments in total were synthesized and all these fragments were 6-bp longer on the 5'- and 3'- prime ends than the primer binding site on the target region. It was designed in this manner to ensure effective and specific binding to the target by the primers. The first was the wild type control, which corresponded completely with the wild type calreticulin sequence found on GenBank (Accession number: NG_029662) of the same region. The second control was a synthesized fragment of the region that contains the 52-bp deletion of the calreticulin type 1 mutation. The third control was a synthesized fragment of the region of interest which contained the 5-bp insertion of the calreticulin type 2 mutation. The manufactured controls are shown in Appendix A6.

2.2.6. Conventional in-house PCR

The conventional in-house PCR was performed according to the HotStar HiFidelity Polymerase PCR kit (Qiagen, Hilden, Germany) Handbook protocol. The HotStar HiFidelity PCR Buffer (containing dNTPs and MgSO₄) (Qiagen) and primer solutions were thawed. The solutions were briefly vortexed (Velp Scientifica) and centrifuged with the Z 100 M minicentrifuge (Hermle AG, Gosheim, Germany) before use to ensure homogenous solutions. A reaction mix was prepared according to Table 2.2.

Table 2.2: Conventional PCR reaction setup

Component	Volume/reaction	Final concentration
5x HotStar HiFidelity PCR Buffer (Qiagen)	5.00 µl	1 x
Forward Primer (10.00 µM)	1.00 µl	1.00 µM
Reverse Primer (10.00 µM)	1.00 µl	1.00 µM
HotStar HiFidelity DNA Polymerase (Qiagen) (2.50 units/µl)	0.50 µl	1.25 units
Template DNA	Variable	±100 ng
Double distilled H ₂ O (ddH ₂ O)	Fill up to 25.00 µl	–
Total volume	25.00 µl	–

After adding all the reagents to prepare the reaction mix, the mixture was briefly vortexed (Velp Scientifica) and pulse centrifuged (Hermle AG) before use to ensure homogenous solutions and appropriate volumes were dispensed into PCR tubes. During each PCR, the appropriate controls were included to serve as a confirmation of whether a product was the wild type, type 1 or type 2 allele. A no template control (NTC), to which sterile double distilled water (ddH₂O) was added instead of template DNA, was also included to ensure that no contamination of reagents had taken place. Template DNA was added to the individual tubes containing the reaction mix. The concentrations of the DNA determined by the NanoDrop™ 2000c Spectrophotometer (Thermo Fisher Scientific) differed greatly between each sample of extracted DNA. Therefore, the volume of DNA added to each reaction mix was individually determined to ensure that a total DNA content of 100 ng was added to the PCR reaction tubes. Sterile double distilled water was added to make up the reaction to a total volume of 25 µl. The BioRad DNA Engine® Peltier Thermal Cycler (Bio-Rad, Hercules, CA, USA) was programmed as indicated in Table 2.3.

Table 2.3: Conventional PCR cycling protocol on the BioRad DNA Engine® Peltier Thermal Cycler (Bio-Rad)

	Number of Cycles	Time	Temperature
Initial activation step	1	5 min	95°C
3-step cycling:	40		
Denaturation		15 sec	94°C
Annealing		1 min	56°C
Extension		1 min	72°C
Final extension step	1	10 min	72°C
Hold step	-	Indefinite	4°C

After the cycling protocol was completed, PCR products were analyzed. This was done using agarose gel electrophoresis for the detection of *CALR* type 1 mutation, as described in section 2.2.9.

2.2.7. Purification of PCR products

Purification of conventional PCR products was performed using the Zymo Research DNA Clean & Concentrator TM-25 kit (Zymo Research Corporation, Irvine, CA, USA) handbook protocol . In a 1.5 ml microcentrifuge tube, 100 µl of DNA Binding Buffer was added to 20 µl of DNA sample and mixed briefly by vortexing (Velp Scientifica). The mixture was transferred to a Zymo-Spin™ Column in a collection tube and centrifuged using the Mikro 200R (Hettich) centrifuge at 13,000 x g for 30 seconds. Two hundred microlitres of the DNA Wash Buffer was then added to the column and it was centrifuged (Hettich) at 13,000 x g for 30 seconds. This wash step was repeated. Thirty microlitres DNA Elution Buffer was added directly to the column matrix and incubated at room temperature (20°C to 24°C) for one minute. The column was subsequently transferred to a 1.5 ml microcentrifuge tube and centrifuged (Hettich) at 13,000 x g for 30 seconds to elute the DNA.

2.2.8. Restriction enzyme analysis

A ten microlitre aliquot of the purified PCR product was subjected to restriction enzyme digestion with *Mfe*I (New England Biolabs Inc., Ipswich, MA, USA). Purification of PCR products was done prior to restriction enzyme digestion, to minimise possible inhibition of the RE by PCR components (New England Biolabs, 2017). The reaction mix was prepared according to Table 2.4. A restriction digest negative reaction was also included when a reaction mix was prepared and in this reaction the PCR product was substituted with sterile ddH₂O. The products of the RE digestion reaction containing the type 2 mutation were expected to be 222-bp and 182-bp in length.

Table 2.4: Restriction enzyme digestion reaction setup

Component	Volume/reaction	Final concentration
10x Restriction Buffer (New England Biolabs, Inc, MA)	5.00 µl	1x
<i>Mfe</i> I (10 U/µl)	1.00 µl	10 U
PCR product	10.00 µl	–
ddH ₂ O	34.00 µl	–
Total volume	50.00 µl	–

The reactions were incubated in a water bath (Labcon Laboratory Equipment, Krugersdorp, South Africa) at 37°C for two hours. The digestion products were then analyzed using agarose gel electrophoresis, for the detection of *CALR* type 2 mutation as described in 2.2.9.

2.2.9. Agarose gel electrophoresis

Products of the conventional PCR, as well as the restriction enzyme digestion, were separated on a 2% agarose gel. The gel was prepared using 2.4 g of agarose powder (Sigma-Aldrich, St. Louis, MO, USA) to which 120 ml of 1 X TBE (Tris/Borate/EDTA) buffer (Sigma-Aldrich) was added and mixed well.

The mixture was then heated in the microwave, while stirring occasionally, until all the granules of agarose powder had disappeared. The agarose mixture was then left to cool and once it had obtained a temperature of 50°C, 5 µl of 10 mg/ml ethidium bromide solution (EtBr) (Amresco LLC, Cleveland, OH, USA) was added to the mixture. The agarose mixture was mixed well and then poured into a 100 mm X 150 mm casting tray to create a gel that was 10 mm thick. The comb used for making the wells was either a 15 well comb or a 20 well comb, depending on the amount of products that had to be analysed. The gel took approximately 30 minutes to set, after which the comb was removed from the gel. The gel, along with the casting tray, was then submerged inside the electrophoresis tank (Bio-Rad) in 1 X TBE buffer up to approximately two mm above the level of the gel. The products to be analysed were selected and recorded by well number. Two microlitres DNA loading dye (Bio-Rad) was then added to five microlitres PCR product, mixed well and then five microlitres of the mixture was added to the appropriate well. Two microlitres of a 100-bp DNA ladder (Thermo Fisher Scientific) was added to certain wells and was used to determine the sizes of the amplified products. The power supply was switched on and run at 84 Volts (5 V/cm) for approximately 65 minutes.

Visualisation of the gels took place using EtBr (Amresco LLC) as the intercalating dye and UV illumination. The instrument used for the UV illumination of the gels, was a Molecular Imager Gel Doc™ XR (Bio-Rad) and the software that was used for the viewing and analysis of the gels was Quantity One® 1-D Analysis Software Version 4.6.5 (Bio-Rad).

2.2.10. Conventional PCR using a commercial kit

Conventional PCR using a commercial kit (Genequality *CALR* Mutation, AB Analitica, Padua, Italy) was performed according to the manufacturer's guidelines. The Genequality *CALR* Mutation PCR Master Mix (AB Analitica) was thawed on ice before use. The solutions were briefly vortexed (Velp Scientifica) and centrifuged (Hermle AG) before use to ensure homogenous solutions. A reaction mix was prepared according to Table 2.5.

Table 2.5: Conventional PCR using a commercial kit reaction setup (AB Analitica, 2015)

Component	Volume/reaction	Final concentration
<i>CALR</i> Master Mix (Qiagen)	20.00 µl	1 x
Template DNA	5.00 µl	80.00 ng/reaction
Total volume	25.00 µl	–

The reaction mix was briefly vortexed (Velp Scientifica) and centrifuged (Hermle AG) before use to ensure homogenous solutions and appropriate volumes were dispensed into PCR tubes. During each PCR, the appropriate controls were included to serve as a confirmation of whether a product was the wild type, type 1 or type 2 allele. A NTC, to which sterile ddH₂O was added instead of template DNA, was also included to ensure that no contamination of reagents had taken place. Template DNA was added to the individual tubes containing the reaction mix. The BioRad DNA Engine® Peltier Thermal Cycler (Bio-Rad) was programmed as indicated in Table 2.6.

Table 2.6: Conventional PCR using a commercial kit's cycling profile on the BioRad DNA Engine® Peltier Thermal Cycler (Bio-Rad) (AB Analitica, 2015)

	Number of Cycles	Time	Temperature
Initial activation step	1	2 min	95°C
3-step cycling:	35		
Denaturation		30 sec	95°C
Annealing		30 sec	60°C
Extension		30 sec	72°C
Final extension step	1	10 min	72°C
Hold step	-	Indefinite	4°C

A 4% agarose gel was prepared to visualize the PCR products using reagents included in the commercial kit. Four grams of agarose was added to 100 ml of TAE (Tris/Acetic acid/EDTA). The mixture was heated in the microwave, while stirring occasionally, until all the granules of agarose powder had disappeared.

The agarose mixture was left to cool at room temperature (20°C to 24°C) and once it had obtained a temperature of 50°C, 10 µl of 2.5 mg/ml ethidium bromide solution (AB Analitica) was added and mixed well into the agarose solution. The agarose was poured into a 10 mm x 15 mm casting tray to create a gel.

The comb used for making the wells was a 15 well comb. The gel took approximately 30 minutes to set, after which the comb was removed from the gel. The gel, along with the casting tray, was submerged inside the electrophoresis tank (Bio-Rad) in 1 X TAE buffer up to approximately two mm above the level of the gel.

According to the manufacturer's instructions, pre-treatment of patient sample products was required prior to analysis using agarose gel electrophoresis. The Post-PCR reagent (AB Analitica) was thawed, mixed well and centrifuged (Hermle AG) briefly. Sufficient 0.2 ml PCR tubes for all the samples and controls were prepared and 5 µl of the Post-PCR reagent (AB Analitica) was dispensed into each 0.2 ml tube. Five microliters of each PCR product was then added to the corresponding tube. The tubes were vortexed (Velp Scientifica) and pulse centrifuged (Hermle AG) briefly. A short program was then run on the BioRad DNA Engine® Peltier Thermal Cycler (Bio-Rad) as shown in Table 2.7.

Table 2.7: Pre-treatment of PCR product cycling conditions (AB, Analitica 2015)

Cycles	Time	Temperature
1	5 min	95°C

The tubes were removed from the thermal cycler, mixed and pulse centrifuged (Hermle AG) briefly. The products were allowed to cool at room temperature (20°C to 24°C) for 5 minutes. The products to be analysed were then selected and recorded by well number. Samples were prepared according to Table 2.8. Each patient sample therefore has one pre-treated PCR product and one untreated PCR product. Two microlitres bromophenol blue (BB) (loading dye) (AB Analitica) was then added to five microlitres PCR product, mixed well and then all seven microlitres of the mixture was loaded to the appropriate well (Table 2.9).

Ten microlitres of a molecular weight marker (AB Analitica) was added to certain wells and was used to determine the sizes of the amplified products. The power supply was switched on and run at 100 Volts for approximately 60 minutes.

Table 2.8: Method for preparing samples on parafilm before electrophoresis (AB, Analytica 2015)

2 µl bromophenol blue (BB) + 5 µl	PCR product of no template control
2 µl BB + 5 µl pre-treated	PCR product of Controls (WT/T1/T2)
2 µl BB + 5 µl	PCR product of clinical sample
2 µl BB + 5 µl pre-treated	PCR product of clinical sample
2 µl BB + 10 µl	molecular weight marker

Table 2.9: Indication of expected results (AB, Analytica 2015)

2 µl BB + 5 µl	PCR product of no template control
2 µl BB + 5 µl pre-treated	PCR product of WT control
2 µl BB + 5 µl pre-treated	PCR product of T1 control
2 µl BB + 5 µl pre-treated	PCR product of T2 control
2 µl BB + 5 µl	PCR product of clinical sample
2 µl BB + 5 µl pre-treated	PCR product of clinical sample
2 µl BB + 10 µl	molecular weight marker

Visualisation of the gels took place using EtBr (Bio-Rad) as the intercalating dye and UV illumination. The instrument used for the UV illumination of the gels, was a Gel Doc™ XR (Bio-Rad) imaging system and the software that was used for the viewing and analysis of the gels was Quantity One® 1-D Analysis Software Version 4.6.5 (Bio-Rad). Before the interpretation of the results could take place, the quality of the PCR had to be determined by evaluation of the controls (Table 2.10). If the controls showed the expected results, the analysis of the clinical samples could take place. Table 2.11 and Figure 2.1 indicate how the results should be interpreted according to the Genequality *CALR* Mutation (AB Analytica, Padua, Italy) user manual protocol.

Table 2.10: Evaluation of the commercial PCR session (AB Analytica 2015)

Control	Result	Interpretation
No template control	No band	No contamination
WT Control	One band at 285-bp	PCR and visualization by gel electrophoresis have worked correctly
T1 Control	Two bands at 285-bp and 233-bp	
T2 Control	Two bands at 285-bp and 290-bp	

Table 2.11: Guide to interpreting results of the commercial PCR (AB Analitica 2015)

Clinical Sample	Band(s) on gel	Genotype of sample
PCR product Pre-treated PCR product	285-bp 285-bp	Homozygous for wild type <i>CALR</i>
PCR product Pre-treated PCR product	285-bp and 233-bp 285-bp and 233-bp	Heterozygous for <i>CALR</i> mutation type 1
PCR product Pre-treated PCR product	233-bp 285-bp and 233-bp	Homozygous for <i>CALR</i> mutation type 1
PCR product Pre-treated PCR product	285-bp and 290-bp 285-bp and 290-bp	Heterozygous for <i>CALR</i> mutation type 2
PCR product Pre-treated PCR product	285-bp 285-bp and 290-bp	Homozygous for <i>CALR</i> mutation type 2
PCR product Pre-treated PCR product	285-bp and ≠ 285-bp 285-bp and ≠ 285-bp	Heterozygous for <i>CALR</i> with unspecified mutation*
PCR product Pre-treated PCR product	285-bp 285-bp and ≠ 285-bp	Homozygous for <i>CALR</i> with unspecified mutation*
PCR product Pre-treated PCR product	No band 285-bp	Sample not suited for this assay Repeat PCR or DNA extraction

*The unspecified mutations are insertions, deletions or combinations of both that results in an at least 4-bp longer or shorter *CALR* sequence.

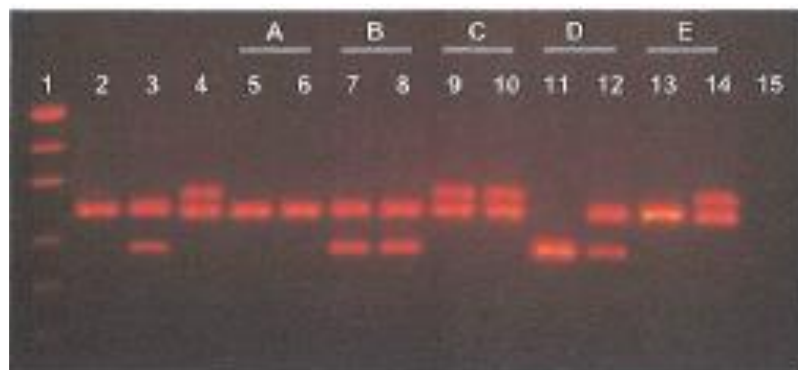


Figure 2.1: Representative example of a gel and the interpretation of its results. Sample A: wild type *CALR*, Sample B: heterozygous for type 1 mutation, Sample C: heterozygous for type 2 mutation, Sample D: homozygous for type 1 mutation, Sample E: homozygous for type 2 mutation. 1. Molecular weight marker, 2. Wild type control, 3. Type 1 control, 4. Type 2 control, 5. PCR product sample A, 6. Pre-treated PCR product sample A, 7. PCR product sample B, 8. Pre-treated PCR product sample B, 9. PCR product sample C, 10. Pre-treated PCR product sample C, 11. PCR product sample D, 12. Pre-treated PCR product sample D, 13. PCR product sample E, 14. Pre-treated PCR product sample E, 15. Negative control (no template control) (AB Analitica, 2015)

The cost analysis was performed by comparing the cost of running a 20 well gel using the conventional PCR to that of running a 20 well gel using the commercially available kit. The cost of all reagents (controls, PCR kit, gel electrophoresis reagents and the commercial PCR kit) required to reach a diagnostic conclusion were included in the cost analysis.

2.3. Results and Discussion

Conventional PCR produced fragments of 399-bp for normal alleles and 347-bp for alleles with the type 1 mutation in the calreticulin gene. This was detected using agarose gel electrophoresis, as shown in Figure 2.2, using a 100-bp DNA ladder (Thermo Fisher Scientific), as well as the synthesized fragments of DNA which served as controls. The control fragments for the wild type as well as the type 1 mutation were used when determining whether a sample had the type 1 mutation, whereas the control fragments for the wild type as well as the type 2 mutation were used when determining whether a sample had the type 2 mutation.

Normal individuals had one DNA band corresponding with the 400-bp marker on the DNA ladder (Thermo Fisher Scientific). In the case of a type 1 mutation, which is a 52-bp deletion, patients were expected to have either two different sized bands (for the two different sized alleles) or one band (for the two identical sized alleles) depending on whether they were heterozygous or homozygous for the mutation. The presence of the type 2 mutation in the set of samples could not be excluded by the initial gel electrophoresis (as the 5-bp insertion would not be clearly visible due to the resolution of the gel) which was run to confirm the presence of PCR products and the presence of the type 1 mutation. A restriction digest reaction was; however, performed to indicate the presence of the type 2 mutation in each set of samples. Extraction negative samples were analysed to indicate that DNA cross-contamination did not occur during the extraction step/process.

A gel was run to specifically detect the type 1 mutation as shown in Figure 2.2. From this figure it is clear that samples 24, 25, 26, 27, 28, 29 and 30 corresponded with the wild type control to the 400-bp mark on the ladder, which is what was expected from the normal 399-bp fragment. Sample 23 had a wild type band as well as a faint 52-bp deletion which was shown by the type 1 (T1) mutation control and thus has a band corresponding to the type 1 control fragment which migrated between the 400-bp and 300-bp mark. The presence of both bands indicated that the patient was heterozygous for the *CALR* type 1 mutation. The faint bands below the actual fragments indicate the possible presence of non-specific amplification which could be reduced by further optimization.

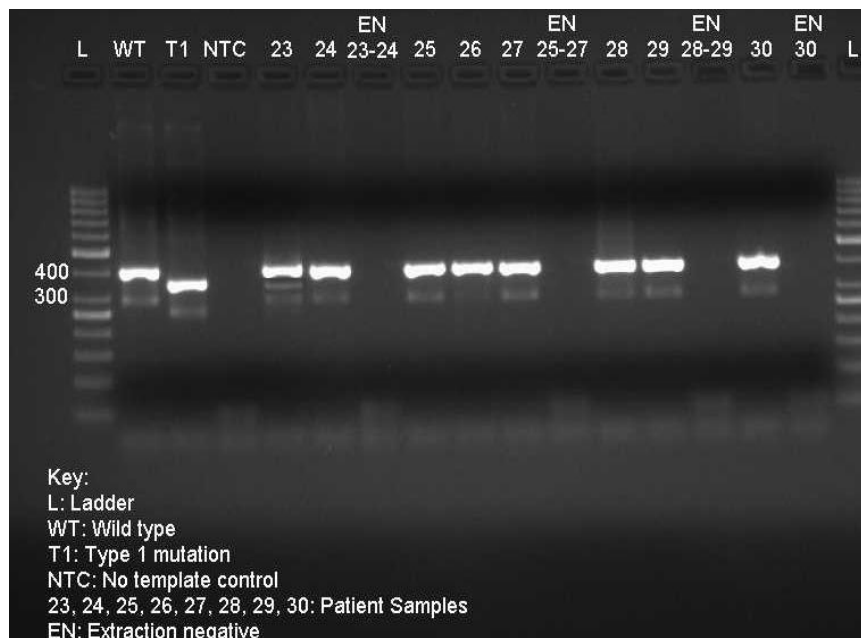


Figure 2.2: Agarose gel electrophoresis of *CALR* exon 9 amplicons from selected patients, namely 23-30

In Figure 2.3 it is clear that samples J37, J38, J39, J40, J41, J42, J43, J44, and J45 corresponded with the wild type control to the 400-bp mark on the ladder, which is what was expected from the normal 399-bp fragment. Sample J36 had a wild type band as well as a faint 52-bp deletion which was shown by the type 1 (T1) mutation control and thus had a band corresponding to the type 1 control fragment which migrated between the 400-bp and 300-bp mark.

The faint band visible as the 52-bp deletion of sample J36 could be due to possible genomic DNA degradation, as a result of prolonged storage. Unfortunately there was not enough sample material available to repeat the run. The presence of both bands indicated that the patient was heterozygous for the *CALR* type 1 mutation.

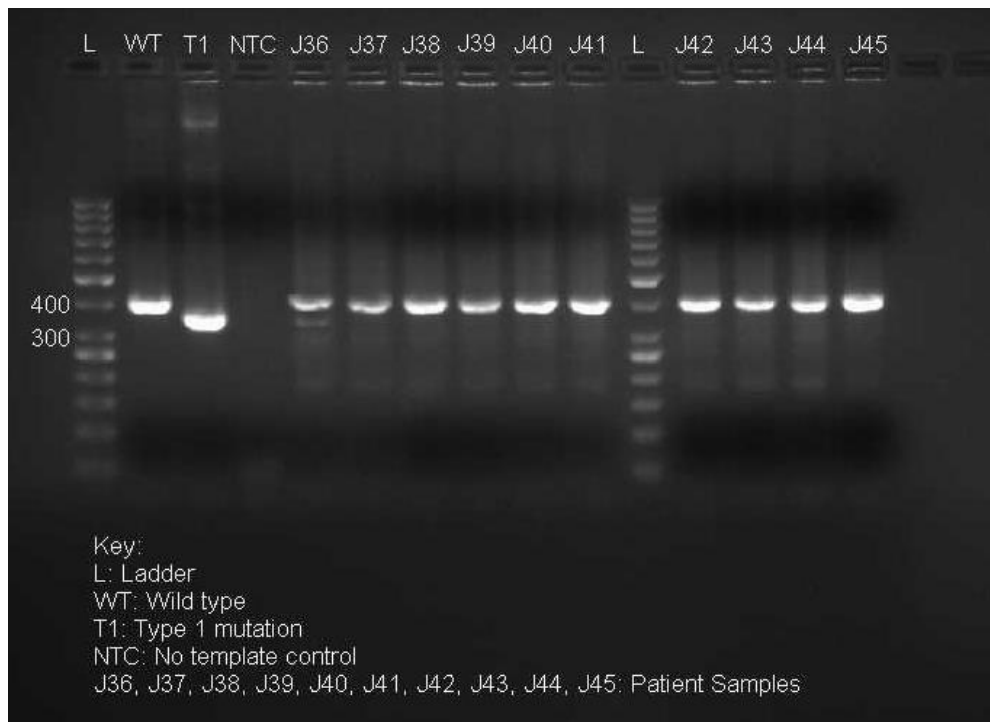


Figure 2.3: Agarose gel electrophoresis of *CALR* exon 9 amplicons from selected patients, namely J36-J45

A gel was run to specifically detect the type 1 mutation as shown in Figure 2.4. Results show that samples 6.2, J22 and INS appears to correspond with the wild type control to the 400-bp mark on the ladder, which is what was expected from the normal 399-bp fragment. The fragments are however not perfectly aligned as it appears as if that fragments on the right hand side of the gel migrated at a slower rate than the fragments on the left side. Unfortunately there was not enough sample material available to repeat the run.

The sample labelled Known Deletion (DEL), had a wild type band as well as a faint 52-bp deletion which was shown by the type 1 (T1) mutation control and thus had a band corresponding to the type 1 control fragment which migrated between the 400-bp and 300-bp mark (347-bp). The presence of both bands indicated that the patient was heterozygous for the *CALR* type 1 mutation.

Although the type 2 mutation was thought to be invisible before RE digestion, the samples J22 and the Known Insertion (INS), produced what appeared to be a double fragment on the gel before restriction digest (Figure 2.4), indicating that it may be possible to observe the type 2 mutation without restriction digest, provided the gel is run long enough. A restriction digest reaction was performed and the presence of the type 2 mutation was confirmed in J22 and INS (Figure 2.5 and Figure 2.6) and was excluded in the rest of this batch of samples.



Figure 2.4: Agarose gel electrophoresis of *CALR* exon 9 amplicons from selected patients, namely 6.2, J22, DEL and INS

Fragments of DNA produced by PCR of the type 2 mutation were 404-bp in length whereas fragments of DNA of the normal sequence were 399-bp in length. This resulted in a size difference of only 5-bp which was not always clearly visible with normal agarose gel electrophoresis.

Restriction enzyme digestion followed by gel electrophoresis was used to detect the 5-bp insertion of the calreticulin type 2 mutation as this created a restriction enzyme digest site. The restriction enzyme, *MfeI* was able to recognize the target sequence (which was created by the 5-bp insertion) 5'-CAATTG-3' and cut the DNA between the cytosine (C) and the adenine (A) bases to produce two fragments of 222-bp and 182-bp in length.

From Figure 2.5 it is clear that samples 6.2 and J19 on the gel corresponded with the wild type control (400-bp in size). Samples DEL and J36 were confirmed as type 1 mutations by the time that this gel was run for the restriction enzyme digestion analysis. Samples J22 and INS corresponded with the type 2 control to the bands on either side of the 200-bp mark on the ladder, which as expected from the type 2 mutation fragments of 222-bp and 182-bp.

The sample labelled INS did not photograph well as the 222-bp and 182-bp fragments were very faint and it was subsequently rerun with more DNA on another gel (Figure 2.6). The samples also had a band that corresponded with the wild type control to the 400-bp mark on the ladder, which is what is expected from the normal fragment of 399-bp.

The sample labelled INS on the gel (Figure 2.6) corresponded with the type 2 control to the 222-bp and 182-bp bands. The sample also had a band that corresponded with the wild type control to the 400-bp mark on the ladder. This was indicative of the fact that the sample INS appears to be heterozygous for the calreticulin type 2 mutation as it had both a mutant and a wild type allele as shown in Figure 2.5 and 2.6.

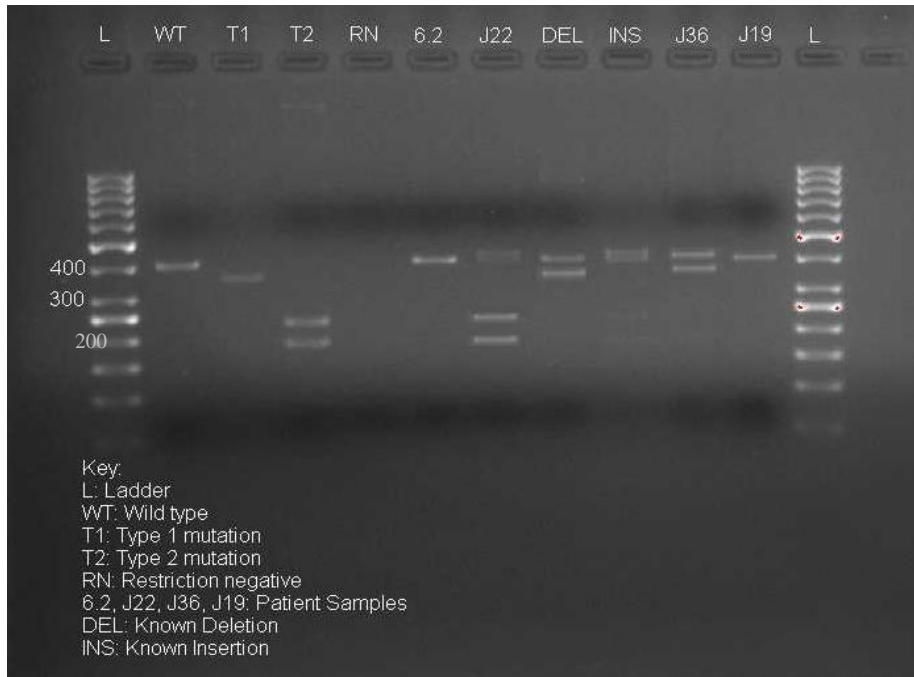


Figure 2.5: Agarose gel electrophoresis of *CALR* exon 9 amplicons, after RE digest, from selected patients, namely J22 and INS

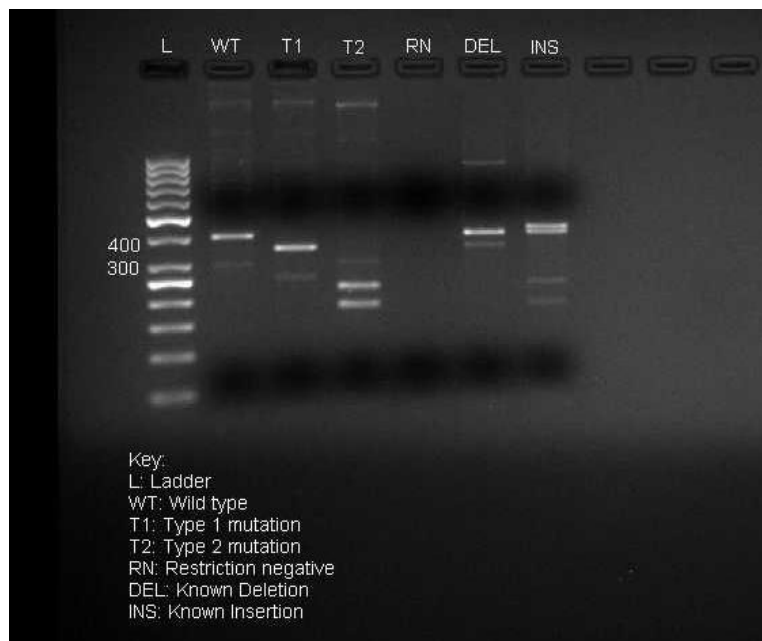


Figure 2.6: Agarose gel electrophoresis of *CALR* exon 9 amplicons, after RE digest, from selected patients, namely DEL and INS

A commercially available conventional PCR kit (Genequality *CALR* Mutation, AB Analitica) for the detection of the calreticulin type 1 and type 2 mutations was included in this study. The purpose of this comparison was to compare the results to those obtained with the conventional in-house PCR as well as to do a cost comparison to determine which method would be the most cost-effective. The commercially available conventional PCR kit was sufficient for 50 reactions.

Since running all 50 collected samples would require more than 50 reactions, when controls were included, it was decided to run the samples that: 1) tested positive for the type 1 or type 2 mutation (with the exception of J36 no DNA was left), 2) normal samples within the range of the acceptable A260/A280 ratio (Appendix A5), 1.7-1.9 for the kit, as well as 3) samples above and below the acceptable A260/A280 ratio (to determine whether samples outside the ratio would yield normal results).

Figure 2.7 indicates that the pre-treated lane for sample 23 as well as the untreated PCR product of sample 23 had two bands corresponding to the type 1 control bands. This was the same for the lanes of sample DEL. Using the key in Table 2.11 and Figure 2.1, these results were interpreted as a heterozygous type 1 calreticulin mutation in both samples. This corresponded with the results achieved by the in-house conventional PCR. Figure 2.7 also shows that the pre-treated sample in the lane for sample INS as well as the untreated PCR product of sample INS had two bands corresponding to the type 2 control bands. Using the key in Table 2.11 and Figure 2.1, this result was interpreted as a heterozygous type 2 calreticulin mutation. This corresponded with the results achieved by the in-house conventional PCR.

To summarise the results, samples 23, J36 and DEL were positive for the *CALR* type 1 mutation, while samples J22 and INS tested positive for the *CALR* type 2 mutation. All other samples included in this study tested negative for these two mutations.

For the commercial kit, the ladder sizes were not specified. The agarose was difficult to dissolve and therefore the agarose particles appeared to cause the artefacts apparent in some lanes of the gels (Figure 2.7 and Figure 2.8)

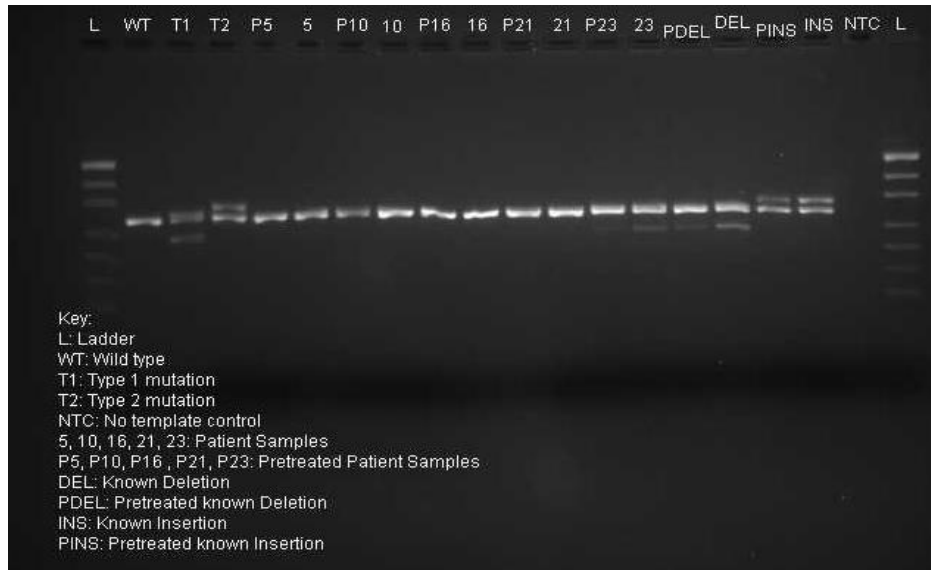


Figure 2.7: Agarose gel electrophoresis of *CALR* exon 9 amplicons detected using a commercially available conventional PCR kit, from selected patients namely 5, 10, 16, 21, 23, DEL and INS

Figure 2.8 shows the run with a sample with an acceptable A260/A280 ratio (J43) as well as samples with A260/A280 ratios outside of the recommended acceptable range (samples 31, J9, J22, A8 J6). These samples gave satisfactory results when used with the commercial kit as can be seen in Figure 2.8.

The gel also showed that the sample in the pre-treated lane for sample J22 as well as the untreated PCR product of sample J22 had two bands corresponding to the type 2 control bands. Using the key in Table 2.11 and Figure 2.1, this result was interpreted as a heterozygous type 2 calreticulin mutation. This corresponded with the results achieved by the in-house conventional PCR. As this is a commercially manufactured kit, artefacts visible in the gel could not be improved as the kit is advertised as an optimized assay for detecting *CALR* mutations. The PCR and gel electrophoresis were run exactly to the specifications of the manufacturer.



Figure 2.8: Agarose gel electrophoresis of *CALR* exon 9 amplicons detected using a commercially available conventional PCR kit, from selected patients namely J43, 31, J9, J22, 18 and J6

Finally, a cost comparison was done by examining the cost of the commercial kit and everything it contains to that of the developed in-house conventional PCR. The analysis is shown in Table 2.12 and 2.13.

When a full 20 well gel is run using the in-house conventional PCR method, the entire gel costs R2 275.02 and the cost per patient (if a full gel is run) is determined by dividing the amount of R2 275.02 by 14 patients per run (four wells are for controls and two is for the molecular weight marker) which is equal to R162.50 per test for the developed PCR method. If the entire gel is not utilized and only one patient is run per gel with a potential to run 14 patients, a test will cost R863.44.

Table 2.12: Cost analysis of the in-house conventional PCR assay

Component	Total cost	Number of reactions	Unit cost/run	Units needed for 1 patient sample per gel	Total	Units needed for a 15 well PCR	Total
Controls (All 3)	R10 498.94	50	R209.98	1	R209.98	1	R209.98
PCR Kit	R3 738.14	80	R46.73	5	R233.63	18	R841.14
Agarose	R765.35	42	R18.37	2	R36.73	2	R36.73
TBE Buffer	R1 194.06	83	R14.33	2	R28.66	2	R28.66
Ladder	R1 117.17	100	R11.17	4	R44.68	4	R44.68
Restriction Digest Kit	R1 236.92	20	R61.85	5	R309.23	18	R1113.3
EtBr	R525.43	2000	R0.26	2	R0.53	2	R0.53
Price for one sample on a full 20 well gel					R863.44	Price for one 20 well gel	R2 275.02

Table 2.13: Cost analysis of the commercially available PCR kit

Component	Total cost	Number of reactions	Unit cost/run	Units needed for 1 patient sample per gel	Total	Units needed for a 15 well PCR	Total
PCR kit (incl. controls & gel reagents)	R17,236.80	50	R344.74	5	R1,723.68	18	R6 205.32
Price for one sample on a full 20 well gel					R1,723.68	Price for one 20 well gel	R6 205.32

When a full 20 well gel is run using the commercially available kit PCR method, the entire gel costs R6205.32 and the cost per patient (if a full gel is run) is determined by dividing the amount of R6205.32 by 14 patients per run (four wells are for controls and two is for the molecular weight marker) which is equal to R443.24 per test for the commercial PCR method. If the entire gel is not utilized and only one patient is run per gel with a potential to run 14 patients, a test will cost R1723.68.

It is therefore always more cost-effective to batch samples until there are enough to run a full gel. This is due to the high cost of the reagents that are needed in the same amount for each sample and the commercial controls.

The in-house conventional PCR assay for the detection of the calreticulin type 1 and type 2 mutations proved to be an effective and relatively simple test to perform. Conventional PCR reactions are usually very time consuming. Even though the newly developed in-house PCR assay takes up to 2.5 hours, the analysis has shown that the assay is very accurate in determining whether a patient has the type 1 or type 2 mutation. On the other hand, a full gel with 20 wells could effectively run 14 samples at a time (taking into account the wells for the ladder, wild type control, type 1 control, type 2 control and the no template control).

As previously mentioned, a recently published article describes the use of a conventional PCR and agarose gel electrophoresis that was developed to screen for *CALR* type 1 and type 2 mutations before using Sanger sequencing to confirm the results (Jeong *et al.*, 2016). The researchers used a method whereby two forward primers and one reverse primer was added to a reaction mix and a PCR was performed (Jeong *et al.*, 2016). The first forward primer would bind to a region upstream of the type 1 mutation and the second forward primer was specific for the 5-bp insertion of the type 2 mutation (Jeong *et al.*, 2016). Depending on the presence of the wild type, type 1 or type 2 mutations the length of the fragments would be 357-bp, 302-bp or 272-bp respectively (Jeong *et al.*, 2016). This PCR showed perfect agreement with Sanger sequencing in detecting the presence of type 1 and type 2 mutations, although a novel mutation was missed by the screening PCR (Jeong *et al.*, 2016).

Another study recently performed in South Africa and previously mentioned, evaluated the use of a PCR followed by capillary electrophoresis using a 6-FAM labelled forward primer (De Kock, 2016). However, there is no evidence or information available of a conventional PCR assay that employs the use of gel electrophoresis as the detection method in the South African government health care sector.

Previous studies have used PCR followed by Sanger sequencing to determine the presence of *CALR* mutations or used fragment analysis PCR as it is considered to be more sensitive than a conventional PCR using gel electrophoresis as the method of visualization (Park *et al.*, 2015; Jeong *et al.*, 2016). Conventional PCR using gel electrophoresis has been shown to be an effective and simple method for detecting type 1 and type 2 mutations, especially in laboratories without specialised equipment for sequencing and fragment analysis PCR (Jeong *et al.*, 2016).

2.4. Conclusion

The comparison of the in-house PCR assay with that of a commercially available kit indicated that the newly developed PCR yielded the same results as the commercial PCR kit and that it is a more economically viable option to use in government funded diagnostic laboratories. The analysis also indicated that the A260/A280 ratio for DNA does not need to be between 1.7-1.9 in order for the commercial kit to generate results. The newly developed in-house conventional PCR followed by gel electrophoresis was able to detect the 52-bp deletion of the *CALR* type 1 mutation and conventional PCR followed by restriction enzyme digestion and gel electrophoresis was able to detect the 5-bp insertion of the *CALR* type 2 mutation.

References

AB Analitica 2015. *GENEQUALITY CALR MUTATION*, AB Analitica.

Bain, BJ, Bates, I, Laffan, MA and Lewis, SM 2012. Molecular and cytogenetic analysis. In: Houston, M. (ed.) *Dacie and Lewis Practical Haematology*. Churchill Livingstone Elsevier, 139-174.

Baxter, EJ, Scott, LM, Campbell, PJ, East, C, Fourouclas, N, Swanton, S, Vassiliou, G, Bench, AJ, Boyd, EM, Curtin, N, Scott, MA, Erber, WN and Green, AR 2005. Acquired mutation of the tyrosine kinase JAK2 in human myeloproliferative disorders. *Mechanisms of disease*, 365, 1054-1061.

Chacon-Cortes, D and Griffiths, LR 2014. Methods for extracting genomic DNA from whole blood samples: current perspectives. *Journal of Biorepository Science for Applied Medicine*, 2, 1-9.

De Kock, A. 2016. *RE: Screening for calreticulin mutations in a Free State cohort suspected of having a myeloproliferative neoplasm*. Type to Prinsloo, A.

Dehar, N and Singh, H 2006. Polymerase Chain Reaction. *Asian Journal of Chemistry*, 18, 3437-3441.

Furtado, LV, Weigelin, HC, Elenitoba-Johnson, KSJ and Betz, BL 2013. Detection of MPL Mutations by a Novel Allele-Specific PCR-Based Strategy. *Journal of Molecular Diagnostics*, 15, 810-818.

Integrated DNA Technologies. 2015. *PrimerQuest Tool* [Online]. Integrated DNA Technologies. [Accessed September 30th 2015].

Jeong, JH, Lee, HT, Seo, JY, Seo, YH, Kim, KH, Kim, MJ, Lee, JH, Park, J, Hong, J, Park, PW and Ahn, JY 2016. Screening PCR Versus Sanger Sequencing: Detection of CALR Mutations in Patients With Thrombocytosis. *Annals of Laboratory Medicine*, 36, 291-299.

Johnson, PH 1977. Electrophoresis of DNA in Agarose Gels. Optimizing Separations of Conformational Isomers of Double- and Single-Stranded DNAs. *Biochemistry*, 16, 4217-4225.

Lalam, N 2006. Estimation of the reaction efficiency in polymerase chain reaction. *Journal of Theoretical Biology*, 242, 947-953.

Malacinski, GM 2003. *Essentials of Molecular Biology*, USA, Jones and Bartlett Publishers, Inc.

Mullis, K, Faloona, F, Scharf, S, Saiki, R, Horn, G and Erlich, H 1986. Specific enzymatic amplification of DNA *In Vitro*: the polymerase chain reaction. *Cold Spring Harbor Symposia on Quantitative Biology*, 51, 263-273.

New England Biolabs. 2017. *Restriction Endonucleases* [Online]. Ipswich, MA, USA. Available: <https://www.neb.com/products/restriction-endonucleases/restriction-endonucleases> [Accessed 26 January 2017].

Nussbaum, RL, McInnes, RR and Willard, HF 2007. *Thompson & Thompson Genetics in Medicine*, Philadelphia, PA, Elsevier Ltd.

Park, J-H, Sevin, M, Ramla, S, Truffot, A, Verrier, T, Bouchot, D, Courtois, M, Bas, M, Benali, S, Bailly, F, Favre, B, Guy, J, Martin, L, Maynadié, M, Carillo, S and Girodon, F 2015. Calreticulin Mutations in Myeloproliferative Neoplasms: Comparison of Three Diagnostic Methods. *PLoS One*, 10, 1-7.

Prediger, E. 2015. *Designing PCR Primers and Probes* [Online]. Integrated DNA Technologies, Inc. [Accessed September 30th 2015].

Scitable. 2014. *Gel electrophoresis* [Online]. Nature Education. Available: <http://www.nature.com/scitable/definition/gel-electrophoresis-286> [Accessed 29 June 2016].

Solanki, G 2012. Polymerase Chain Reaction. *International Journal of Pharmacological Research*, 2, 98-102.

Steensma, DP 2006. JAK2 V617F in Myeloid Disorders: Molecular Diagnostic Techniques and Their Clinical Utility: A Paper from the 2005 William Beaumont Hospital Symposium on Molecular Pathology. *Journal of Molecular Diagnostics*, 8, 397-411.

Tiselius, A 1937. A new apparatus for electrophoretic analysis of colloidal mixtures. *Transactions of the Faraday Society*, 33, 524-531.

Turgeon, ML 2012. Myeloproliferative Neoplasms. *Clinical Haematology: Theory and Procedures*. 5th ed. Philadelphia PA: Lippincott Williams and Wilkins, 361-385.

Wang, X and Seed, B 2006. High-throughput primer and probe design. *In: Dorak, M. (ed.) Real-time PCR*. Taylor & Francis Group, 93-106.

Chapter 3

Sequencing

3.1. Introduction to techniques

Below follows a short explanation on the techniques used for sequencing of part of the *CALR* gene. The methodology used follows thereafter.

3.1.1. Sanger sequencing

The analysis of Sanger sequencing products is according to the following principle: DNA base pairs (bp) adenine (A), cytosine (C), guanine (G) and thymine (T) are each chemically labelled using a different fluorescent dye that facilitates detection and identification of the deoxyribonucleic acid (DNA) sequence of interest (Applied Biosystems, 2010a). Molecules from the samples are injected into thin, fused-silica capillaries that have been filled with a polymer (Applied Biosystems, 2010a). High voltage is then applied between the positive electrode and a negative electrode so that the negatively charged DNA will migrate through the polymer towards the positive electrode (Applied Biosystems, 2010a).

The fluorescently labelled DNA fragments, which are at this point separated by size, move through the path of a laser beam before reaching the positive electrode. The laser beam causes the dyes on the bases to fluoresce (Applied Biosystems, 2010a). An optical detection device, the charge-coupled device (CCD) camera, then captures the fluorescent signals and the Data Collection Software converts the fluorescence signal to digital data (Applied Biosystems, 2010a). After the data is processed, it is analyzed using specific Analysis Software and displayed as chromatograms (Applied Biosystems, 2010a).

3.1.2. Next generation sequencing

As previously mentioned, the initial discovery of the calreticulin exon 9 mutations occurred in 2013 when two groups performed whole exome sequencing and targeted re-sequencing of the calreticulin exon 9 (Klampfl *et al.*, 2013; Nangalia *et al.*, 2013). Libraries were sequenced using the Illumina HiSeq platform, a type of next generation sequencing method (Klampfl *et al.*, 2013; Nangalia *et al.*, 2013).

Since 2009, there has been a major move away from the use of Sanger sequencing for the analysis of genomes (Metzker, 2010). Before this move, the automated Sanger sequencing method had dominated the industry for almost two decades, undergoing many technical improvements in this time (Metzker, 2010). Despite this, the limitations of automated Sanger sequencing indicated a need for novel and enhanced technologies for sequencing an immense number of human genomes (Metzker, 2010). These novel technologies, referred to as next-generation sequencing (NGS), are made up of various strategies that depend on a combination of: 1) template preparation, 2) sequencing and imaging, and 3) and genome alignment and assembly methods (Metzker, 2010). Next-generation sequencing is a blanket term that is used to refer to the high throughput DNA sequencing technologies available which can sequence a large number of different DNA sequences in a single reaction (Rizzo and Buck, 2012). The major advantage offered by NGS is the ability to produce an enormous amount of data within a short time frame (Metzker, 2010).

The aim of this chapter was to use Sanger sequencing to determine the nucleotide sequences of the exon 9 amplicons obtained from the patient samples. Sanger sequencing was used as it was the most cost-effective and readily available method in this study setting. This was done to confirm the results obtained by conventional polymerase chain reaction (PCR) and to compare those results with the available sequencing data as sequencing is currently the most effective method in *CALR* mutation testing.

3.2. Materials and Methods

3.2.1. Sanger sequencing

Sanger sequencing of the conventional PCR products was performed using the BigDye® Terminator v3.1 Cycle Sequencing kit (Applied Biosystems, Foster City, CA, USA) protocol on the ABI 3130 Genetic Analyzer (Thermo Fisher Scientific, Waltham, MA, USA) (Applied Biosystems, 2010b).

Polymerase chain reaction products that were purified using the DNA Clean & Concentrator TM-25 kit (Zymo Research Corporation, Irvine, CA, USA) were used in the sequencing reactions. This was done according to section 2.2.7. The products were eluted in 30 µl of Elution Buffer (Zymo Research Corporation). The reaction mixtures were prepared according to Table 3.1 where there existed a forward and a reverse reaction for each sample. The primers used for the reaction mixtures for Sanger sequencing were identical to the primers described in section 2.2.4.

Table 3.1: Preparation of reaction mixtures for Sanger sequencing

Component	Volume/reaction (1 X)	Final concentration
5x sequencing buffer	3.00 µl	0.75 X
Terminator mix	1.00 µl	(1/8 reaction)
Forward/Reverse primer (3.2 pmol/µl)	1.00 µl	3.20 pmol/reaction
ddH ₂ O	13.00 µl	
PCR product	2.00 µl	
Total	20.00 µl	

The reactions mixtures were vortexed (Velp Scientifica, Usmate Velate, Italy) and pulse centrifuged (Hermle AG, Gosheim, Germany) briefly. The tubes were placed in the BioRad DNA Engine® Peltier Thermal Cycler (Bio-Rad, Hercules, CA, USA) and subjected to the PCR cycling parameters in Table 3.2.

Table 3.2: Cycle sequencing program on the BioRad DNA Engine® Peltier Thermal Cycler (Bio-Rad)

	Number of cycles	Time	Temperature
Initial denaturation	1	3 min	94°C
3-step cycling:	25		
Denaturation		30 sec	94°C
Annealing		10 sec	50°C
Extension		4 min	60°C
Purify		HOLD	4°C

After PCR, the products were purified for analysis by adding 2 µl of 125 mM EDTA, 2 µl of 3 M sodium acetate (NaAc, pH 5.2) and 50 µl of absolute ethanol (EtOH). The mixture was vortexed briefly to ensure proper mixing and then incubated at room temperature (20°C to 24°C) for 15 minutes. The sample was centrifuged (Hettich, Tuttlingen, Germany) at 14,000 x g for 20 minutes at 4°C and the supernatant was subsequently removed by pipetting. The pellet was washed with 100 µl of 70% EtOH and spun again at 14,000 x g for 10 minutes at 4°C. The supernatant was again removed by pipetting. Finally the sample was dried at 95°C for 5 minutes using the heating block of the BioRad DNA Engine® Peltier Thermal Cycler (Bio-Rad).

The sample was submitted for sequencing analysis to be performed at the Human Genetics department on the ABI 3130 Genetic Analyzer (Applied Biosystems). The bioinformatic analysis of the sequencing data was performed, using the CLC Main Workbench version (Qiagen, USA). The electropherograms were expected to show single peaks at each nucleotide position up to the point where the mutation (52-bp deletion or 5-bp insertion) is detected. The peaks were individually read and compared to the known sequence of the wild type reference sequence, obtained from GenBank (Accession number: NG_029662). Sequence alignments were generated using the CLC Main Workbench (Qiagen), to show the presence of the deletion or insertion of the mutant allele.

3.3. Results and Discussion

The purpose of this study was to compare a host of molecular methods for detecting *CALR* mutation type 1 and type 2 with results obtained by sequencing of a fragment of the calreticulin gene at exon 9. The electropherograms depicted in Figure 3.1 indicates what a wild type sequence should look like at both mutation points. The artefacts visible in A, could be due to the presence of unused and partially removed dye which may appear as a large peak. The electropherograms shown in Figure 3.2 shows the sequences of the sample labelled DEL (A) and the sample labelled INS (B). In the case of a type 1 mutation, the first 7-bp of the deletion area are identical to the first 7-bp following the deletion area. This is why no double peaks were observed for this part of the sequencing data.

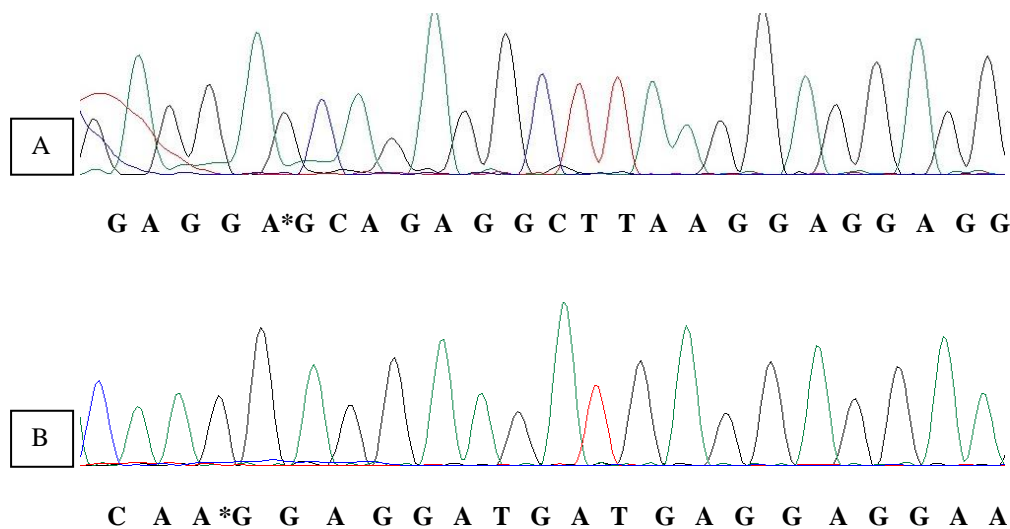


Figure 3.1: Sanger sequencing electropherograms of sequences exhibiting no type 1 (A) or type 2 (B) mutations. The asterisks (*) indicate where mutations would have occurred in both cases. Both sequences are from patient 19

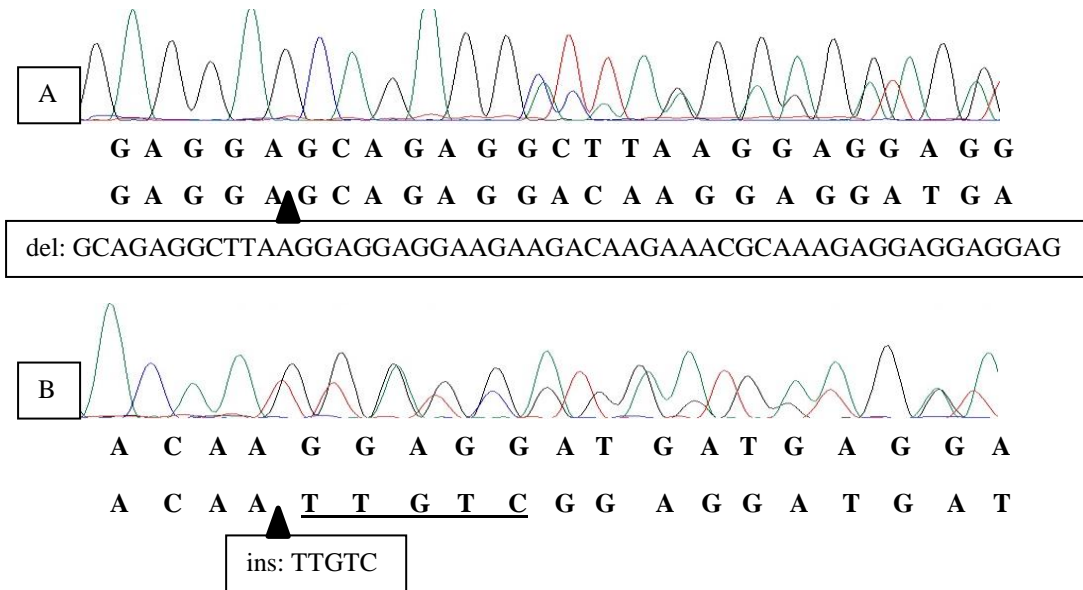


Figure 3.2: Sanger sequencing electropherograms of the two samples representative of the type 1 (A) and type 2 (B) mutations. A: sample DEL, B: sample INS. The top row of nucleotides refers to the sequence of the wild type strand and the bottom row refers to the sequence of the mutated strand. The box below each figure indicates the change to the strand and the sequence of the specific change

From the literature, it is known that Sanger sequencing can obtain a sensitivity and specificity of 89.3% and 100% when detecting calreticulin mutations (Park *et al.*, 2015). The sequencing data that was obtained in this study indicated that 45 of the samples did not contain either the type 1 or type 2 calreticulin mutation. Three of the samples showed the presence of the type 1 mutation and two of the samples showed the presence of the type 2 mutation. Sanger sequencing confirmed the presence or absence of the calreticulin mutations that were found using conventional PCR. The presence in the study population of the type 1 and type 2 mutations were only 6% and 4% respectively, (with a combined total of 10% in the study population), and no other mutations were detected in the sequenced fragments. Access to patients limited the required sample size of 62 to 50 patients. In the study a 100% agreement (Cohen’s Kappa=1, Sensitivity=100%, Specificity=100% and hence no false positives and false negatives) between sequencing and the developed in-house PCR assay were observed.

Compared to literature where the prevalence of the *CALR* type 1 and type 2 mutations was 50% to 70% and 33% to 58% in European and Asian populations, respectively, this study showed that only 10% (N=50; 95% CI) of patients had type 1 or type 2 mutations (Klampfl *et al.*, 2013; Nangalia *et al.*, 2013). Table 3.3 provides a summary of the mutations found in this study.

Table 3.3: Samples found to contain type 1 or type 2 mutations

Patient	Mutation type	Diagnosis	Sex	Ethnicity	JAK2+/MPL+
23	Type 1	ET	F	Caucasian	Negative
J22	Type 2	ET	F	Caucasian	Negative
J36	Type 1	ET	F	Caucasian	Negative
DEL	Type 1	Unknown	Unknown	Unknown	Unknown
INS	Type 2	Unknown	Unknown	Unknown	Unknown

These results showed that while our population does not necessarily contain the type 1 or the type 2 mutations (which are the most prevalent *CALR* mutations); our population might be harbouring a higher frequency of the less common *CALR* mutations. Further evaluation of the sequencing data should be done in order to determine whether this is the case. A bigger sample size will be needed in the future to perform a formal method validation. Next generation sequencing might also be a helpful tool in the analysis of *CALR* mutations.

3.4. Conclusion

Sanger sequencing confirmed the absence and presence of the *CALR* type 1 and type 2 mutations in the 50 samples that were analysed in the study. Both the in-house and commercial conventional PCR methods' results were in 100% agreement to the sequencing results which indicated that the conventional PCR, followed by restriction enzyme digestion, successfully detected the wild type as well as the type 1 and type 2 mutations.

References

Applied Biosystems 2010a. *Applied Biosystems 3130/3130xl Genetic Analyzers Getting Started Guide* CA, USA, AppliedBiosystems.

Applied Biosystems 2010b. *BigDye® Terminator v3.1 Cycle Sequencing Kit*, Applied Biosystems.

Klampfl, T, Gisslinger, H, Harutyunyan, AS, Nivarthi, H, Rumi, E, Milosevic, JD, Them, NCC, Berg, T and Gisslinger, B 2013. Somatic Mutations of Calreticulin in Myeloproliferative Neoplasms. *New England Journal of Medicine*, 369, 2379-2390.

Metzker, ML 2010. Sequencing technologies — the next generation. *Nature Reviews Genetics*, 11, 31-46.

Nangalia, J, Massie, CE, Baxter, EJ, Nice, FL, Gundem, G, Wedge, DC, Avezov, E, Li, J, Kollman, K, Kent, DG, Aziz, A, Godfrey, AL, Hinton, J, Martincorena, I, Van Loo, P, Jones, AV, Guglielmelli, P, Tarpey, P and Harding, HP 2013. Somatic *CALR* Mutations in Myeloproliferative Neoplasms with Nonmutated JAK 2. *New England Journal of Medicine*, 369, 2391-2405.

Park, J-H, Sevin, M, Ramla, S, Truffot, A, Verrier, T, Bouchot, D, Courtois, M, Bas, M, Benali, S, Bailly, F, Favre, B, Guy, J, Martin, L, Maynadié, M, Carillo, S and Girodon, F 2015. Calreticulin Mutations in Myeloproliferative Neoplasms: Comparison of Three Diagnostic Methods. *PLoS One*, 10, 1-7.

Rizzo, JM and Buck, MJ 2012. Key Principles and Clinical Applications of "Next-Generation" DNA Sequencing. *American Association for Cancer Research*, 5, 887-900.

Chapter 4

Real-time PCR

4.1. Introduction to techniques

Real-time PCR has been widely used in clinical diagnostics since its introduction in the late 1990s (Hughes and Branford, 2006). This technique uses the same principles that a conventional PCR does, except for the fact that a fluorescent reporter is attached to a probe which binds to the product formed and reports its presence and amount by fluorescence (Kubista *et al.*, 2006).

4.1.1. Real-time PCR

The detection and quantification of chromosomal translocations in clinical oncology is regarded as a useful method to diagnose various types of haematological malignancies, to confirm whether treatment is successful and to monitor minimal residual disease (MRD) after treatment (Klein, 2002; Hughes and Branford, 2006). The advantages of real-time polymerase chain reaction (PCR) over conventional or nested PCR include: 1) the ability to quantify transcripts, 2) a high technical sensitivity, 3) high precision, 4) no post-PCR steps (minimizing the risk of contamination), 5) high throughput, 6) a decreased turnaround time and 7) the ability to measure products as they accumulate (Ginzinger, 2002; Klein, 2002; Vrsalović *et al.*, 2007).

The ability of the qPCR assay to accurately quantify MRD is a significant selling point for the use of qPCR, especially when dealing with follow-up patients, as mere detection of disease transcripts does not allow for correct prediction of the course of the disease (Bustin and Mueller, 2005). Real-time PCR is also employed to monitor the effects of graft-versus-lymphoma effects after stem cell transplantation (Klein, 2002).

Fluorescence is almost exclusively used as the detection method in qPCR and the employment of fluorescent chemistry is used to effect the kinetic measurement of product accumulation (Kubista *et al.*, 2006; Tevfik Dorak, 2006). These may include compounds that are non-specific such as the DNA intercalating dye, SYBR Green, or oligoprobes specific for certain sequences which employ fluorescent resonance energy transfer (FRET) (Tevfik Dorak, 2006).

Asymmetric cyanine dyes such as SYBR Green I have become the most popular dyes for use in qPCR (Kubista *et al.*, 2006). These dyes become brightly fluorescent when they bind to double-stranded DNA with the amount of fluorescence increasing as the amount of product formed increases per cycle (Kubista *et al.*, 2006).

High resolution melt (HRM) analysis is another technique that makes use of saturated double stranded DNA binding dyes (Tevfik Dorak, 2006). The technique makes use of mutation scanning by melting analyses which makes it inherently inexpensive as well as sensitive (Tevfik Dorak, 2006).

Fluorescently labelled probes are based on nucleic acids and can be of two kinds: 1) fluorophores with intrinsically strong fluorescence, and 2) fluorophores whose fluorescent properties change upon binding nucleic acids (Kubista *et al.*, 2006). Currently, there are several distinct assay systems that employ the use of probes: 1) hydrolysis probes, 2) Molecular Beacons, 3) minor groove binding (MGB) probes, 4) Locked nucleic acid (LNA) probes, and 5) hybridization probes (FRET probes) (Tevfik Dorak, 2006).

The most well-known probe-based system is the *TaqMan* system which utilizes the 5'-3' exonuclease activity of *Taq* polymerase to assess target sequences in samples (Figure 4.1) (Pfaffl, 2004; Arya *et al.*, 2005). Attached to the 5'-end of the *TaqMan* probe, is a fluorescent reporter dye and attached to the 3'-end is a quencher dye (Arya *et al.*, 2005).

When the probe's target is present on the DNA sequence, the probe binds downstream from one of the primer sequences (Arya *et al.*, 2005). During the extension step of the PCR, the fluorogenic probe is cleaved by the 5'-nuclease activity of the *Taq* polymerase enzyme (Arya *et al.*, 2005).

As long as the probe is still intact, fluorescent emission of the reporter dye is absorbed by the quenching dye (Arya *et al.*, 2005). Cleavage or hydrolysis of the probe by *Taq* polymerase causes the fluorophore to separate from the quencher which results in the release of a fluorescent signal (Pfaffl, 2004; Arya *et al.*, 2005).

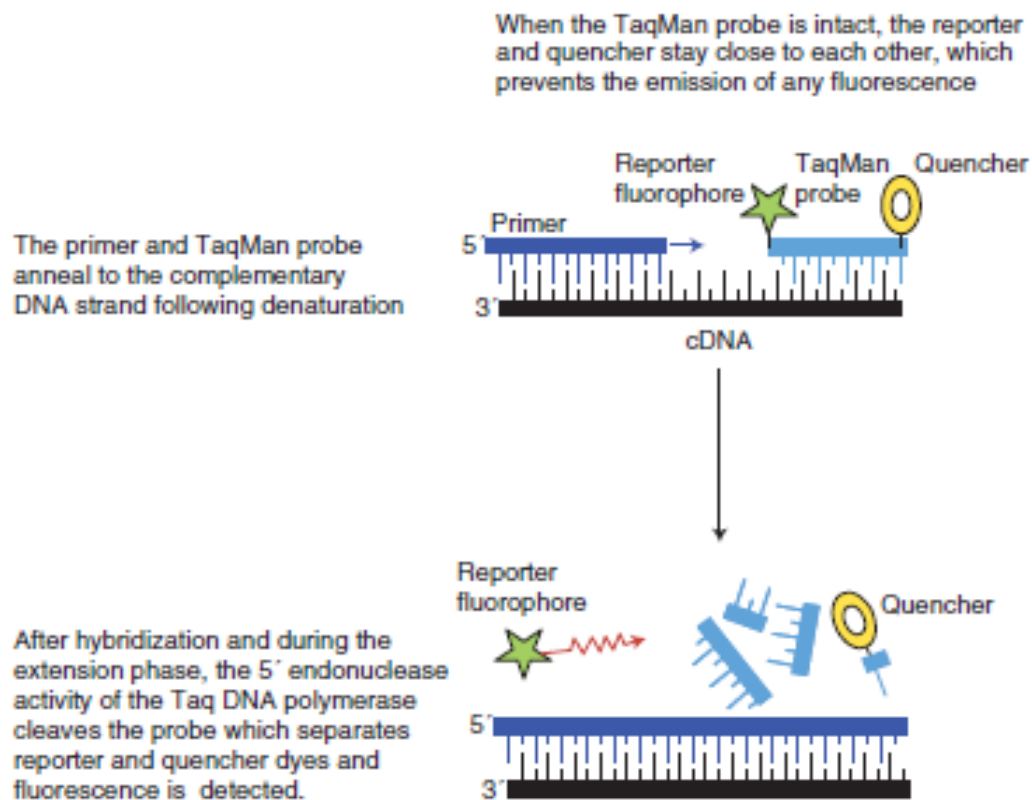


Figure 4.1: Hydrolysis probes (e.g., *TaqMan* assay) (Arya et al. 2005)

Limited data is available on the use of qPCR for the detection of *CALR* type 1 and type 2 mutations. The aim of this chapter was to develop and test a qPCR assay using SYBR Green, an HRM analysis using EvaGreen and a qPCR assay using hydrolysis probes.

4.2. Materials and Methods

The concentrations of the DNA determined by the NanoDrop™ 2000c Spectrophotometer (Thermo Fisher Scientific, Waltham, MA, USA) differed greatly between each sample of extracted DNA. Therefore, the volume of DNA added to each reaction mix was individually determined to ensure that a total DNA content of 100 ng was added to the PCR reaction tubes.

In the case of probe-based qPCR, it was later determined that a total content of 20 ng of the controls' DNA added to the reaction yielded a better result. The primers used for the qPCR using SYBR Green, the qPCR using HRM as well as the qPCR using probes, are described in section 2.2.4.

4.2.1. Real-time PCR using SYBR Green

Two kits were used to test qPCR using SYBR Green. Below follows both methodologies.

4.2.1.1. QuantiNova™ SYBR® Green PCR

A qPCR assay using SYBR Green was performed according to the QuantiNova™ SYBR® Green PCR kit (Qiagen, Hilden, Germany) protocol. The 2x QuantiNova SYBR Green PCR Master Mix (Qiagen), template DNA, primers (Integrated DNA Technologies, Coralville, IO, USA), and sterile double distilled water (ddH₂O) were thawed on ice and a reaction mix was prepared according to Table 4.1.

Table 4.1: Preparation of real-time PCR with QuantiNova (Qiagen) SYBR Green reaction setup on the SmartCycler® (Cepheid)

Component	Volume/reaction	Final concentration
2x QuantiNova SYBR Green PCR Master Mix (Qiagen)	12.50 µl	1x
Forward Primer (10.00 µM)	1.75 µl	0.70 µM
Reverse Primer (10.00 µM)	1.75 µl	0.70 µM
ddH ₂ O	Variable	-
Template DNA	Variable	≤100 ng/reaction
Total reaction volume	25.00 µl	

The reaction mix was mixed thoroughly and appropriate volumes were dispensed into SmartCycler® tubes (Cepheid, Sunnyvale, CA, USA). Template DNA was added to the individual tubes containing the reaction mix.

Double distilled water was added to make up a total volume of 25 µl. The real-time SmartCycler® (Cepheid, Sunnyvale, CA, USA) was programmed according to the program outlined in Table 4.2. Data acquisition was performed during the combined annealing/extension step.

Table 4.2: Real-time PCR with QuantiNova (Qiagen) SYBR Green cycler conditions on the SmartCycler® (Cepheid)

Step	Number of cycles	Time	Temperature
PCR initial activation step	1	2 min	95°C
Two-step cycling: Denaturation Combined annealing/extension	40	5 sec 10 sec	95°C 60°C
Melting curve analysis: 45°C-95°C at 0.2°C/sec			

The SmartCycler® (Cepheid) tubes were briefly pulse centrifuged (Hermle AG, Gosheim, Germany), placed in the real-time SmartCycler® (Cepheid) and the cycling program was started. Melt curve analysis of the PCR products was performed to distinguish between the wild type and the type 1 and type 2 *CALR* mutations.

The qPCR using QuantiNova SYBR Green PCR Master Mix (Qiagen) was also performed on another instrument in the Department of Chemical Pathology. There, the Rotor-Gene® Q (Qiagen) was used and the reaction was set up according to Table 4.3.

Table 4.3: Real-time PCR with QuantiNova (Qiagen) SYBR Green reaction setup on the Rotor-Gene® Q (Qiagen)

Component	Volume/reaction	Final concentration
2x QuantiNova SYBR Green PCR Master Mix (Qiagen)	10.00 µl	1x
Forward Primer (10.00 µM)	1.40 µl	0.70 µM
Reverse Primer (10.00 µM)	1.40 µl	0.70 µM
ddH ₂ O	Variable	-
Template DNA	Variable	≤100 ng/reaction
Total reaction volume	20.00 µl	

The reaction mix was mixed thoroughly and appropriate volumes were dispensed into 200 µl PCR tubes. Template DNA was added to the individual tubes containing the reaction mix. Double distilled water was added to make up a total volume of 20 µl. The Rotor-Gene® Q (Qiagen) was programmed according to the program outlined in Table 4.4. Data acquisition was performed during the combined annealing/extension step.

Table 4.4: Real-time PCR with QuantiNova (Qiagen) SYBR Green cyclers conditions on the Rotor-Gene® Q (Qiagen)

Step	Number of cycles	Time	Temperature
PCR initial activation step	1	2 min	95°C
Two-step cycling: Denaturation Combined annealing/extension	40	5 sec 10 sec	95°C 60°C
Melting curve analysis: 45°C-95°C at 0.2°C/sec			

The 200 µl tubes were placed in the Rotor-Gene® Q (Qiagen) and the cycling program was started. Melt curve analysis of the PCR products was performed to distinguish between the wild type and the type 1 and type 2 *CALR* mutations.

4.2.1.2. SensiFAST™ SYBR® Green PCR

A qPCR assay using SYBR Green was also performed according to the SensiFAST™ SYBR No-ROX PCR kit (Bioline, London, UK) handbook protocol. The SensiFAST™ SYBR No-ROX PCR Master Mix (Bioline), template DNA, primers (Integrated DNA Technologies), and sterile ddH₂O were thawed on ice and a reaction mix was prepared according to Table 4.5.

Table 4.5: Real-time PCR with SensiFAST™ SYBR® No-ROX (Bioline) SYBR Green reaction setup on the Rotor-Gene® Q (Qiagen)

Component	Volume/reaction	Final concentration
SensiFAST™ SYBR® No-ROX PCR Master Mix (Bioline)	10.00 µl	1x
Forward Primer (10.00 µM)	0.80 µl	0.40 µM
Reverse Primer (10.00 µM)	0.80 µl	0.40 µM
ddH ₂ O	Variable	-
Template DNA	Variable	≤100 ng/reaction
Total reaction volume	20.00 µl	

The reaction mix was mixed thoroughly and appropriate volumes were dispensed into 200 µl PCR tubes. Template DNA was added to the individual tubes containing the reaction mix. Double distilled water was added to make up a total volume of 20 µl. The Rotor-Gene® Q (Qiagen) was programmed according to the program outlined in Table 4.6.

Table 4.6: Real-time PCR with SensiFAST™ SYBR® No-ROX (Bioline) SYBR Green cycler conditions on the Rotor-Gene® Q (Qiagen)

Step	Number of cycles	Time	Temperature
PCR initial activation step	1	3 min	95°C
3-step cycling: Denaturation Annealing Extension	40	5 sec 10 sec 20 sec	95°C 60°C 72°C
Melting curve analysis: 45°C-95°C at 0.2°C/sec			

Melt curve analysis of the PCR products was performed to distinguish between the wild type and the type 1 and type 2 *CALR* mutations.

4.2.1.3. SensiFAST™ High Resolution Melt PCR

A qPCR assay using HRM EvaGreen® was performed according to the SensiFAST™ HRM kit (Bioline) protocol. The SensiFAST™ HRM Master Mix (Bioline), template DNA, primers (Integrated DNA Technologies), and ddH₂O were thawed on ice and a reaction mix was prepared according to Table 4.7.

Table 4.7: Real-time PCR with SensiFAST™ HRM (Bioline) reaction setup on the Rotor-Gene® Q (Qiagen)

Component	Volume/reaction	Final concentration
SensiFAST™ HRM Master Mix (Bioline)	10.00 µl	1x
Forward Primer (10.00 µM)	0.80 µl	0.40 µM
Reverse Primer (10.00 µM)	0.80 µl	0.40 µM
ddH ₂ O	Variable	-
Template DNA	Variable	≤100 ng/reaction
Total reaction volume	20.00 µl	

The reaction mix was mixed thoroughly and appropriate volumes were dispensed into 200 μ l PCR tubes. Sterile double distilled water was added to make up a total volume of 20 μ l. The Rotor-Gene® Q (Qiagen) was programmed according to the program outlined in Table 4.8. Data acquisition was performed during the extension step.

Table 4.8: Real-time PCR with SensiFAST™ HRM (Bioline) SYBR Green cycler conditions on the Rotor-Gene® Q (Qiagen)

Step	Number of cycles	Time	Temperature
PCR initial activation step	1	3 min	95°C
3-step cycling:	40		
Denaturation		5 sec	95°C
Annealing		10 sec	60°C
Extension		20 sec	72°C
Melting curve analysis: 45°C-95°C at 0.2°C/sec			

Melt curve analysis of the PCR products was performed. This was done to distinguish between the wild type and the type 1 and type 2 *CALR* mutations.

4.2.2. Probe design for real-time PCR

Probes (Table 4.9) were designed using the online qPCR probe design tool on the PrimerQuest Tool as well as the OligoAnalyzer 3.1 Tool of the Integrated DNA Technologies' (IDT) (Integrated DNA Technologies, Coralville, IO, USA) website (Integrated DNA Technologies, 2015). When designing probes it was ensured that the guidelines for correct probe design were met. These guidelines included (Tevfik Dorak, 2006): 1) having a probe T_m that is up to 10°C higher than that of both primers, 2) avoiding the use of guanine at the 5'-end of the probe as guanine bases cause quenching of the reporter sequence, 3) having a GC content of 35-65%, and 4) the probe should not be prone to forming secondary structures by self-annealing.

Table 4.9: Probe sequences and characteristics

Probe	Sequence	Length	GC Content	T _m	5'-Modification	3'-Modification
Type 1 Wild Type	5'-CAG AGG CTT AAG GAG GAG GAA GAA GAC-3'	27-bp	51.8 %	67.6°C	6-FAM	BHQ-1™
Type 1 Mutant	5'-CGA GGA GCA GAG GAC AAG GAG G-3'	22-bp	63.6 %	68.2°C	TET	BHQ-1™
Type 2 Wild Type	5'-CAA GGA GGA AGA TGA GGA GGA AGA TGT C-3'	28-bp	50.0 %	67.5°C	Cal 610	BHQ-2™
Type 2 Mutant	5'-TTG TCG GAG GAA GAT GAG GAG GAA G-3'	25-bp	52.0 %	66.2°C	Cy5	BHQ-2™

The Type 1 Wild Type probe was designed to bind on the second nucleotide (C) of the 52-bp deletion while the Type 1 Mutant probe was designed to bind six nucleotides before the area where the 52-bp deletion occurs and 16-bp after it. The Type 2 Wild Type probe was designed to bind three nucleotides before the area where the 5-bp insertion occurs and 20-bp after it while the Type 2 Mutant probe was designed to bind on the first nucleotide (T) of the 5-bp insertion.

4.2.3. Real-time PCR using probes

A qPCR assay using hydrolysis probes was performed according to the QuantiNova™ Probe PCR kit (Qiagen) protocol. The 2x QuantiNova Probe PCR Master Mix (Qiagen), template DNA, primers (Integrated DNA Technologies), probes (Inqaba Biotechnical Industries, Pretoria, South Africa), and ddH₂O were thawed on ice and a reaction mix was prepared according to Table 4.10.

Table 4.10: Real-time PCR with QuantiNova (Qiagen) Probe PCR kit reaction setup on the SmartCycler® (Cepheid)

Component	Volume/reaction	Final concentration
2x QuantiNova Probe PCR Master Mix (Qiagen)	12.50 µl	1x
Forward Primer (10.00 µM)	1.00 µl	0.40 µM
Reverse Primer (10.00 µM)	1.00 µl	0.40 µM
T1 WT Probe (5.00 µM)	1.00 µl	0.20 µM
T1 Mutant Probe (5.00 µM)	1.00 µl	0.20 µM
T2 WT Probe (5.00 µM)	1.00 µl	0.20 µM
T2 Mutant Probe (5.00 µM)	1.00 µl	0.20 µM
ddH ₂ O	Variable	-
Template DNA	Variable	~20 ng/reaction (Controls) ~100 ng/reaction (Patients)
Total reaction volume	25.00 µl	

The reaction mix was mixed thoroughly and appropriate volumes were dispensed into SmartCycler® tubes (Cepheid). Template DNA was added to the individual tubes containing the reaction mix. Sterile double distilled water was added to make up a total volume of 25 µl. The real-time SmartCycler® (Cepheid) was programmed according to the program outlined in Table 4.11.

Table 4.11: Real-time PCR with QuantiNova (Qiagen) probe PCR kit cycler conditions on the SmartCycler® (Cepheid)

Step	Number of cycles	Time	Temperature
PCR initial activation step	1	2 min	95°C
Two-step cycling:	40		
Denaturation		5 sec	95°C
Combined annealing/extension		5 sec	60°C

The SmartCycler® (Cepheid) tubes were pulse centrifuged (Hermle AG) briefly, placed in the real-time SmartCycler® (Cepheid) and the cycling program was started. Data acquisition was performed during the combined annealing/extension step.

The qPCR using hydrolysis probes on the Rotor-Gene® Q was performed according to the QuantiNova™ Probe PCR kit (Qiagen). The reaction mix was prepared according to Table 4.12.

Table 4.12: Real-time PCR with QuantiNova (Qiagen) Probe PCR kit reaction setup on the Rotor-Gene® Q (Qiagen)

Component	Volume/reaction	Final concentration
2x QuantiNova Probe PCR Master Mix (Qiagen)	10.00 µl	1x
Forward Primer (10.00 µM)	0.80 µl	0.40 µM
Reverse Primer (10.00 µM)	0.80 µl	0.40 µM
T1 WT Probe (5.00 µM)	0.80 µl	0.20 µM
T1 Mutant Probe (5.00 µM)	0.80 µl	0.20 µM
T2 WT Probe (5.00 µM)	0.80 µl	0.20 µM
T2 Mutant Probe (5.00 µM)	0.80 µl	0.20 µM
ddH ₂ O	Variable	-
Template DNA	Variable	~20 ng/reaction (Controls) ~100 ng/reaction (Patients)
Total reaction volume	20.00 µl	

The reaction mix was mixed thoroughly and appropriate volumes were dispensed into 200 µl PCR tubes. Template DNA was added to the individual tubes containing the reaction mix. Double distilled water was added to make up a total volume of 20 µl. The Rotor-Gene® Q (Qiagen) was programmed according to the program outlined in Table 4.13.

Table 4.13: Real-time PCR with QuantiNova (Qiagen) Probe PCR kit cycler conditions on the Rotor-Gene® Q (Qiagen)

Step	Number of cycles	Time	Temperature
PCR initial activation step	1	2 min	95°C
Two-step cycling:	40		
Denaturation		5 sec	95°C
Combined annealing/extension		5 sec	60°C

The tubes were placed inside the Rotor-Gene® Q (Qiagen) and the cycling program was started. Data acquisition was performed during the combined annealing/extension step.

4.3. Results and Discussion

4.3.1. Real-time PCR using SYBR Green

Real-time PCR using SYBR Green was initially performed using the QuantiNova™ SYBR® Green PCR kit (Qiagen), as described in 4.2.1., on the SmartCycler® system (Cepheid). As shown in Figure 4.2, the controls were the only samples run in order to first test the SYBR Green run on the SmartCycler® (Cepheid) and to see whether the controls would yield expected results.

The results obtained from this assay were not satisfactory as the melting curves produced double peaks which are associated with heterozygous sequences whereas the controls that were used throughout the analysis were homozygous. The double peaks could be due to possible primer dimer formation during the qPCR analysis. Primer dimers can be avoided by re-designing the primers. Unfortunately, due to budgetary constraints primers could not be re-ordered. When the melting curves were observed closer by zooming in, (Figure 4.2 C), the analysis did not show a typical melt curve analysis.

After the analysis of the qPCR results, the PCR products were analysed using gel electrophoresis (section 2.2.9) to determine whether the PCR protocol was successful and whether it yielded the expected product. The photograph of the gel (Figure 4.3) indicated that the PCR protocol was successful and there was no explanation for the unexpected results observed in the amplification curve or melt curve.

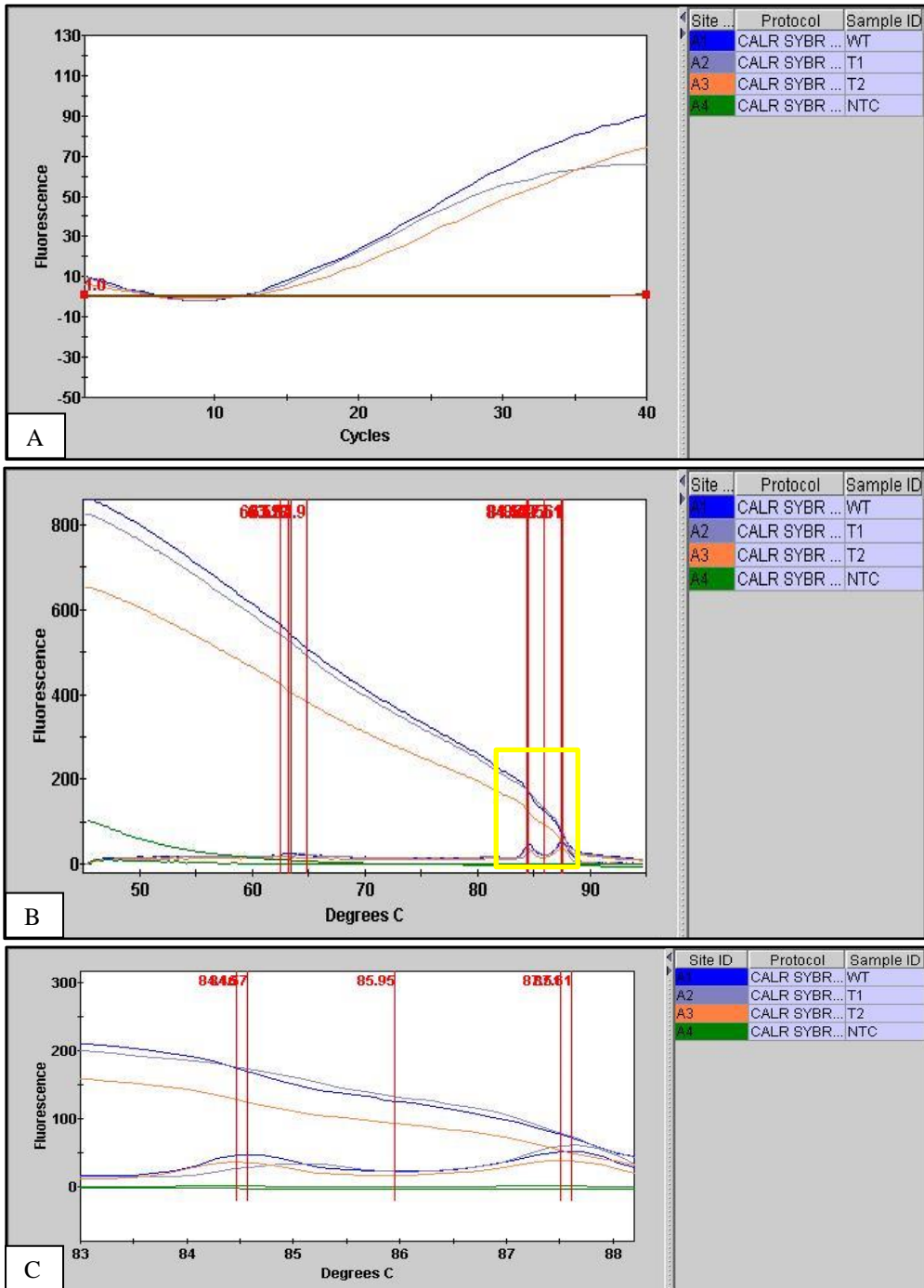


Figure 4.2: SYBR Green analysis using the SmartCycler® (Cepheid) system. A) Amplification curve, B) melting curve (middle) and C) a zoomed in view of the yellow square on the melting curve of a SYBR Green analysis using the QuantiNova (Qiagen) kit

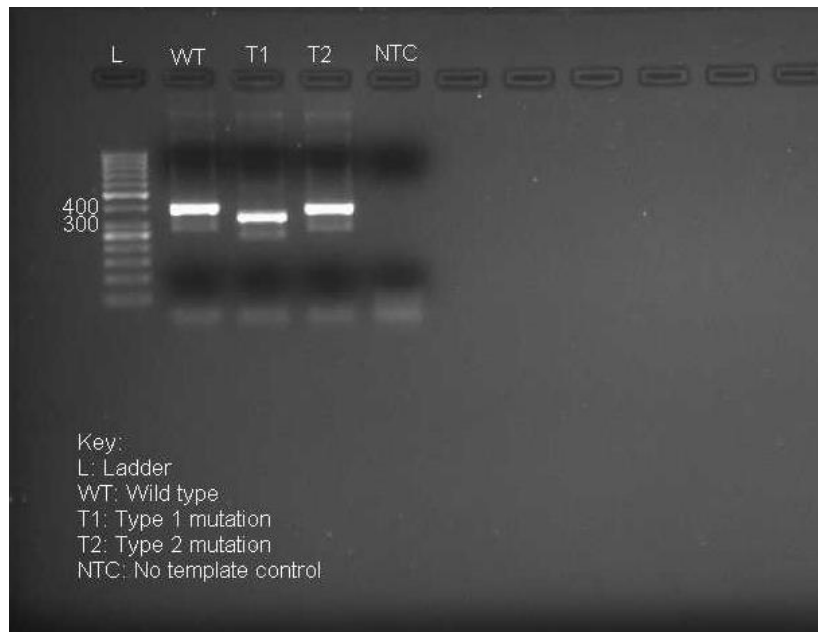


Figure 4.3: Agarose gel electrophoresis of *CALR* exon 9 amplicons produced by a real-time PCR using SYBR Green QuantiNova (Qiagen) kit on the SmartCycler® (Cepheid) system

The unexpected results were at first thought to have been caused by either the SmartCycler® (Cepheid) or the type of kit that was used. It was then decided to compare another kit with the first kit that was tried [the QuantiNova kit (Qiagen)] and to also perform the run on another instrument i.e. the Rotor-Gene® Q (Qiagen). The purpose of using two different kits was to assess whether one of them could give a result that could be pursued and optimized.

From the results of the run (data unavailable), it is clear that the PCR yielded results that could not be interpreted. An agarose gel was prepared using the method outlined in section 2.2.9 and run using the products of this PCR to confirm whether the PCR was successful and produced the expected product sizes. The photograph of the gel (Figure 4.4) confirmed that the PCR itself was successful once again using the QuantiNova kit (Qiagen) on the Rotor-Gene® Q (Qiagen) system.

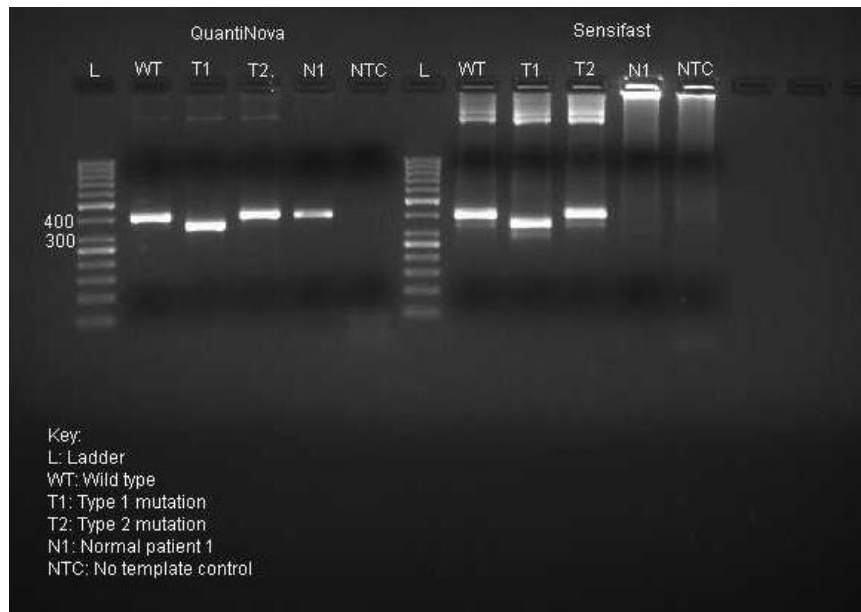


Figure 4.4: Agarose gel electrophoresis of *CALR* exon 9 amplicons produced by a real-time PCR using SYBR Green, comparing the QuantiNova (Qiagen) and SensiFAST™ (Bioline) kits on the Rotor-Gene® Q (Qiagen)

It was found that the run to compare the QuantiNova (Qiagen) and SensiFAST™ (Bioline) kits yielded much the same results as the run on the SmartCycler® (Cepheid). The difference in kits might not have been an optimal experiment as the SensiFAST™ master mix (Bioline) itself was old and might have already expired (no expiry date was listed on the tube). This could have caused and explained the smearing of the PCR products seen in the SensiFAST™ (Bioline) lanes on Figure 4.4.

The different instruments and kits used confirmed that the SYBR Green real-time analysis was not successful and it was not because of the instrument or the kit used. The wild type control and that of the patients' DNA (which were identical in terms of the calreticulin type 1 and type 2 mutations) in both attempts to use SYBR Green, did not yield the same result, which meant that the peaks of the manufactured controls on the melt curve did not correspond with those of the patients' samples. The SYBR Green could not be pursued using the two kits on the two instruments as it was unable to distinguish between the wild type, type 1 and type 2 mutations.

Following the failure of the SYBR Green analyses, a HRM run was also performed. As HRM is very sensitive and able to detect base pair (bp) changes of even 1-bp, it was thought that this analysis would improve the results obtained. As shown in Figure 4.5, the results of the HRM run on the Rotor-Gene® Q indicated that the wild type (WT) control and the normal sample did not yield similar results and the efficacy of the PCR itself was once again confirmed using gel electrophoresis (Figure 4.6).

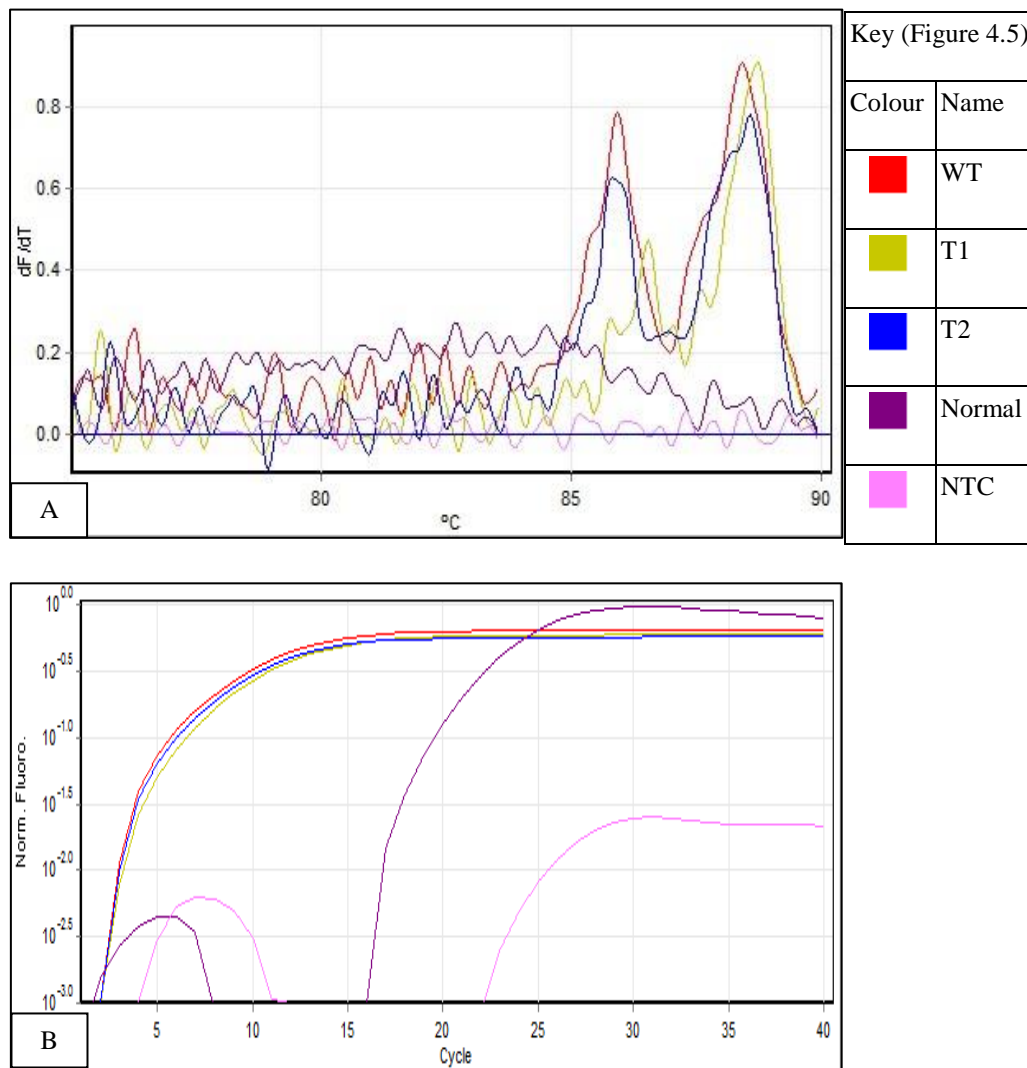


Figure 4.5: Analysis of the HRM run on the Rotor-Gene® Q (Qiagen). A) Melt curve analysis and B) Amplification plot

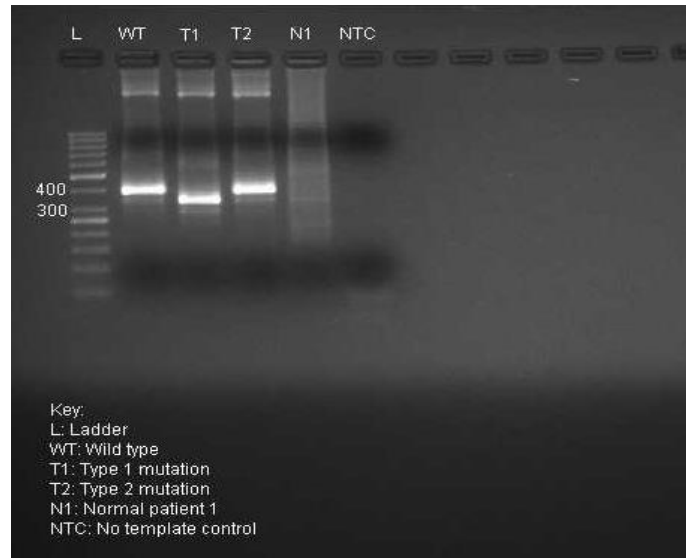


Figure 4.6: Agarose gel electrophoresis of *CALR* exon 9 amplicons produced by a real-time PCR using HRM analysis on the Rotor-Gene® Q (Qiagen)

As an alternative, another PCR using the SYBR Green detection method was attempted using the LightCycler® 2.0 (Roche, Basel, Switzerland) using the protocol outlined in Table 4.1 and Table 4.2. The amplification curves as shown in Figure 4.7 did not have the characteristic sigmoidal shape that is expected from a SYBR Green run and it was not possible to differentiate between the different peaks on the melt curve analysis (Figure 4.8 and Figure 4.9).

As shown in Figure 4.10, sample 2 did not contain enough PCR product in order to be visualized on a gel. The controls did; however, yield the expected results, which again could not provide an explanation as to the unexpected results generated by the LightCycler® 2.0 (Roche) run.

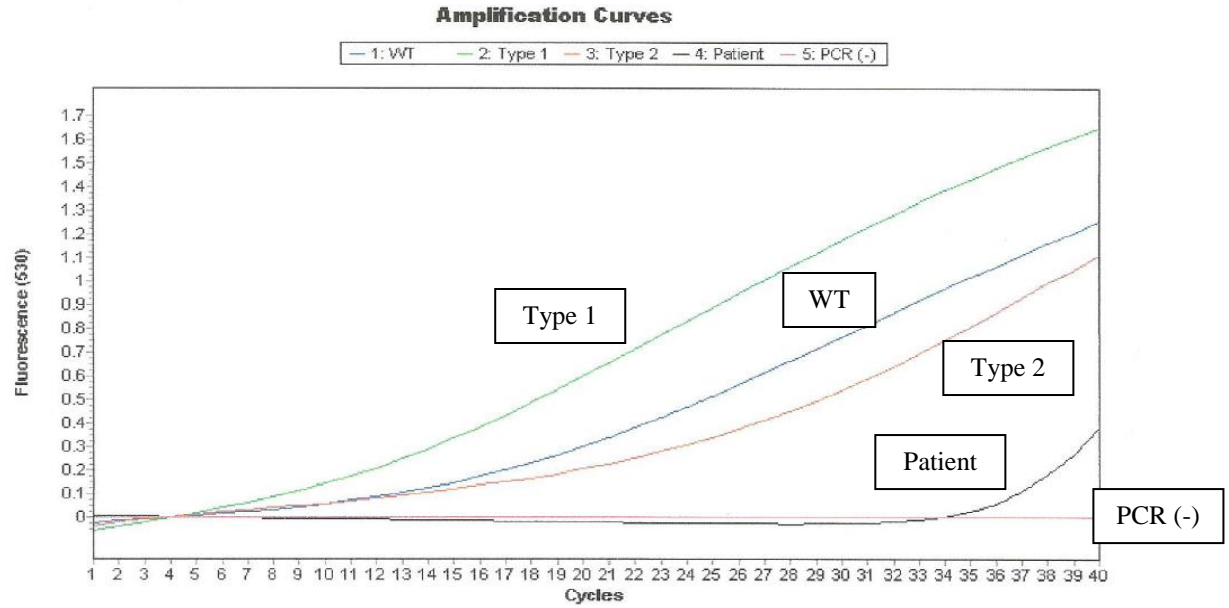


Figure 4.7: Amplification curve analysis of the real-time PCR using SYBR Green on the LightCycler® 2.0 (Roche)

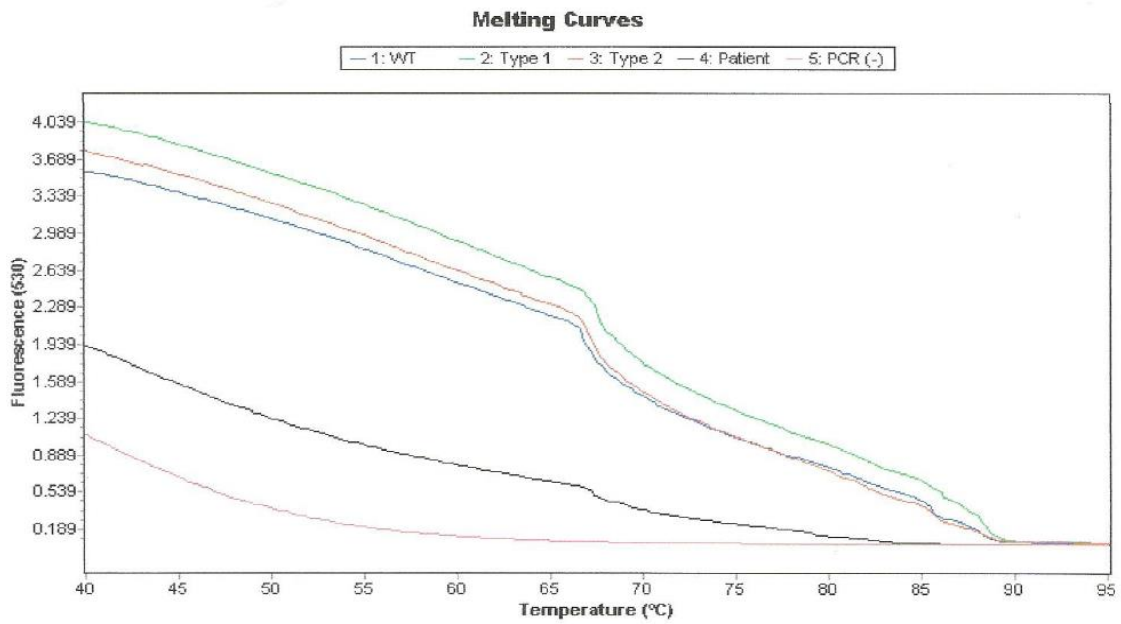


Figure 4.8: Melting curve analysis of the real-time PCR using SYBR Green on the LightCycler® 2.0 (Roche)

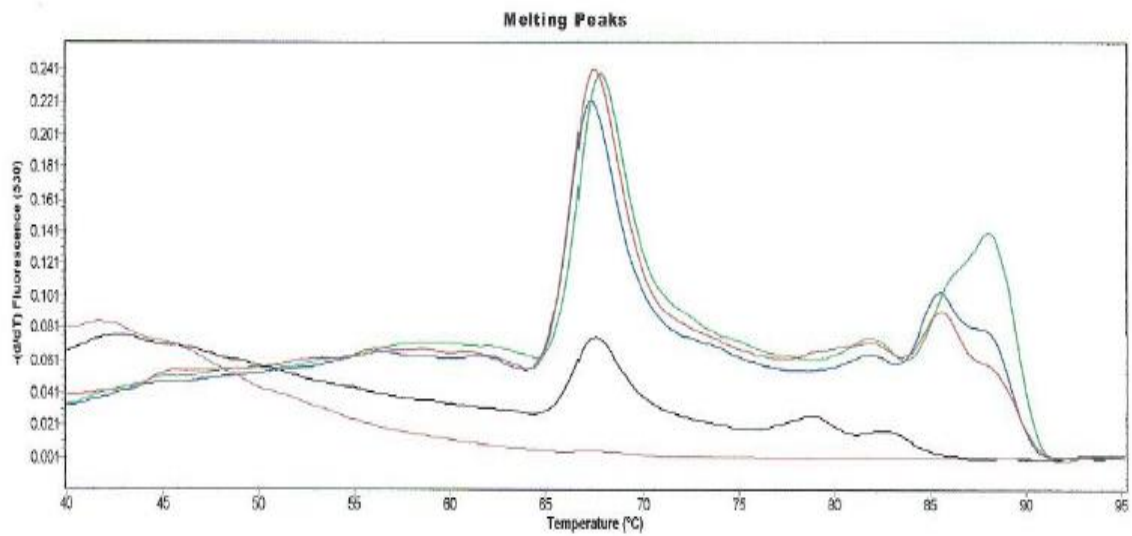


Figure 4.9: Melting peaks of the real-time PCR using SYBR Green on the LightCycler® 2.0 (Roche)

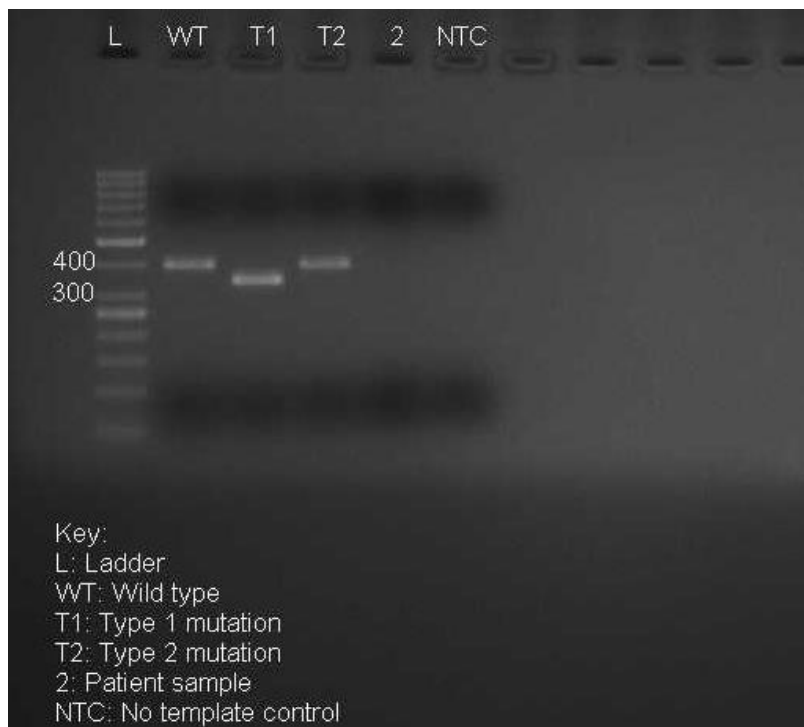


Figure 4.10: Agarose gel electrophoresis of *CALR* exon 9 amplicons produced by a real-time PCR using SYBR Green on the LightCycler® 2.0 (Roche)

The SYBR Green cycling conditions were then changed in a last effort to optimize the run and produce the characteristic sigmoid curves that indicate a good SYBR Green run. The cycling conditions were changed to a three step PCR and the melt curve conditions were modified by increasing the temperature at a slower rate (0.1 degrees/second). As shown in Figure 4.11, even with a newly designed cycling protocol, the real-time SYBR Green assay still did not yield interpretable results. This can be attributed to the fact that the manufactured controls may be producing unexpected results due to the DNA being synthesized in a laboratory rather than being biological in origin. The SYBR Green and HRM analysis was thus abandoned.

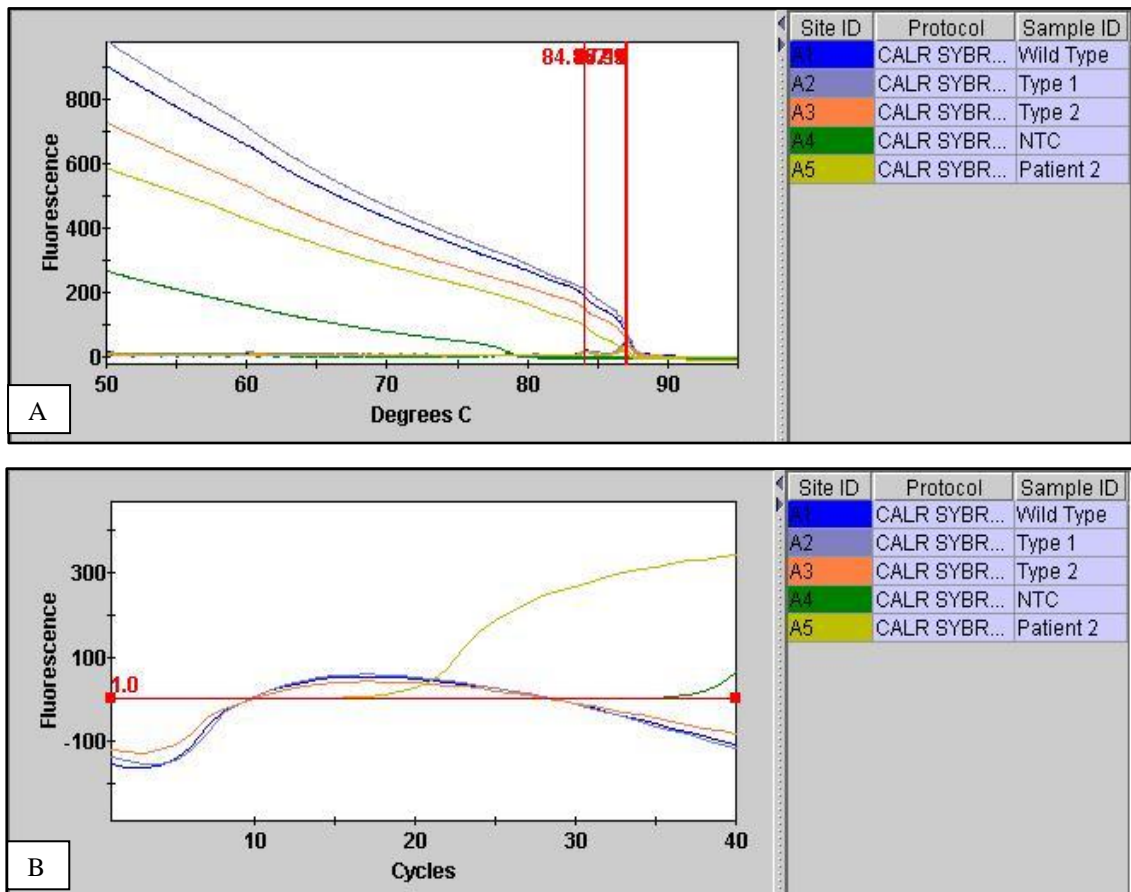


Figure 4.11: A) Melt curve and B) amplification curve analysis of a SYBR Green run using a more optimized protocol on the SmartCycler® (Cepheid)

The use of HRM in the literature to detect the presence of the *CALR* type 1 and type 2 mutations has been widely studied (Bilbao-Sieyro *et al.*, 2014; Enblom *et al.*, 2015; Lim *et al.*, 2015a; Lim *et al.*, 2015b). One of these studies showed that there were distinct HRM patterns to be observed between the type 1 and type 2 mutations and that the HRM used displayed no false positives and mutants could be detected in up to a 3.13% dilution (Bilbao-Sieyro *et al.*, 2014). As previously mentioned, fragment analysis PCR, HRM and Sanger sequencing was compared and it was found that the sensitivity and specificity of HRM to be 96.4% and 96.3% respectively (Park *et al.*, 2015). This technique has proven to be a fast, reliable, economical and high-throughput screening method for the detection of a patient's *CALR* mutation status.

After detecting a mutation, Sanger sequencing is, however, necessary to correctly categorize the mutants seeing as, for example, type 2 mutations are not the only 5-bp insertions that can occur (Bilbao-Sieyro *et al.*, 2014). This is why SYBR Green and HRM, which are assays that rely solely on the melting temperatures of amplified DNA fragments, cannot serve as mutation assays specific for detecting the type 1 and type 2 mutations, but rather as screening assays whose results are to be confirmed by another method.

4.3.2. Real-time PCR using probes

The first qPCR run using probes was performed using the SmartCycler® (Cepheid). The initial run with the first batch of probes was set-up with all four probes present per reaction. Seeing as this was the first test run of the method, only the three commercial controls, as well as a normal sample of DNA and a NTC was included in this run (in order to save reagents). The results of the run showed no fluorescent curves whatsoever (Figure 4.12). The PCR products were immediately run on an agarose gel to determine the presence of any amplified DNA as it seemed as though the qPCR completely failed.

The photograph of the gel on which the PCR products were run clearly indicated that the PCR itself was successful (Figure 4.13). The N1 reaction did not yield optimal results due to the high DNA content.

It was later determined that adding a lower amount of DNA improved the results of this assay. The PCR also produced the appropriately sized fragments which meant that the binding sites for the probes had to be present on the fragments.

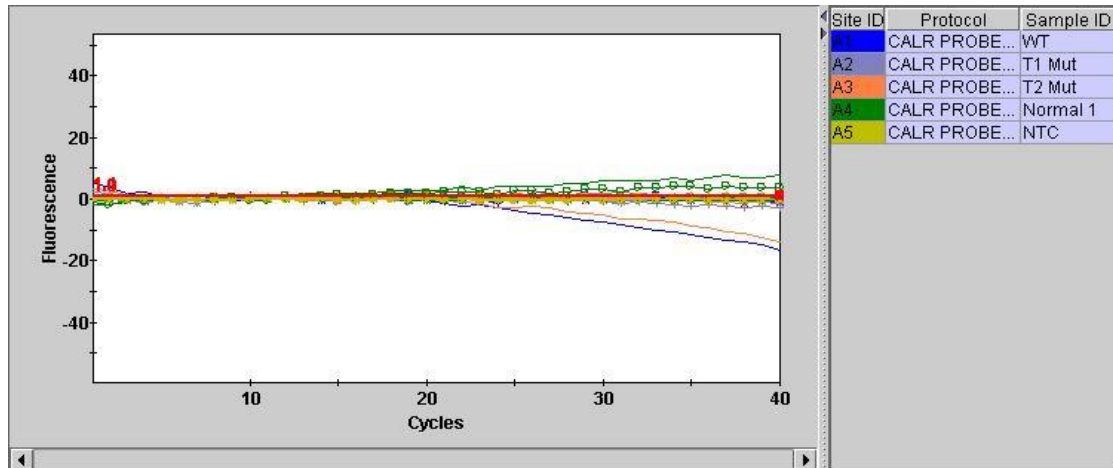


Figure 4.12: Amplification curves of the first attempt at real-time PCR using probes run on the SmartCycler® (Cepheid)

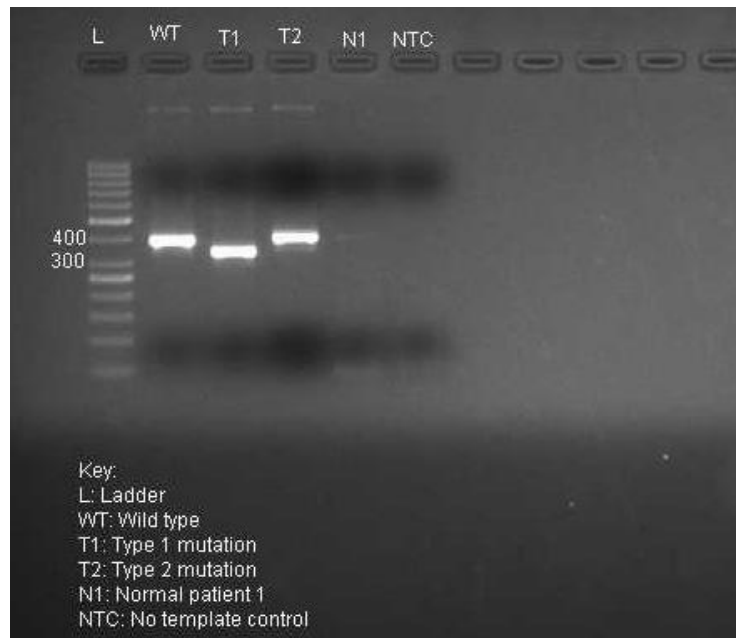


Figure 4.13: Agarose gel electrophoresis of the first real-time PCR amplicons using probes on the SmartCycler® (Cepheid)

The lack of fluorescence from the probes indicated a possible problem with the probes themselves. It was initially thought that the probes were binding to one another, therefore being unable to produce any fluorescence on the real-time graphs.

A new run was set up to test whether the probes were interfering with one another, each reaction only contained the appropriate probe that was supposed to bind to it. The key on Figure 4.14 indicates which probe was added to which sample. Again, only the three commercial controls, as well as a normal sample of DNA and a NTC were included in this run. From Figure 4.14 it is clear that there was still no fluorescence on the graph, which could indicate that the probes were not binding or no fluorescence was detected. The PCR products were run on an agarose gel to determine the presence of any amplified DNA and the gel confirmed that the PCR itself was successful (results not shown).

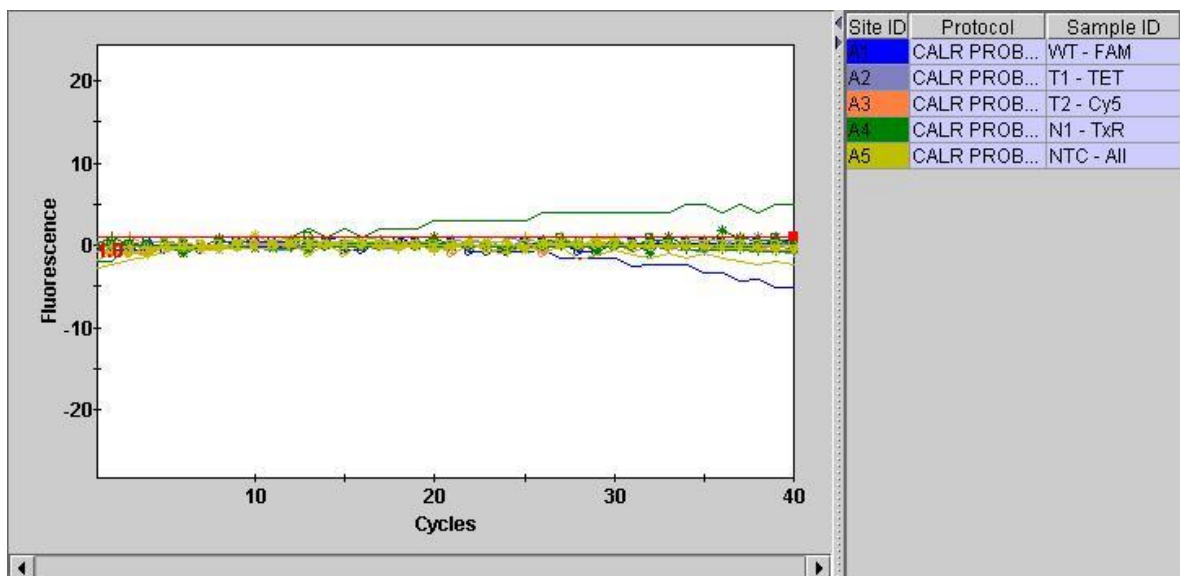


Figure 4.14: Amplification curves of a real-time PCR using probes run using one probe per tube on the SmartCycler® (Cepheid)

The variable that was adjusted next for troubleshooting of the qPCR using probes was the annealing temperature of the reaction. It was considered that the annealing temperature of 60°C that was used at the time might be too high for the different T_m values of the probes (Table 4.9).

The annealing temperature was decreased by 2°C so that the T_m 's of the probes could be within a more acceptable temperature range to the annealing temperature of the primers (Table 2.1). Only the wild type control along with a wild type probe designed to bind to it (labelled with 6-FAM) and an NTC was run in order to save reagents.

The results from Figure 4.15 indicate that the lowering of the T_m did not influence the run in any way and that the probes were still not binding/showing any fluorescence. No additional temperature changes were therefore tested. The PCR products were run on an agarose gel to determine the presence of any amplified DNA and the gel confirmed that the PCR itself was successful (results not shown).

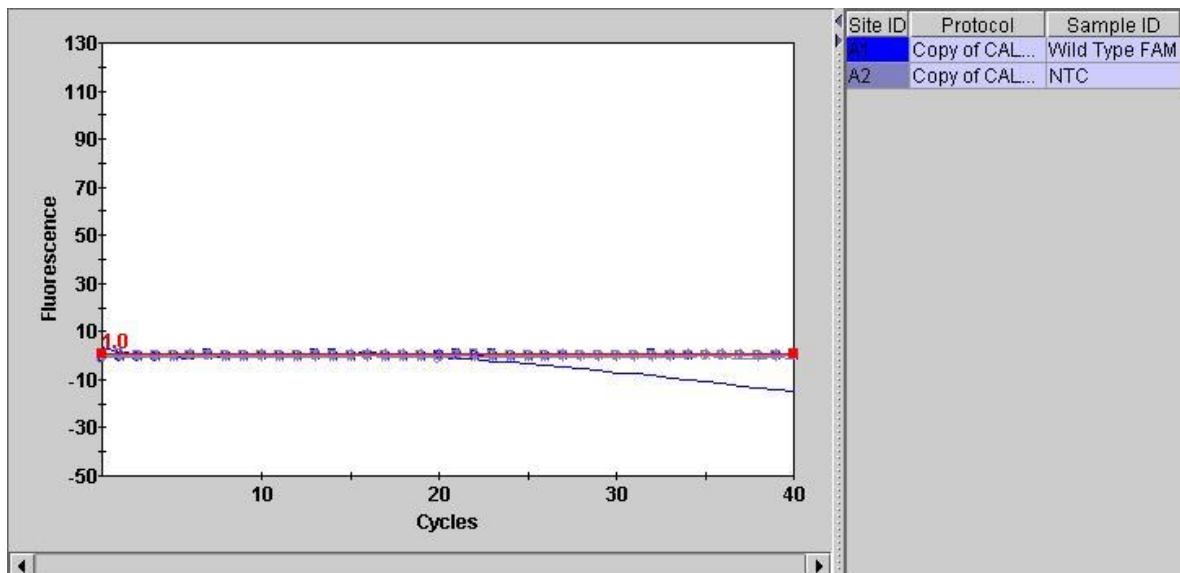


Figure 4.15: Amplification curves of a real-time PCR using probes run with annealing temperature changed on the SmartCycler® (Cepheid)

After the third run with the probes did not produce any results the manufacturers were contacted and troubleshooting assistance was requested. The manufacturer resynthesized the probes and a new batch was received. The first run with the new probes was set up using only the three commercial controls, as well as a patient sample of DNA (labelled J5) and a NTC (Figure 4.16). Each reaction tube again only contained one probe in order to test whether the probes were binding to the sequence they were required to bind to.

The sample in site A1 contained the Type 1 WT probe; the sample in site A2 contained the Type 1 Mutant probe; the sample in site A3 contained the Type 2 Mutant probe; the sample in site A4 contained the Type 2 WT probe and the NTC in site A5 contained all the probes. From Figure 4.16 it is clear that the probes did not fluoresce as was intended.

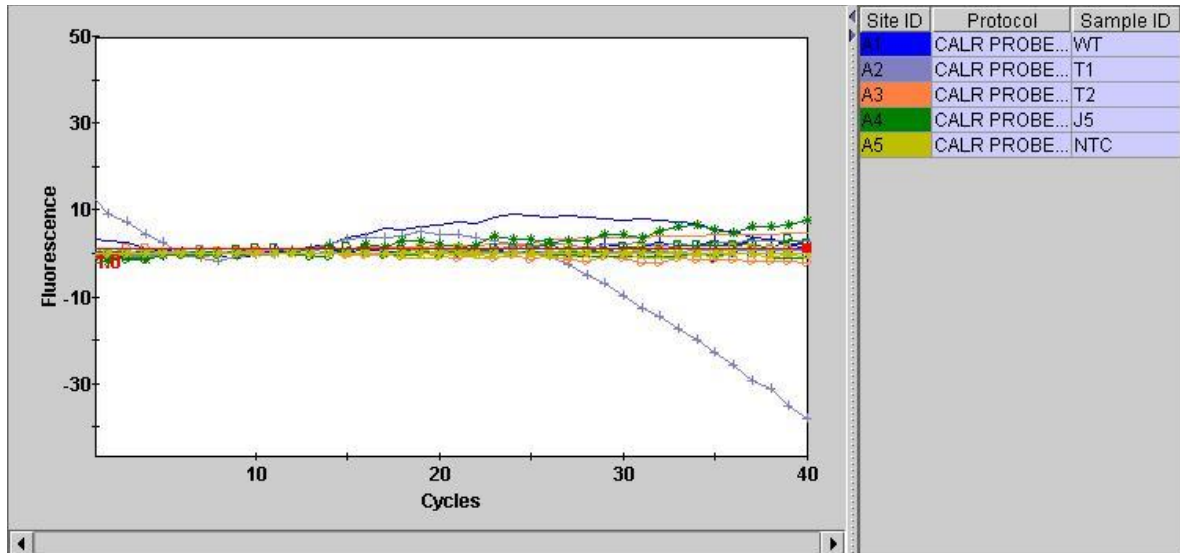


Figure 4.16: Amplification curves of a real-time PCR using new probes run with one probe per tube on the SmartCycler® (Cepheid)

Another variable that was adjusted on the qPCR assay using the SmartCycler® was the DNA amount added to the samples to see whether that would enable the probes to bind. The run was set up to include a total DNA content of 20 ng and 40 ng per control reaction and a total DNA content of 50 ng for the patient (N1) reaction (Figure 4.17).

In all the previous qPCR experiments, a total DNA content of 100 ng was used. The DNA of the patient sample was therefore halved and because of the purity of the manufactured controls, the DNA content was significantly reduced and tested at two lower amounts (20 ng and 40 ng).

The run set up is on the right panel in Figure 4.17. Results showed that sites A3 and A4 performed the best in this run. They both contained the probe labelled with TET and it clearly shows that the sample with the lower amount of DNA (site A4, type 1 Mutant 20 ng) of DNA had the higher peak of fluorescence.

The SmartCycler® (Cepheid) sites A1 and A2, containing reaction mixtures with probes labelled with 6-FAM, also showed an increase in fluorescence, although not as pronounced as the fluorescence in sites A3 and A4. The sample with the lower total DNA (A2 containing the wild type Mutant [20 ng]) of DNA had the higher peak of fluorescence. However, no clear sigmoidal amplification curves were obtained in this experiment.

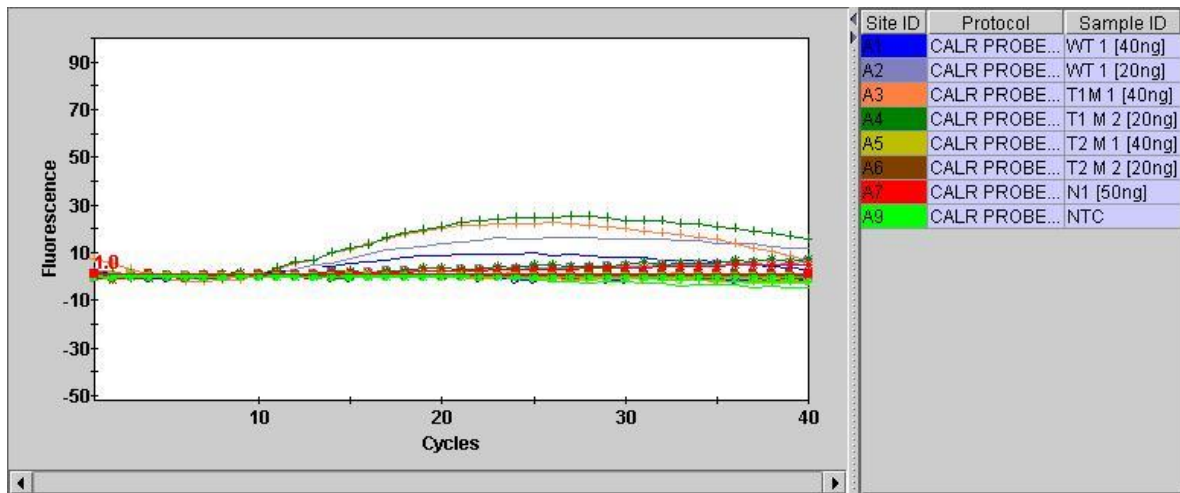


Figure 4.17: Amplification curves of a real-time PCR using new probes run with one probe per tube and different amounts of DNA on the SmartCycler® (Cepheid)

The control samples with a lower DNA content thus performed better in the 6-FAM and TET bound samples. The samples in site A5 and A6, had probes labelled with Cy5, while the sample in site A7 had the Texas Red equivalent probe (Cal 610) added to it. Both of these probes did not fluoresce with no indication as to why. The NTC (with all probes added) showed no amplification as was expected.

Because the newly synthesized probes were still not yielding expected results, the next variable to adjust was the choice of thermal cycler. Subsequently, the Rotor-Gene® Q (Qiagen) was used as alternative. Since it can only read the channels for 6-FAM and TET, only the type 1 mutation's probes could be tested initially.

Figure 4.18 shows the first run performed with the Rotor-Gene® Q (Qiagen) using the type 1 probes with the DNA of the samples set at different amounts of DNA content in order to determine the effect of the different amounts of DNA on the Rotor-Gene® Q (Qiagen). In both the WT and T1 M samples, the number 1 sample had a DNA content of 40 ng whereas the number 2 sample had a DNA content of 20 ng.

As shown in Figure 4.18, the TET probe in T1 M 1 and T1 M 2 produced the most fluorescence (as in the run in Figure 4.17). The probe (6-FAM) in T1 WT 1 and T1 WT 2 also fluoresced as expected. In both cases, the reaction tube with the least amount of DNA (T1 WT 2 and T1 M 2) performed the best, giving the highest fluorescent peaks.

After the satisfactory peaks achieved by the run in Figure 4.18, probes for the type 2 mutation were re-ordered and labelled with 6-FAM and TET as well. This would thus require the assays to be set up as two reactions per patient (one type 1 mutation reaction and a type 2 mutation reaction).

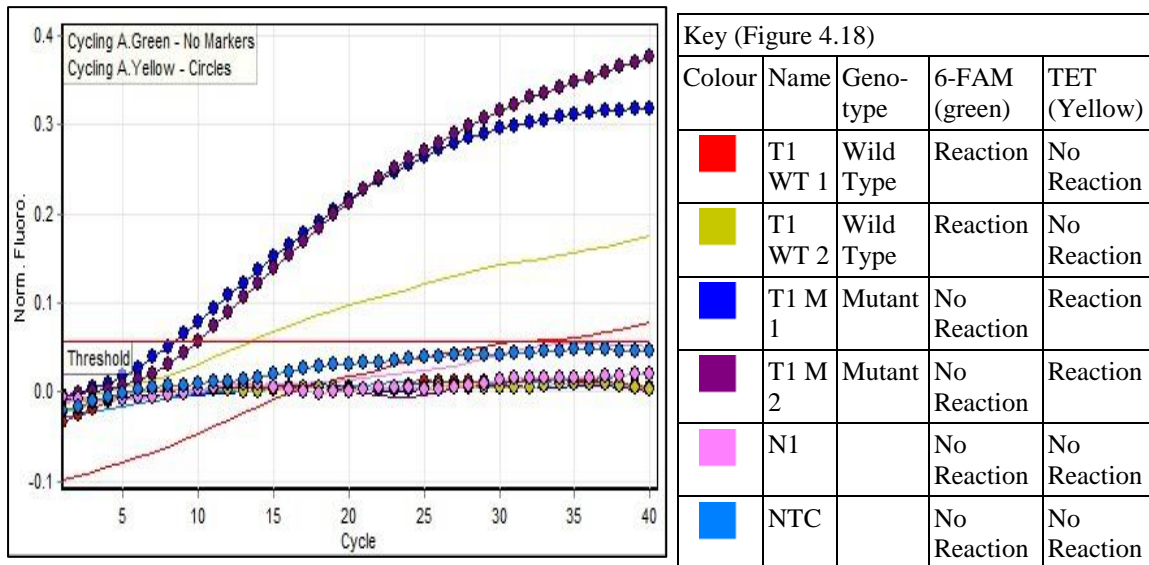


Figure 4.18: Amplification curves of a real-time PCR, using new probes, run with one probe per tube (type 1 probes) and different DNA concentrations on the Rotor-Gene® Q (Qiagen)

Following the initial success of the qPCR performed on the Rotor-Gene® Q (Qiagen), a full run for the type 1 mutation was set up and run on the instrument. During this reaction, both probes were added to the reaction mixture per tube.

According to the results from Figure 4.19 and its key, both probes bound to all samples except for the NTC reaction (where no probes bound as expected) and J6 reaction (where only the mutant probe, TET, fluoresced). Due to the fact that the wild type and mutant probes were both binding to both the wild type and type 1 mutant controls, the entire run's results were rejected.

The probes were also showing fluorescence in the 6-FAM and TET channels on all the patient samples excluding patient J6. This result is impossible as the mutations have been confirmed to be absent in all the samples in this qPCR reaction by means of both conventional PCR and Sanger sequencing.

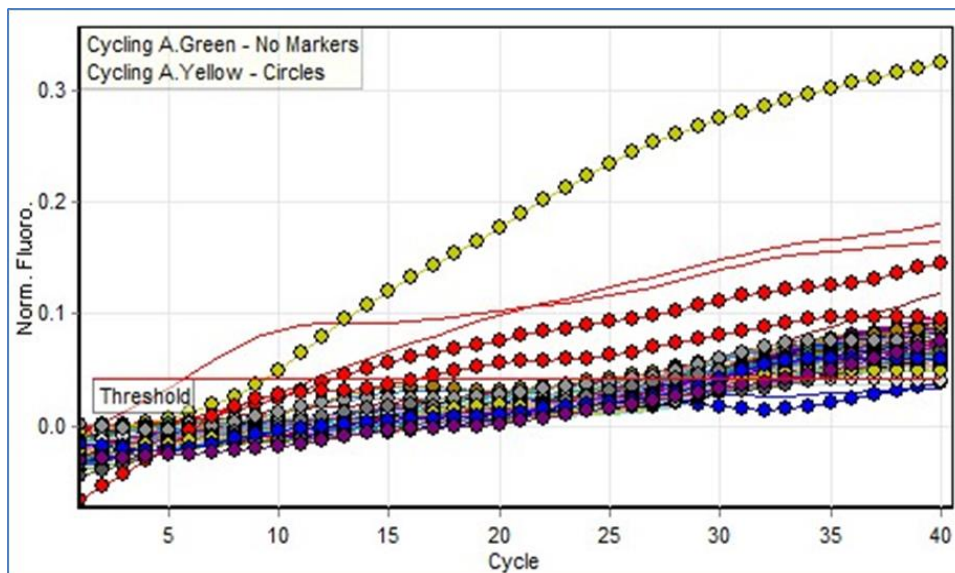































Figure 4.19: Amplification curves of a real-time PCR using new probes run with two probes per tube for the type 1 mutation on the Rotor-Gene® Q (Qiagen)

Key (Figure 4.19)				
Colour	Name	Genotype	6-FAM (green)	TET (yellow)
■	WT	Heterozygous	Reaction	Reaction
■	T1	Heterozygous	Reaction	Reaction
■	NTC		No Reaction	No Reaction
■	2	Heterozygous	Reaction	Reaction
■	4	Heterozygous	Reaction	Reaction
■	5	Heterozygous	Reaction	Reaction
■	10	Heterozygous	Reaction	Reaction



Key (Figure 4.19)

Colour	Name	Genotype	6-FAM (green)	TET (yellow)
	11	Heterozygous	Reaction	Reaction
	12	Heterozygous	Reaction	Reaction
	13	Heterozygous	Reaction	Reaction
	14	Heterozygous	Reaction	Reaction
	15	Heterozygous	Reaction	Reaction
	16	Heterozygous	Reaction	Reaction
	18	Heterozygous	Reaction	Reaction
	19	Heterozygous	Reaction	Reaction
	20	Heterozygous	Reaction	Reaction
	21	Heterozygous	Reaction	Reaction
	23	Heterozygous	Reaction	Reaction
	24	Heterozygous	Reaction	Reaction
	25	Heterozygous	Reaction	Reaction
	26	Heterozygous	Reaction	Reaction
	27	Heterozygous	Reaction	Reaction
	28	Heterozygous	Reaction	Reaction
	29	Heterozygous	Reaction	Reaction
	30	Heterozygous	Reaction	Reaction
	31	Heterozygous	Reaction	Reaction
	J5	Heterozygous	Reaction	Reaction
	J6	Mutant	No Reaction	Reaction
	J9	Heterozygous	Reaction	Reaction
	J19	Heterozygous	Reaction	Reaction
	J23	Heterozygous	Reaction	Reaction
	J25	Heterozygous	Reaction	Reaction
	J26	Heterozygous	Reaction	Reaction
	J27	Heterozygous	Reaction	Reaction
	J28	Heterozygous	Reaction	Reaction
	J29	Heterozygous	Reaction	Reaction

From the results of this reaction (Figure 4.19), it is clear that the qPCR using probes was still not producing the results that were expected. The cycling conditions in (Table 4.13) were re-examined and it was suggested to increase the time on the denaturation as well as the combined annealing/extension steps to ten seconds each instead of the five seconds as recommended in the QuantiNova Probe PCR (Qiagen) kit insert. This would allow more time for the probes to bind and subsequently fluoresce.

From Figure 4.20 and its key, it is clear that this adjustment did not improve the results. In the case of the type 1 mutation, both probes were once again binding to all the patient samples (where only FAM was expected to bind) as well as to both controls, which is not what was expected from the design of the assay.

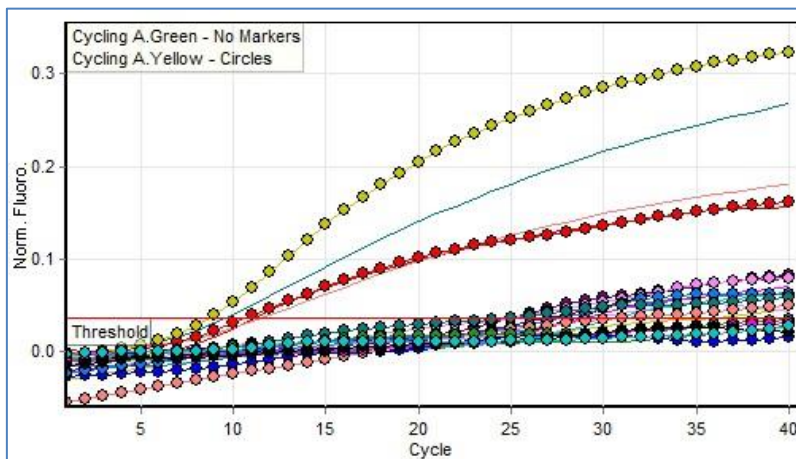






Figure 4.20: Amplification curves of a real-time PCR using new probes run with two probes per tube for the type 1 and type 2 mutations on the Rotor-Gene® Q (Qiagen)

Key (Figure 4.20)				
Colour	Name	Genotype	6-FAM (green)	TET (yellow)
■	T1 WT	Heterozygous	Reaction	Reaction
■	T1 T1	Heterozygous	Reaction	Reaction
■	T1 NTC		No Reaction	No Reaction
■	T1-2	Heterozygous	Reaction	Reaction
■	T1-10	Heterozygous	Reaction	Reaction
■	T1-5	Heterozygous	Reaction	Reaction
■	T2 WT	Heterozygous	Reaction	Reaction
■	T2 T2	Heterozygous	Reaction	Reaction

Key (Figure 4.20)				
Colour	Name	Genotype	6-FAM (green)	TET (yellow)
	T2 NTC		No Reaction	No Reaction
	T2-2	Wild Type	Reaction	No Reaction
	T2-10	Wild Type	Reaction	No Reaction
	T2-5	Wild Type	Reaction	No Reaction

A final run was performed using a sample probe specific for the type 1 wild type which was synthesized by IDT. This probe was obtained when it was suspected that the fault might have occurred during the manufacturing of the original probes. The run was performed on the Rotor-Gene® Q (Qiagen) using the QuantiNova Probe PCR kit (Qiagen). Only one probe was added to this reaction. The results are shown in Figure 4.21.

From the results, the wild type probe (labelled with 6-FAM), seems to exhibit more specific binding properties than the previous probes that were tested. The probe has bound to the WT control as well as the T2 control, both of which have the wild type sequence for the type 1 mutation. The probe has thus behaved in a manner that was expected. The overall efficiency of the probe, however, could not be determined without the presence of another probe for the mutant allele.

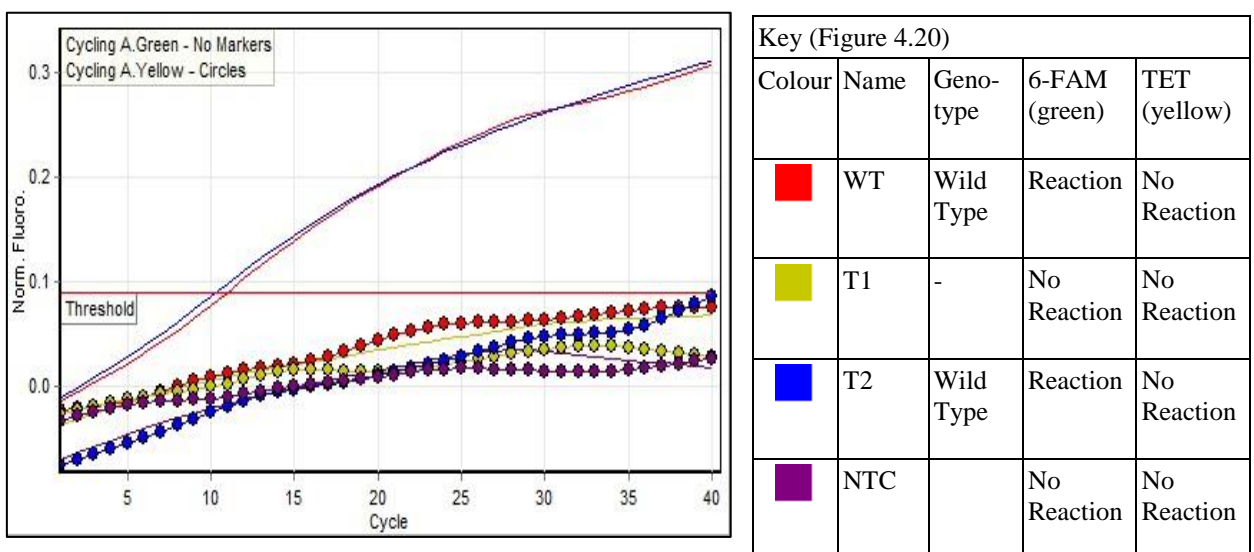


Figure 4.21: Amplification curves of a real-time PCR using a probe from IDT on the Rotor-Gene® Q (Qiagen)

A possible solution to improve the qPCR assay is to redesign and resynthesize the probes in order to create probes that are more specific. While redesigning the probes, the binding sites could be redesigned to better suit the use of *TaqMan* probes. The type of probe used could also be revisited. Probes that would bind more specifically over the areas where the 52-bp deletion and the 5-bp insertion occurs would be more suited for this assay (FRET probes might be a more suitable choice). This is because an assay using FRET probes utilises two probes that hybridize to adjacent DNA sequences, one with a donor at the 3'-end and another with an acceptor at the 5'-end (Didenko, 2001). The FRET system forms after hybridization of the two probes and a fluorescent signal is released (Didenko, 2001).

For the purposes of this analysis, a probe pair could be designed to ensure that one binds to the mutation and the other probe to the site downstream of the mutation. Should the mutation be absent, the first probe would not be able to bind and no fluorescence would be observed.

The qPCR assay using probes was discontinued due to time and budgetary constraints. The lack of qPCR techniques using sequence specific probes in literature is a testament as to how challenging the design and implementation of such an assay might be.

A study was performed in 2014, using a common reverse primer and a pair of different forward primers; one specific for the 52-bp deletion of the type 1 mutation and the other specific for the 5-bp insertion of the type 2 mutation (Chi *et al.*, 2015). A common distal *TaqMan* probe, labelled with FAM, was used in this assay (Chi *et al.*, 2015). The ability of this assay to detect the *CALR* mutations depended on whether the primers would bind in the presence of the type 1 or type 2 mutations, subsequently creating a fluorescent signal when the *TaqMan* probe could bind to the generated fragments (Chi *et al.*, 2015).

In the absence of the specific mutation for which the primer was designed, amplification of the products could not take place and a fluorescent signal was not created (Chi *et al.*, 2015). The probe used in this study was thus not specific for either of the *CALR* mutations, but would rather bind when amplification was taking place (Chi *et al.*, 2015).

A disadvantage of this approach is that in small mutational loads, the type 1 assay starts to cross amplify the type 2 mutation, making it difficult to distinguish the type 1 mutation from the type 2 mutation (Chi *et al.*, 2015). A qPCR assay using probes specific for the two mutations and their wild types would be more sensitive in distinguishing completely between the two mutations.

4.4. Conclusion

After many different attempts using a variety of kits, protocols and instruments, the qPCR using SYBR Green was not successful. SYBR Green has decreased in popularity due to the high specificity of qPCR using probes. The qPCR using SYBR Green was therefore discontinued. In addition the use of TaqMan probes were also investigated without success. However, a qPCR using probes should still be pursued as a possible method for mutation analysis concerning the type 1 and type 2 calreticulin mutations.

References

- Arya, M, Shergill, I, Williamson, M, Gommersall, L, Arya, N and Patel, H 2005. Basic principles of real-time quantitative PCR. *Expert Review of Molecular Diagnostics*, 5, 1-11.
- Bilbao-Sieyro, C, Santana, G, Moreno, M, Torres, L, Santana-Lopez, G, Rodriguez-Medina, C, Perera, M, Bellosillo, B, De la Iglesia, S, Molero, T and Gomez-Casares, M 2014. High Resolution Melting Analysis: A Rapid and Accurate Method to Detect *CALR* Mutations. *PLoS One*, 9, 1-5.
- Bustin, SA and Mueller, R 2005. Real-time reverse transcription PCR (qRT-PCR) and its potential use in clinical diagnosis. *Clinical Science*, 109, 365-379.
- Chi, J, Manoloukos, M, Pierides, C, Nicolaidou, V, Nicolaou, K, Kleopa, M, Vassiliou, G and Costeas, P 2015. *Calreticulin* mutations in myeloproliferative neoplasms and new methodology for their detection and monitoring. *Annals of Hematology*, 94, 399-408.
- Didenko, VV 2001. DNA Probes Using Fluorescence Resonance Energy Transfer (FRET): Designs and Applications. *Biotechniques*, 31, 1106-1121.
- Enblom, A, Lindskog, E, Hasselbalch, H, Hersby, D, Bak, M, Tetu, J, Girodon, F and Andréasson, B 2015. High rate of abnormal blood values and vascular complications before diagnosis of myeloproliferative neoplasms. *European Journal of Internal Medicine*, 26, 344-347.
- Ginzinger, DG 2002. Gene quantification using real-time quantitative PCR: An emerging technology hits the mainstream. *Experimental Hematology*, 30, 503-512.
- Hughes, T and Branford, S 2006. Molecular monitoring of *BCR-ABL* as a guide to clinical management in chronic myeloid leukaemia. *Blood*, 20, 29-41.
- Integrated DNA Technologies. 2015. *PrimerQuest Tool* [Online]. Integrated DNA Technologies. [Accessed September 30th 2015].
- Klein, D 2002. Quantification using real-time PCR technology: applications and limitations. *Trends in Molecular Medicine*, 8, 257-260.

Kubista, M, Andrade, JM, Bengtsson, M, Forootan, A, Jonák, J, Lind, K, Sindelka, R, Sjöback, R, Sjögreen, B, Strömbom, L, Ståhlberg, A and Zoric, N 2006. The real-time polymerase chain reaction. *Molecular Aspects of Medicin*, 27, 95-125.

Lim, K-H, Chang, Y-C, Chen, CG-S, Lin, H-C, Wang, W-T, Chiang, Y-H, Cheng, H-I, Su, N-W, Lin, J, Chang, Y-F, Chang, M-C, Hsieh, R-K, Kuo, Y-Y and Chou, W-C 2015a. Frequent *CALR* exon 9 alterations in *JAK2* V617F-mutated essential thrombocythemia detected by high resolution melting analysis. *Blood Cancer Journal*, 5, 1-4.

Lim, K-H, Lin, H-C, Chen, CG-S, Wang, W-T, Chang, Y-C, Chiang, Y-H, Lin, C-S, Su, N-W, Su, Y-W, Lin, J, Chang, Y-F, Chang, M-C, Hsieh, R-K, Kuo, Y-Y and Chou, W-C 2015b. Rapid and sensitive detection of *CALR* exon 9 mutations using high-resolution melting analysis. *Clinica Chimica Acta*, 440, 133-139.

Park, J-H, Sevin, M, Ramla, S, Truffot, A, Verrier, T, Bouchot, D, Courtois, M, Bas, M, Benali, S, Bailly, F, Favre, B, Guy, J, Martin, L, Maynadié, M, Carillo, S and Girodon, F 2015. Calreticulin Mutations in Myeloproliferative Neoplasms: Comparison of Three Diagnostic Methods. *PLoS One*, 10, 1-7.

Pfaffl, M 2004. Quantification strategies in real-time PCR. In: Bustin, S. A. (ed.) *A-Z of quantitative PCR*. La Jolla, CA, USA: International University Line (IUL),

Tevfik Dorak, M 2006. *Real-time PCR*, New York, NY, Taylor & Francis Group.

Vrsalović, MM, Kušec, R, Pejša, V and Romić, Ž 2007. Comparison of sensitivity of nested PCR and quantitative PCR in Bcr-Abl p210 transcript detection in chronic myelogenous leukemia. *Biochemia Medica*, 17, 109-114.

Chapter 5

Study Outcome

The myeloproliferative neoplasms (MPN), are a group of haematopoietic stem cell (HSC) disorders that are characterized by clonal proliferation of one or more mature myeloid lineages i.e. erythroid, megakaryocytic, or granulocytic cells in the bone marrow and, in some cases, the liver and spleen (Klco *et al.*, 2010; Hoffbrand and Moss, 2012; Turgeon, 2012; Skoda *et al.*, 2015). The group of disorders, now classified as the classic MPNs, include chronic myeloid leukaemia (CML), as well as the Philadelphia (Ph) chromosome-negative MPNs: polycythaemia vera (PV), essential thrombocythaemia (ET) and primary myelofibrosis (PMF) or myelofibrosis (MF) (Santos and Verstovsek, 2012; Klampfl *et al.*, 2013).

Somatic mutations at exon 9 of *CALR*, the gene that encodes for calreticulin, were discovered through whole-exome sequencing and targeted re-sequencing in 50% to 70% and 33% to 58% of European and Asian patients, respectively, with ET and PMF who had neither mutated *JAK2* nor *MPL* (Klampfl *et al.*, 2013; Nangalia *et al.*, 2013; Ha and Kim, 2015). More than 50 different indels (insertions and deletions) have been found in exon 9 of the *CALR* gene (Pietra *et al.*, 2015). Among these mutations, more than 80% of *CALR* mutated patients possess one of only two mutation types: type 1 which is a 52-bp deletion (c.1092_1143del) and type 2 which is a 5-bp insertion (c.1154_1155insTTGTC) (Klampfl *et al.*, 2013; Tefferi *et al.*, 2014). The other indels can be grouped, based on their molecular characteristics, into the categories type 1-like or type 2-like (Guglielmelli *et al.*, 2015). The majority of the calreticulin mutations are heterozygous in nature, with homozygous mutations occurring mostly as 5-bp insertions (Luo and Yu, 2015).

Variable presentations of disease occur depending on which *CALR* mutation is present (Klampfl *et al.*, 2013). This is due to the fact that the mutant protein may possess varying amounts of negatively charged amino acids (Klampfl *et al.*, 2013).

Therefore, type 1/type 1-like and type 2/type 2-like mutations are phenotypically very different (Klampfl *et al.*, 2013; Guglielmelli *et al.*, 2015; Pietra *et al.*, 2015). Type 1/type 1-like mutations are associated with a significant thrombocytosis and an accelerated development to myelofibrosis-like disease with consequential splenomegaly, anaemia, and thrombocytopenia (Guglielmelli *et al.*, 2015). Type 2/type 2-like mutations present with a much milder phenotype as less thrombocytosis is observed as well as a reduced disposition to evolve (Guglielmelli *et al.*, 2015).

In patients with ET, those with type 2/type 2-like *CALR* mutations were younger, had a higher platelet count and lower risk for thrombosis at the time of diagnosis as compared to those with a type 1/type 1-like or *JAK2* mutation (Pietra *et al.*, 2015). It has been noted that the type 1 mutation occurs much more frequently in PMF than in ET (Klampfl *et al.*, 2013). Within the PMF patients, no compelling differences were found between those with type 1-like *CALR* mutations and those with type 2-like *CALR* mutations (Pietra *et al.*, 2015).

Within the MPNs, disease presentation also differs between the *JAK2*, *MPL* and *CALR* mutations. In patients with ET, those with a *CALR* mutation have a lower WBC count, a lower haemoglobin level and a higher platelet count at diagnosis as well as a lower risk of thrombosis than those patients who have mutated *JAK2* (Klampfl *et al.*, 2013; Ahmadzadeh *et al.*, 2015). These patients also have a better thrombosis free survival rate than those with a *JAK2* mutation (Ahmadzadeh *et al.*, 2015). Patients with PMF who have mutated *CALR* are found to have a lower white-cell count and higher platelet count than patients with mutated *JAK2* (Klampfl *et al.*, 2013).

Overall there is a marked difference in the survival rates among the three subgroups of patients with PMF i.e. patients with a somatic mutation of *CALR* have a longer overall survival than those with mutated *JAK2* or *MPL* (Klampfl *et al.*, 2013). Therefore it is of clinical significance to test MPN patients for the presence of the *CALR* type 1 and type 2 mutations.

For this study, the use of conventional polymerase chain reaction (PCR) and real-time PCR (qPCR) was evaluated due to the popularity and widespread use of these techniques as well as the lack of a qPCR assay for the detection of the *CALR* type 1 and type 2 mutations in the South African sector. A qPCR assay for the detection of the type 1 and 2 mutations in *CALR* was deemed most beneficial as qPCR is a technique that is readily available to most diagnostic laboratories. The scarcity (type 1 = 6% and type 2 = 4%; combined total = 10%) of the calreticulin mutations in the population of clinic samples from the Steve Biko Academic Hospital and in the clinical samples from a colleague's *JAK2* study corresponds with findings from another South African study where a very low percentage of positive samples (for type 1 and 2 mutations) were found. The study determined that in a cohort of 89 patients, only three were found to be positive for the type 1 mutation (De Kock, 2016).

Of these three, one was homozygous for the mutation and was also positive for the *JAK2V617F* mutation (De Kock, 2016). The absence of the type 1 and type 2 mutations could be attributed to the African descent of most of the patients which were tested in the study. Three of the five patients in this study, whose ethnicity is known, and who are positive for a calreticulin mutation, are all of Caucasian descent. This is the same for the majority of population groups that have been analysed worldwide, which include populations in Europe and Asia with a *CALR* type 1 and type 2 prevalence of 50% to 70% and 33% to 58%, respectively (Klampfl *et al.*, 2013; Nangalia *et al.*, 2013; Ha and Kim, 2015). Calreticulin type 1 and type 2 mutations have been determined to be very rare in our study population but further studies of other population groups within South Africa will have to be performed to determine whether this is true for the entire population.

Although fragment analysis PCR is the most widely used technique for studying *CALR* mutations; in our study setting the necessary infrastructure and expertise was not available. In future, the qPCR assay using probes should be pursued by redesigning the probes. Method validation should also be performed on all assays that are implemented in the laboratory. This is done by determining the sensitivity and specificity, as well as measuring the precision and accuracy of the assay. Further research, using the sequencing data obtained, should be undertaken to determine whether other, less common, mutations are more likely to be found in this study population.

References

Ahmadzadeh, A, Shirzad, R, Golchin, A, S, S, Shahjahani, M, Seghatoleslami, M and Saki, N 2015. Calreticulin and JAK2^{V617F} Mutations in Essential Thrombocythemia and Their Potential Role in Diagnostics and Prognosis. *Cellular and Molecular Medicine*, 1, 1-11.

De Kock, A. 2016. *RE: Screening for calreticulin mutations in a Free State cohort suspected of having a myeloproliferative neoplasm*. Type to Prinsloo, A.

Guglielmelli, P, Rotunno, G, Fanelli, T, Pacilli, A, Brogi, G, Calabresi, L, Pancrazzi, A and Vannucchi, AM 2015. Validation of the differential prognostic impact of type 1/type 1-like versus type 2/type 2-like *CALR* mutations in myelofibrosis. *Blood Cancer Journal*, 5, 1-3.

Ha, JS and Kim, YK 2015. Calreticulin Exon 9 Mutations in Myeloproliferative Neoplasms. *Annals of Laboratory Medicine*, 35, 22-27.

Hoffbrand, AV and Moss, PA 2012. The non-leukaemic myeloproliferative neoplasms. *Essential Haematology*. 6th ed. West Sussex, UK: Wiley-Blackwell Publishing Ltd, 200-213.

Klampfl, T, Gisslinger, H, Harutyunyan, AS, Nivarthi, H, Rumi, E, Milosevic, JD, Them, NCC, Berg, T and Gisslinger, B 2013. Somatic Mutations of Calreticulin in Myeloproliferative Neoplasms. *New England Journal of Medicine*, 369, 2379-2390.

Klco, JM, Vij, R, Kriesel, FH, Hassan, A and Frater, JL 2010. Molecular Pathology of Myeloproliferative Neoplasms. *American Journal of Clinical Pathology*, 133, 602-615.

Luo, W and Yu, Z 2015. Calreticulin (*CALR*) mutation in myeloproliferative neoplasms (MPNs). *Stem Cell Investigation*, 2, 1-10.

Nangalia, J, Massie, CE, Baxter, EJ, Nice, FL, Gundem, G, Wedge, DC, Avezov, E, Li, J, Kollman, K, Kent, DG, Aziz, A, Godfrey, AL, Hinton, J, Martincorena, I, Van Loo, P, Jones, AV, Guglielmelli, P, Tarpey, P and Harding, HP 2013. Somatic *CALR* Mutations in Myeloproliferative Neoplasms with Nonmutated JAK 2. *New England Journal of Medicine*, 369, 2391-2405.

Pietra, D, Rumi, E, Ferretti, VV, Di Buduo, CA, Milanese, C, Cavalloni, C, Sant'Antonio, E, Abbonante, V, Moccia, F, Casetti, IC, Bellini, M, Renna, MC, Rancoroni, E, Fugazza, E, Astori, C, Boveri, E, Rosti, V, Barosi, G, Balduini, A and

Cazzola, M 2015. Differential clinical effects of different mutation subtypes in *CALR*-mutant myeloproliferative neoplasms. *Leukemia*, 1-8.

Santos, FPS and Verstovsek, S 2012. Breakthroughs in myeloproliferative neoplasms. *Hematology*, 17, 55-58.

Skoda, RC, Duek, A and Grisouard, J 2015. Pathogenesis of myeloproliferative neoplasms. *Experimental Hematology*, 43, 599-608.

Tefferi, A, Wassie, EA, Guglielmelli, P, Gangat, N, Belachew, AA, Lasho, TI, Finke, C, Ketterling, RP, Hanson, CA, Pardanani, A, Wolanskyj, AP, Maffioli, M, Casalone, R, Pacilli, A, Vannucchi, AM and Passamonti, F 2014. Type 1 versus Type 2 calreticulin mutations in essential thrombocythemia: A collaborative study of 1027 patients. *American Journal of Hematology*, 89, 121-124.

Turgeon, ML 2012. Myeloproliferative Neoplasms. *Clinical Haematology: Theory and Procedures*. 5th ed. Philadelphia PA: Lippincott Williams and Wilkins, 361-385.

Appendices

A1	MSc Committee approval form Demographic information of study population	118
A2	Ethics Committee approval form	119
A3	Ethics Committee amendment approval form	120
A4	Informed consent form for the collection of blood samples from non-government institutions	121
A5	DNA concentration of samples used	127
A6	Manufactured control sequences with primer binding sites and the <i>MfeI</i> restriction enzyme digestion site	129



A1. MSc Committee approval form



UNIVERSITEIT VAN PRETORIA
UNIVERSITY OF PRETORIA
YUNIBESITHI YA PRETORIA

Faculty of Health Sciences

MSc Committee
19 November 2015

Dr WB van Zyl
Department of Virology
Faculty of Health Sciences

Dear Dr van Zyl,

Ms LDV du Toit, Student no 10062361

Thank you for submitting the above mentioned student's ethics approval to the MSc Committee. Please receive the comments:

Student name	Ms LDV du Toit	Student number	10062361
Name of study leader	Dr WB van Zyl		
Department	Medical Virology		
Title of MSc	Detection of the calreticulin type 1 and type 2 mutations in a group of myeloproliferative neoplasm patients using the polymerase chain reaction.		
Date of first submission	May 2015		
October 2015	<ul style="list-style-type: none"> • Thank you for submitting the ethics approval letter 		
Decision	<p>This protocol has been approved. Ethics approval obtained.</p> <p>The internal and external examiners should be nominated and submitted for approval 6 months prior to submission of the dissertation.</p>		

Yours sincerely

Prof Riana Cockeran
Chair: MSc Committee



A2. Ethics Committee approval form

The Research Ethics Committee, Faculty Health Sciences, University of Pretoria complies with ICH-GCP guidelines and has US Federal side Assurance.

- PAA 00002957, Approved dd 22 May 2002 and Expires 20 Oct 2018.
- IRB 0000 2235 IORG0001762 Approved dd 22/04/2014 and Expires 22/04/2017.



UNIVERSITEIT VAN PRETORIA
UNIVERSITY OF PRETORIA
YUNIBESITHI YA PRETORIA

Faculty of Health Sciences Research Ethics Committee

27/08/2015

Approval Certificate New Application

Ethics Reference No.: 335/2015

Title: Detection of the calcitriol type 1 and type 2 mutations in a group of myeloproliferative neoplasm patients using molecular methods.

Dear Louise du Toit

The **New Application** as supported by documents specified in your cover letter dated 17/08/2015 for your research received on the 18/08/2015, was approved by the Faculty of Health Sciences Research Ethics Committee on its quorate meeting of 25/08/2015.

Please note the following about your ethics approval:

- Ethics Approval is valid for 1 year
- Please remember to use your protocol number (335/2015) on any documents or correspondence with the Research Ethics Committee regarding your research.
- Please note that the Research Ethics Committee may ask further questions, seek additional information, require further modification, or monitor the conduct of your research.

Ethics approval is subject to the following:

- The ethics approval is conditional on the receipt of 6 monthly written Progress Reports, and
- The ethics approval is conditional on the research being conducted as stipulated by the details of all documents submitted to the Committee. In the event that a further need arises to change who the investigators are, the methods or any other aspect, such changes must be submitted as an Amendment for approval by the Committee.

Additional Conditions:

- *The REC recommends the waiving of Informed Consent for obtaining the blood considering the low risk.*

We wish you the best with your research.

Yours sincerely

Dr R Sommers; MBChB, MMed (Inf); MPharmD.
Deputy Chairperson of the Faculty of Health Sciences Research Ethics Committee, University of Pretoria

The Faculty of Health Sciences Research Ethics Committee complies with the SA National Act 61 of 2003 as it pertains to health research and the United States Code of Federal Regulations Title 45 and 46. This committee abides by the ethical norms and principles for research, established by the Declaration of Helsinki, the South African Medical Research Council Guidelines as well as the Guidelines for Ethical Research: Principles Structures and Processes 2004 (Department of Health).



A3. Ethics Committee amendment approval form

The Research Ethics Committee, Faculty Health Sciences, University of Pretoria complies with ICH-GCP guidelines and has US Federal wide Assurance.

- FWA 00002567, Approved dd 22 May 2002 and Expires 20 Oct 2016.
- IRB 0000 2235 IORG0001762 Approved dd 22/04/2014 and Expires 22/04/2017.



UNIVERSITEIT VAN PRETORIA
UNIVERSITY OF PRETORIA
YUNIBESITHI YA PRETORIA

Faculty of Health Sciences Research Ethics Committee

11/08/2016

**Approval Certificate
Amendment**

(to be read in conjunction with the main approval certificate)

Ethics Reference No.: **335/2015**

Title: Detection of the calreticulin type 1 and type 2 mutations in a group of myeloproliferative neoplasm patients using molecular methods.

Dear Miss Louise du Toit **Dept:** Hematology

The **Amendment** (as supported by documents specified in your cover letter dd 19/07/2016) as described in the documents received on dd 18/07/2016 to be ratified by the Faculty of Health Sciences Research Ethics Committee on the 17/08/2016.

Please note the following about your ethics amendment:

- Please remember to use your protocol number (**335/2015**) on any documents or correspondence with the Research Ethics Committee regarding your research.
- Please note that the Research Ethics Committee may ask further questions, seek additional information, require further modification, or monitor the conduct of your research.

Ethics amendment is subject to the following:

- The ethics approval is conditional on the receipt of 6 monthly written Progress Reports, and
- The ethics approval is conditional on the research being conducted as stipulated by the details of all documents submitted to the Committee. In the event that a further need arises to change who the investigators are, the methods or any other aspect, such changes must be submitted as an Amendment for approval by the Committee.

We wish you the best with your research.

Yours sincerely

Dr R Sommers; MBChB; MMed (Int); MPharMed. Phd

Deputy Chairperson of the Faculty of Health Sciences Research Ethics Committee, University of Pretoria

The Faculty of Health Sciences Research Ethics Committee complies with the SA National Act 61 of 2003 as it pertains to health research and the United States Code of Federal Regulations Title 45 and 46. This committee abides by the ethical norms and principles for research, established by the Declaration of Helsinki, the South African Medical Research Council Guidelines as well as the Guidelines for Ethical Research: Principles Structures and Processes 2004 (Department of Health).

◆ Tel:012-3541330 ◆ Fax:012-3541367 Fax2Email: 0866515924 ◆ E-Mail: fhsethics@up.ac.za
◆ Web: //www.healthethics-up.co.za ◆ H W Snyman Bld (South) Level 2-34 ◆ Private Bag x 323, Arcadia, Pta, S.A., 0007

A4. Informed consent form for the collection of blood samples from non-government institutions

PATIENT OR PARTICIPANT'S INFORMATION & INFORMED CONSENT DOCUMENT

STUDY TITLE: Detection of the calreticulin type 1 and type 2 mutations in a group of myeloproliferative neoplasm patients using molecular methods.

SPONSOR: NHLS Research Trust Fund and RESCOM

Principal Investigator: Louise de Villiers du Toit

Supervisor: Dr Walda van Zyl

Co-supervisor: Mrs Andrea Prinsloo

Institution: University of Pretoria, Department of Haematology

DAYTIME AND AFTERHOURS TELEPHONE NUMBER(S):

Daytime numbers: 012 319 2279 / 073 228 6228

Afterhours: 073 228 6228

DATE AND TIME OF FIRST INFORMED CONSENT DISCUSSION:

dd mm yyyy Time:

Dear Mr. / Mrs. date of consent procedure/...../.....

1) INTRODUCTION

You are invited to volunteer for a research study. This information leaflet is to help you to decide if you would like to participate. Before you agree to take part in this study you should fully understand what is involved. If you have any questions, which are not fully explained in this leaflet, do not hesitate to ask the investigator. You should not agree to take part unless you are completely happy about all the procedures involved. In the best interests of your health, it is strongly recommended that you discuss with or inform your personal doctor of your possible participation in this study, wherever possible.

2) THE NATURE AND PURPOSE OF THIS STUDY

Myeloproliferative neoplasms are a group of blood cancers caused when something goes wrong and your genes (DNA) change. This change is called a mutation. In this study we want to develop a laboratory test that will be used to find two of the most common mutations associated with the myeloproliferative neoplasms in the calreticulin gene. By doing so, we wish to fill a gap that currently exists in the South African health care sector.

3) EXPLANATION OF PROCEDURES TO BE FOLLOWED

This study involves giving a blood sample. This is done by sticking a clean needle into a vein, usually one in the arm, and withdrawing a small amount of blood into a tube. The tube is then labelled with your name and surname, age and sex for statistical purposes. Your blood is then used in the laboratory where it is tested for the two common calreticulin mutations as part of a study to create a test for finding these mutations.

4) RISK AND DISCOMFORT INVOLVED

The only discomfort involved is the taking of blood from a vein. Drawing blood is normally done as part of routine medical care and presents a slight risk of discomfort. Drawing blood may result in a bruise at the puncture site, or less commonly fainting or swelling of the vein, infection and bleeding from the site. Your protection is that the procedures are performed under sterile conditions by experienced personnel. A total of (4.5ml) of blood will be collected over the course of the entire study. The University of Pretoria has limited insurance for research related injuries.

5) POSSIBLE BENEFITS OF THIS STUDY.

The development of a test to find the two mutations will help a lot of people with a myeloproliferative neoplasm that may be suspected of having this change in their calreticulin genes. It will also help your doctor to better treat your disease if a mutation is found.

6) I understand that if I do not want to participate in this study, I will still receive standard treatment for my illness.

7) I may at any time withdraw from this study.

8) HAS THE STUDY RECEIVED ETHICAL APPROVAL?

This protocol was submitted to the Faculty of Health Sciences Research Ethics Committee, University of Pretoria, telephone numbers 012 356 3084 / 012 356 3085 and written approval has been granted by that committee (protocol number 335/2016). The study has been structured in accordance with the Declaration of Helsinki (last update: October 2013), which deals with the recommendations guiding health care professionals in biomedical research involving human/subjects. A copy of the Declaration may be obtained from the investigator should you wish to review it.

9) INFORMATION

If I have any questions concerning this study, I should contact:

Ms Louise du Toit: 073 228 6228

Mrs Andrea Prinsloo: 012 319 2279

10) CONFIDENTIALITY

All records obtained whilst in this study will be regarded as confidential. Results will be published or presented in such a way that patients remain unidentifiable.

11) CONSENT TO PARTICIPATE IN THIS STUDY

I have read or had read to me in a language that I understand the above information before signing this consent form. The content and meaning of this information have been explained to me.

I have been given opportunity to ask questions and am satisfied that they have been answered satisfactorily. I understand that if I do not participate it will not alter my management in any way. I hereby volunteer to take part in this study.

I have received a signed copy of this informed consent agreement.

.....
Patient's name Date

.....
Patient's signature Date

.....
Investigator's name Date

.....
Investigator's signature Date

.....
Witness' name Date

.....
Witness' signature Date

5 of 6

VERBAL PATIENT INFORMED CONSENT (applicable when patients cannot read or write)

I, the undersigned,, have read and have explained fully to the patient, named and/or his/her relative, the patient information leaflet, which has indicated the nature and purpose of the study in which I have asked the patient to participate. The explanation I have given has mentioned both the possible risks and benefits of the study and the alternative treatments available for his/her illness. The patient indicated that he/she understands that he/she will be free to withdraw from the study at any time for any reason and without jeopardizing his/her treatment.

I hereby certify that the patient has agreed to participate in this study.

Patient's name _____

(Please print)

Patient's signature _____

Date _____

Investigator's name _____

(Please print)

Investigator's signature _____

Date _____

Witness name _____

(Please print)

Witness signature _____

Date _____



A5. DNA concentration of samples used

Table A1: DNA concentrations of samples

Patient number	Sample ID	A260/A280	Nucleic Acid Concentration (ng/μl)
(Not a patient)	Normal 1 (N1)	1.83	36.7
1	2	2.17	31.3
2	4	1.95	137.4
3	5*	1.84	32.7
4	6	1.47	22.9
5	10*	1.79	17.2
6	11	1.93	97.4
7	12	1.92	73.2
8	13	1.91	101.8
9	14	1.91	38.7
10	15	1.96	35.2
11	16*	1.88	53.6
12	18**	2.12	35.9
13	19	1.92	34.5
14	20	2.00	35.5
15	21*	1.86	37.1
16	23*	1.89	32.6
17	24	1.86	32.9
18	25	1.97	22.3
19	26	1.87	20.2
20	27	1.91	23.2
21	28	1.87	59.0
22	29	1.94	30.9
23	30	1.81	80.8
24	31**	1.37	19.7
25	J5	2.22	11.6
26	J6**	2.24	9.8
27	J9**	1.53	28.0
28	J19	2.24	20.1
29	J22**	1.41	27.1
30	J23	2.07	13.2
31	J25	2.10	12.1
32	J26	2.12	17.6
33	J27	1.91	12.2
34	J28	2.08	6.20
35	J29	1.97	16.5
36	J32	1.97	52.9
37	J34	1.91	13.1
38	J35	1.95	68.1
39	J36	1.91	172.5
40	J37	1.87	23.6
41	J38	1.85	35.0
42	J39	2.02	37.6
43	J40	1.94	43.3
44	J41	1.97	23.0
45	J42	1.88	53.6



A5. DNA concentration of samples used (continued)			
	Sample ID	A260/A280	Nucleic Acid Concentration (ng/ μ l)
46	J43*	1.84	82
47	J44	1.91	36.9
48	J45	2.01	28.5
49	pos DEL*	1.99	34.0
50	pos INS*	1.91	35.3

*DNA samples used with an A260/A280 ratio within the range of 1.7-1.9, prescribed by the Genequality *CALR* Mutation (AB Analytica, Padua, Italy) kit used in the experiment in section 2.2.10.

**DNA samples used with an A260/A280 ratio outside of the range of 1.7-1.9, prescribed by the Genequality *CALR* Mutation (AB Analytica) kit used in the experiment in section 2.2.10.

A6. Manufactured control sequences with primer binding sites and the *MfeI* restriction enzyme digestion site

Wild type: Fragment size before PCR: 411-bp

 Fragment size after PCR: 399-bp

GAGGCCTGGTCCTGGTCCTGATGTTCGGGGGCGGGCAGGGCTGGCAGGGGGC
AAGGCCCTGAGGTGTGTGCTCTGCCTGCAGGCAGCAGAGAAACAAATGAAG
GACAAACAGGACGAGGAGCAGAGGCTTAAGGAGGAGGAAGAAGACAAGA
AACGCAAAGAGGAGGAGGAGGCAGAGGACAAGGAGGATGATGAGGACAA
AGATGAGGATGAGGAGGATGAGGAGGACAAGGAGGAAGATGAGGAGGAA
GATGTCCCCCGGCCAGGCCAAGGACGAGCTGTAGAGAGGCCTGCCTCCAGGG
CTGGACTGAGGCCTGAGCGCTCCTGCCGCAGAGCTGGCCGCGCCAAATAAT
GTCTCTGTGAGACTCGAGAACTTTCATTTTTTTTCCAGGCTGGTTTCGGATTTGG
GGTGGAT

Type 1 mutation: Fragment size before PCR: 359-bp

 Fragment size after PCR: 347-bp

GAGGCCTGGTCCTGGTCCTGATGTTCGGGGGCGGGCAGGGCTGGCAGGGGGC
AAGGCCCTGAGGTGTGTGCTCTGCCTGCAGGCAGCAGAGAAACAAATGAAG
GACAAACAGGACGAGGAGCAGAGGACAAGGAGGATGATGAGGACAAAGA
TGAGGATGAGGAGGATGAGGAGGACAAGGAGGAAGATGAGGAGGAAGAT
GTCCCCGGCCAGGCCAAGGACGAGCTGTAGAGAGGCCTGCCTCCAGGGCTG
GACTGAGGCCTGAGCGCTCCTGCCGCAGAGCTGGCCGCGCCAAATAATGTC
TCTGTGAGACTCGAGAACTTTCATTTTTTTTCCAGGCTGGTTTCGGATTTGGGG
TGGAT

